Appendix N.

Underwater noise modelling study - FPSO
facility anchor piling (JASCO 2017)

FPSO Facility Anchor Piling Acoustic Modelling

Barossa Field

Suggested citation:

McPherson, C.R, J. Quijano. 2017. *FPSO Facility Anchor Piling Acoustic Modelling, Barossa Field*. JASCO Document 01346, Version 1.0. ConocoPhillips Document BAA-00-HS-RPT-00009. Technical report by JASCO Applied Sciences for ConocoPhillips Australia.

Revision History Table

Person who prepared content	Person who approved content	Date of preparation/approval
J. Quijano	C. McPherson	7 March 2017
C. McPherson	D. Hannay	9 March 2017
C. McPherson	C. McPherson	28 March 2017

Contents

Contents

Figures

Tables

1. Introduction

This report presents the results of an acoustic modelling study designed to estimate potential effects on marine fauna associated with pile driving activities in the Barossa field.

The modelling study specifically assesses distances from pile driving operations at which underwater sound levels decay to thresholds corresponding to various levels of impact near submerged pile driving. The animal types considered here include marine mammals, fishes (including fish eggs and larvae) and turtles. Due to the variety of species considered, there are several different thresholds for evaluating effects, including: mortality, injury, temporary hearing acuity reduction and behavioural disturbance.

This study considers multiple alternative scenarios for the installation of subsea anchor cylindrical piles, and how noise levels generated by these activities are influenced by pile dimensions, bathymetry, and choice of pile driving equipment.

2. Acoustic Impact Criteria

The perceived loudness of sound, especially impulsive noise such as that generated by pile driving, is not generally proportional to the instantaneous acoustic pressure. Rather, perceived loudness depends on pulse rise-time and duration, and frequency content. Thus, several sound level metrics are commonly used to evaluate noise and its effects on marine life. The metrics applied in this report, including peak pressure level (PK), sound pressure level (SPL), and sound exposure level (SEL), are defined in Appendix A.1. The period of accumulation associated with SEL is defined, with this report referencing either a 'per strike' assessment or accumulation over 24 hours, SEL_{24h}. Any applied frequency weighting is indicated by appropriate subscripts, with unweighted SEL defined as required. Recent updates to the ANSI and ISO standards for acoustic terminology, ANSI-ASA S1.1 (ANSI S1.1-2013 R2013) and ISO/DIS 18405.2:2016 (2016, draft) have also been incorporated into the acoustic metrics applied in this report.

The assessment criteria applied in this study arose from several recognised scientific sources that have defined acoustic exposure levels applicable to marine fauna. Since 2007, several expert groups have investigated an SEL-based assessment approach for injury, with a handful of key papers published on the topic. Likewise, the number of studies investigating the level of disturbance to marine fauna by underwater noise has increased substantially. This section discusses the proposed methods and thresholds applied in the current study, which are consistent with those applied for other recent projects in the Barossa field (McPherson et al. 2016).

Results of the modelling study are presented in terms of the following noise criteria, which have been chosen to include thresholds commonly applied in Australia and outlined in Sections 2.1 and 2.2:

1. Single shot threshold for cetaceans (unweighted per-pulse SEL of 160 dB re 1 $\mu Pa^2 \cdot s$) (from marine seismic surveys).This process is outlined in the Australian Environment Protection and Biodiversity Conservation (EPBC) Act Policy Statement 2.1, Department of the Environment, Water, Heritage and the Arts (DEWHA 2008).This has been provided for reference for single strikes from piling operations.

2. Marine mammal behavioural disturbance threshold based on the current interim United States National Marine Fisheries Service (NMFS) criterion (NMFS 2013) for marine mammals of 160 dB re 1 μPa SPL for impulsive sound sources.

3. M-weighted sound exposure level (SEL_{24h}) thresholds for marine mammal injury based on Wood et al. (2012).

4. Sound exposure guidelines for fish, including temporary threshold shift (TTS), and injury to fish, fish eggs and fish larvae, and turtles proposed by Popper et al. (2014).

5. Threshold for turtle behavioural response (NSF 2011), 166 dB re 1 μPa (SPL), applied by the US National Marine Fisheries Service.

2.1. Marine Mammals

The criteria applied in this study to assess possible effects of noise generated by pile driving activities on cetaceans are summarised in Table 1 and detailed in Sections 2.1.1 and 2.1.2, with frequency weighting explained in Appendix A.2.

Table 1. The unweighted per-strike SPL, SEL and SEL$_{24h}$ thresholds for acoustic effects on cetaceans.

Hearing group	DEWHA (2008)	NMFS (2013)	Wood et al. (2012)
	Unweighted per-pulse SEL (dB re 1 µPa2·s)	SPL (dB re 1 µPa)	M-weighted SEL$_{24h}$ (dB re 1 µPa2·s)
		Behaviour	Injury (PTS)
Low-frequency cetaceans			192
Mid-frequency cetaceans	160	160	198
High-frequency cetaceans			179

2.1.1. Behavioural Response

Southall et al. (2007) extensively reviewed marine mammal behavioural responses to sounds as documented in the literature. Their review found that most marine mammals exhibit varying responses between an SPL of 140 and 180 dB re 1 µPa, but a lack of convergence in the data from multiple studies prevented them from suggesting explicit step functions. Why studies varied included the lack of control groups, imprecise measurements, inconsistent metrics, and context dependency of responses including the animal's activity state. To create meaningful qualitative data from the collected information, Southall et al. (2007) proposed a severity scale that increased with increasing sound levels.

Wood et al. (2012) published an updated set of criteria for injury that built upon the work undertaken by Southall et al. (2007) in a study in which Southall was a co-author, thus criteria were developed with some consistency. The new criteria suggested by Wood et al. (2012) include M-weighting similarly to Southall et al. (2007).

NMFS has historically used a relatively simple sound level criterion to measure potential disturbance to marine mammals. For impulsive sounds, this criterion is an SPL of 160 dB re 1 µPa for pinnipeds and cetaceans (NMFS 2013), which this report refers to as the NMFS marine mammal behavioural response criterion.

2.1.2. Injury and Hearing Sensitivity Changes

For seismic surveys in Australian waters, the EPBC Act Policy Statement 2.1 determines suitable exclusion zones with an unweighted per-pulse SEL threshold of 160 dB re 1 µPa^2·s (DEWHA 2008). This threshold minimises the likelihood of TTS in mysticetes and large odontocetes. The Policy Statement does not apply to smaller dolphins and porpoises because DEWHA assessed these cetaceans as having peak hearing sensitivities that occur at higher frequency ranges than those that seismic arrays typically produce. Recent regulation updates in the US (NMFS 2016) and publications on higher frequency components of airgun signals (Hermannsen et al. 2015) suggest that the policy might need to be updated. The Policy Statement can also be applied to other impulsive sources such as pile driving.

There are two categories of auditory threshold shifts or hearing loss: permanent threshold shift (PTS), a physical injury to an animal's hearing organs, and TTS, a temporary reduction in an animal's hearing sensitivity as the result of receptor hair cells in the cochlea becoming fatigued.

To assess the potential for marine mammals to be injured from pile driving, this report applies the EPBC Act Policy Statement 2.1 and the criteria recommended by Wood et al. (2012) for PTS, as outlined in Appendix A.2.1. The report excludes ranges to the PK components of this criteria because the ranges to the 24 h SEL criteria are significantly greater.

2.2. Fish and Turtles

In 2006, the Working Group on the Effects of Sound on Fish and Turtles was formed to continue developing noise exposure criteria for fish and turtles, work begun by a NOAA panel two years earlier. The resulting guidelines included specific thresholds for different levels of effects and for different groups of species (Popper et al. 2014). These guidelines defined quantitative thresholds for three types of immediate effects:

- Mortality, including injury leading to death.

- Recoverable injury, including injuries unlikely to result in mortality, such as hair cell damage and minor haematoma.

- Temporary Threshold Shift.

Masking and behavioural effects are assessed qualitatively, by assessing relative risk rather than by specific sound level thresholds. As the presence or absence of a swim bladder has a role in hearing, susceptibility to injury from noise exposure varies depending on the fish species and the presence and possible role of a swim bladder in hearing. Thus, different thresholds were proposed for fish without a swim bladder (also appropriate for sharks and applied to whale sharks in the absence of other information), fish with a swim bladder not used for hearing, and fish that use their swim bladders for hearing. Turtles, fish eggs, and fish larvae are considered separately.

This report applies the Popper et al. (2014) threshold criteria for the TTS-based impairment of fish exposed to pile driving. Table 2 summarises the effects thresholds from Popper et al. (2014). In general, any adverse effects of impulsive sound on fish behaviour depends on the species, the state of the individuals exposed, and other factors. While it is evident that animals might adjust their behaviour when they are exposed to pile driving sounds, there are few data appropriate to develop guidelines (Popper et al. 2014). Estimates of the behavioural responses can be conducted using the relative-risk criteria. The SEL metric integrates noise intensity over an exposure period. As the period of integration for regulatory assessments is not well defined for sounds that do not begin or end at a specific time, or for exposures that last a long time, Popper et al. (2014) recommended an integration time of 24 hours, similar to the Southall et al. (2007) criteria for marine mammals. Integration times in this study have been applied over the time a single pile was driven since only one pile will be driven per day.

Table 2. Criteria for pile driving noise exposure for fish and turtles, adapted from Popper et al. (2014).

| Type of animal | Mortality and potential mortal injury | Impairment | | | Behaviour |
		Recoverable injury	TTS	Masking	
Fish I: No swim bladder (particle motion detection)	> 219 dB 24 h SEL or > 213 dB PK	> 216 dB 24 h SEL or > 213 dB PK	>> 186 dB 24 h SEL	(N) Moderate (I) Low (F) Low	(N) High (I) Moderate (F) Low
Fish II: Swim bladder not involved in hearing (particle motion detection)	210 dB 24 h SEL or > 207 dB PK	203 dB 24 h SEL or > 207 dB PK	>> 186 dB 24 h SEL	(N) Moderate (I) Low (F) Low	(N) High (I) Moderate (F) Low
Fish III: Swim bladder involved in hearing (primarily pressure detection)	207 dB 24 h SEL or > 207 dB PK	203 dB 24 h SEL or > 207 dB PK	186 dB 24 h SEL	(N) High (I) High (F) Moderate	(N) High (I) High (F) Moderate
Turtles	210 dB 24 h SEL or > 207 dB PK	(N) High (I) Low (F) Low	(N) High (I) Low (F) Low	(N) High (I) Moderate (F) Low	(N) High (I) Moderate (F) Low
Fish eggs and fish larvae	> 210 dB 24 h SEL or > 207 dB PK	(N) Moderate (I) Low (F) Low	(N) Moderate (I) Low (F) Low	(N) Moderate (I) Low (F) Low	(N) Moderate (I) Low (F) Low

Peak sound pressure level dB re 1 µPa; 24 h SEL dB re 1µPa^2·s. All criteria are presented as sound pressure even for fish without swim bladders since no data for particle motion exist. Relative risk (high, moderate, low) is given for animals at three distances from the source defined in relative terms as near (N), intermediate (I), and far (F).

2.2.1. Turtle Behavioural Response

To inform this report, a review of available literature on how turtles respond to acoustic exposure was undertaken. Most information is available from behavioural response to seismic sources, in lieu of specific information about pile driving.

McCauley et al. (2000) observed the behavioural response of caged turtles—green (*Chelonia mydas*) and loggerhead (*Caretta caretta*)—to an approaching seismic airgun. For received levels above 166 dB re 1 µPa (SPL), the turtles increased their swimming activity and above 175 dB re 1 µPa they began to behave erratically, which was interpreted as an agitated state. The 166 dB re 1 µPa level has been used as the threshold level for a behavioural disturbance response by NMFS and applied in the Arctic Programmatic Environment Impact Statement (PEIS) (NSF 2011). At that time, and in the absence of any data from which to determine the sound levels that could injure an animal, TTS or PTS onset were considered possible at an SPL of 180 dB re 1 µPa (NSF 2011). Some additional data suggest that behavioural responses occur closer to an SPL of 175 dB re 1 µPa, and TTS or PTS at even higher levels (Moein et al. 1994), but the received levels were unknown and the NSF (2011) PEIS maintained the earlier NMFS criteria levels of 166 and 180 dB re 1 µPa (SPL) for behavioural response and injury, respectively.

Popper et al. (2014) suggested injury to turtles could occur for sound exposures above 207 dB re 1 µPa (PK) or above 210 dB re 1 µPa^2·s (SEL$_{24h}$) (Table 2). Sound levels defined by Popper et al. (2014) show that animals are very likely to exhibit a behavioural response when they are near a pile driving (tens of metres), a moderate response if they encounter the source at intermediate ranges (hundreds of metres), and a low response if they are far (thousands of metres) from the pile driving. Both the NMFS criteria for behavioural disturbance (SPL of 166 dB re 1 µPa) and the Popper et al. (2014) injury criteria were included in this analysis.

3. Methods

This section details the methodology for predicting the source levels, modelling the sound propagation, and assessing distances to the selected impact criteria.

3.1. Modelling Overview

The alternative scenarios have been selected to account for water depth, hammer strength and pile diameter, and geological resistance. These considerations are explained in detail in Sections 3.1.1 to 3.1.3.

3.1.1. Water Depth

While the Barossa project is at an early stage of project definition, it is possible that subsea impact pile driving might need to be used to install anchor piles for the Floating Production, Storage and Offloading (FPSO) facility. To inform an early assessment of potential pile driving activities, two representative locations within the Barossa field were selected. Available information indicates that the geology and sound speed profiles are consistent across the region (Sections 3.6.2 and 3.6.3). Due to this similarity, the factor that has the greatest influence on the sound propagation across the Barossa field is bathymetry, including the depth at individual locations and the seabed profile of the surrounding area. To understand how the sound propagates depends upon bathymetry, in addition to the operational parameters. The selection of the two representative locations was based on bathymetry(Table 3 and Figure 1) and represent the range of shallow and deeper waters that the FPSO may be located within the Barossa field.

Table 3. Representative locations of piling activities.

| Site | Water depth (m) | Latitude | Longitude | UTM (Zone 52S) | |
				X (m)	Y (m)
1	235	9° 52' 35.7683" S	130° 11' 8.3587" E	630000	8908000
2	288	9° 44' 58.8305" S	130° 16' 34.8945" E	640000	8922000
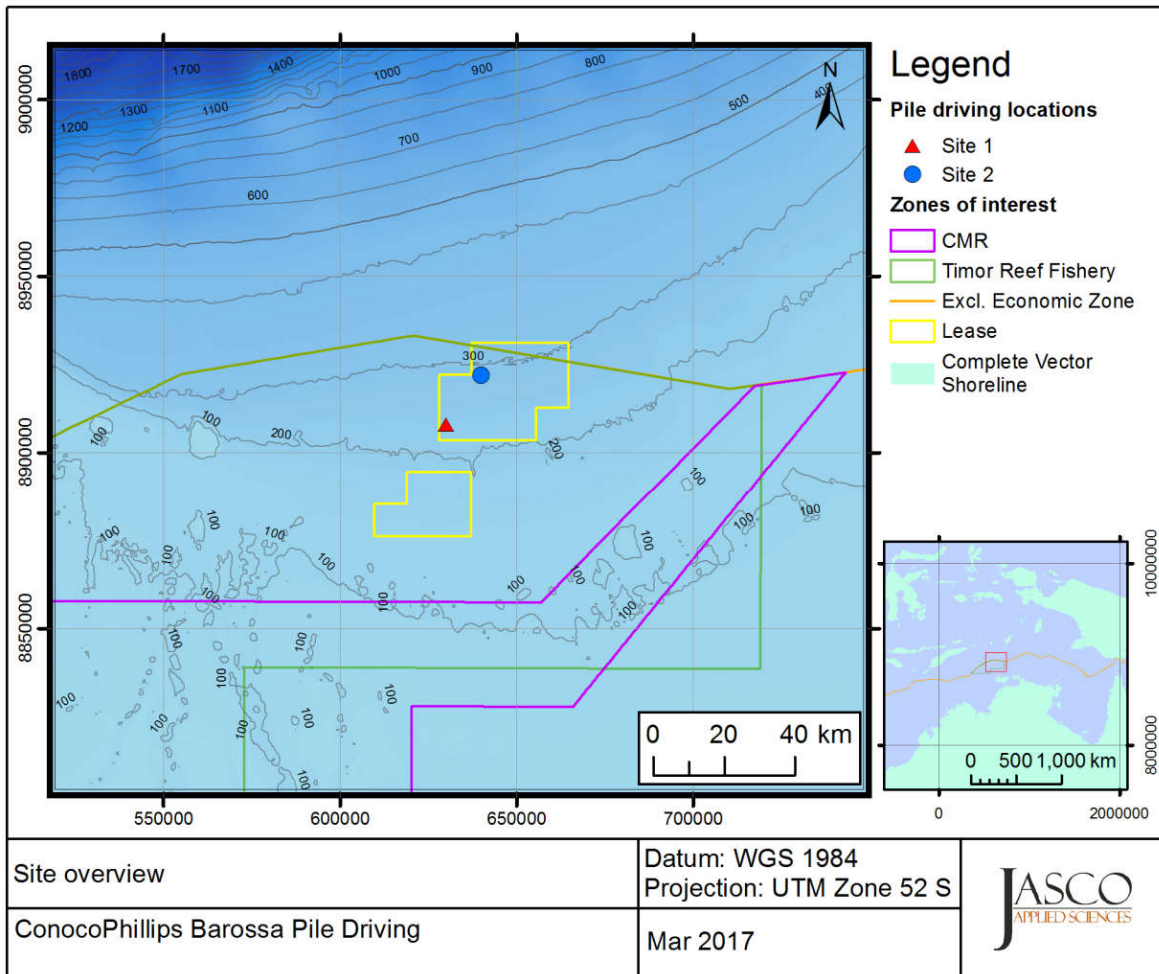
Figure 1. Survey region and modelling locations (note, CMR refers to the Oceanic Shoals Commonwealth Marine Reserve).

3.1.2. Hammer Strength and Pile Diameters

As the engineering design for the project is yet to be finalised, the modelling study considers a combination of a range of possible hammers, pile diameters and lengths. The range of considered inputs, in addition to modelling sites at two different water depths (Table 3), provides a comprehensive overview of possible noise footprints, and the factors related to sound propagation across the Barossa field. The study includes two different hammers with energies of 600 kJ and 1730 kJ, and two different pile diameters of 4 and 5 m. Two different pile lengths of 43 or 39 m were also considered, with 15 m always remaining above the sea floor.

Due to the depth of water these will be driven in to the sediment using subsea hammers. Table 4 defines the modelling scenarios. Only one pile will be driven each day so pile driving equipment can be relocated and setup. It is assumed that the pile will only experience negligible settling before driving commences. We have assumed maximum rated hammer energy over the duration of the drive, derived from GRLWEAP (Section 3.2), which is a very conservative assumption.

3.1.3. Geological Resistance

To determine cumulative effects of pile driving activities, the expected number of strikes needed to drive each pile into the sediment is required. Given it is not yet known whether pile driving will be required, a conservative estimate of the number of strikes needed for each hammer and pile combination has been applied based on practical experience from similar pile driving activities, an assessment of the piling model applied by JASCO and the geological profile that defined the geoacoustics (Section 3.6.2). In practice the number of strikes required will be affected by factors

such as soil resistance (i.e. high soil resistance requires more strikes) and hammer settings (i.e. shorter strike distance require more strikes). To understand how the sound propagation/noise footprint would vary if fewer hammer strikes were required, which could occur given a lower soil resistance, two scenarios (9 and 10 in Table 4) with a lower average strike count for the larger hammer were also modelled.

3.1.4. Modelling Scenarios

The modelling scenarios were numbered initially per modelling site, with the order of pile size and hammer applied the same for both sites. Scenarios 9 and 10, although being at different locations, were grouped together based upon soil resistance characteristics, as they consider a different soil resistance to the other eight scenarios.

In summary, to understand how different parameters would influence the sound propagation across the Barossa field, the alternative scenarios have been selected to consider:

- a premise case of an indicative FPSO location within the Barossa field (i.e. Scenarios 1-4)

- a change in the FPSO facility location to a deeper water depth (i.e. Scenarios 5-8)

- a change in geological resistance (i.e. Scenario 9-10).

The model assumed no acoustic mitigation around the pile driving operation. Therefore, the modelling scenarios represent the maximum noise footprint from pile driving activities as a conservative estimate.

Table 4. Modelling scenario details.

Scenario	Location	Pile dimensions* (m)			Hammer†	Strikes to full penetration	Penetration rate (mm/strike)	Total driving time (min)
		Length	Diameter	Penetration				
1	Site 1	43	4	28	MHU 600T	1843	15.2	61
2		43	4	28	MHU 1700S	433	64.7	14
3		39	5	24	MHU 600T	1579	15.2	53
4		39	5	24	MHU 1700S	371	64.7	12
5	Site 2	43	4	28	MHU 600T	1843	15.2	61
6		43	4	28	MHU 1700S	433	64.7	14
7		39	5	24	MHU 600T	1579	15.2	53
8		39	5	24	MHU 1700S	371	64.7	12
9	Site 1	39	5	24		301	79.7	10
10	Site 2	39	5	24		301	79.7	10

* All piles modelled as having 50 mm pile wall thickness.
† MHU 600T (660 kJ energy) and MHU 1700S (1730 kJ energy) operating at a 30 strikes/minute.

3.2. Acoustic Source and Propagation Models

The following three steps comprise the general approach this study applies to modelling pile driving activities:

1. Piles driven into the sediment by impact driving are characterised as sound-radiating sources. This characterisation strongly depends on local properties such as pile dimensions, pile driving equipment, and rate and extent of pile penetration.

2. The theory of underwater sound propagation is applied to predict how sound propagates from the pile into the water column as a function of range, depth, and azimuthal direction. Propagation

depends on several conditions including the frequency content of the sound, the bathymetry, the sound speed in the water column, and sediment geoacoustics.

3. The propagated sound field is used to compute received levels over a grid of simulated receivers, from which distances to criteria thresholds and maps of ensonified areas can be generated.

This section describes the characterisation of the sound at the pile wall resulting from a single hammer strike. Details on sound propagation and computation of specific metrics are provided in the in the subsections of these Methods and in Appendix B.2.

To model sounds resulting from impact pile driving of cylindrical pipes, JASCO's Pile Driving Source Model (PDSM), a physical model of pile vibration and near-field sound radiation (MacGillivray 2014), was used in conjunction with the GRLWEAP 2010 wave equation model (GRLWEAP, Pile Dynamics 2010). Once the impact pile driver model and the pile dimensions were input into GRLWEAP, it was possible to compute the force at the top of the pile generated by the driver (Figure 2) and then input that into the PDSM.
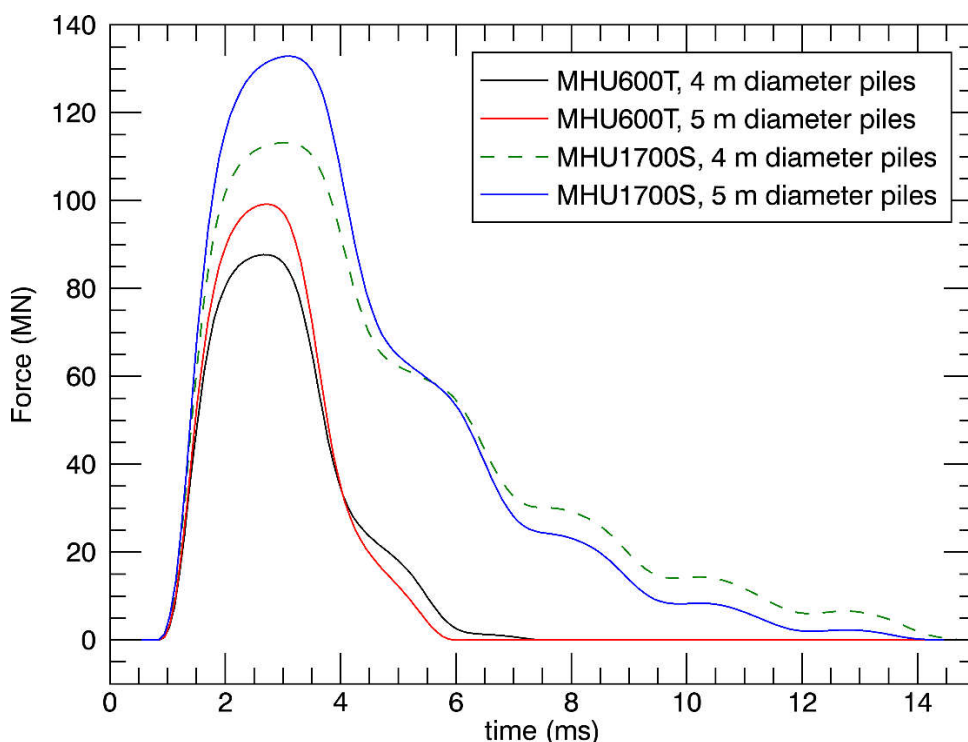
Figure 2. Force at the top of the pile corresponding to impact pile driving of 4 m and 5 m diameter piles, computed using the GRLWEAP 2010 wave equation model for the MHU 600T and the MHU 1700S hammers.

Forcing functions (Figure 2) were input to the PDSM to obtain equivalent pile driving signatures consisting of a vertical array of discrete point sources (Appendix B.1); these represent the pile as an acoustic source and accounted for several parameters that determined the operation: pile type, material, size, and length; the pile driving equipment; and approximate pile penetration rate. The amplitude and phase of the point sources along the array were computed so that they collectively mimicked the time-frequency characteristics of the acoustic wave at the pile wall that results from a hammer strike at the top of the pile. This approach accurately estimates spectral levels within the band 10–800 Hz where most of the energy from impact pile driving is concentrated.

JASCO's Marine Operations Noise Model (MONM; Appendix B.2.2) computes received per-pulse (in this case, per-strike) SEL for directional impulsive sources at a specified source depth. It is a far-field transmission loss model, which assumes that the separation between the source and receiver is sufficiently large that the physical dimensions of the source can be neglected. JASCO's time-domain Full Waveform Range-dependent model (FWRAM; Appendix B.2.3) on the other hand calculates sound propagation from physically distributed sources such as those obtained from PDSM. FWRAM, while valid at all distances, becomes computationally inefficient at long ranges. For this reason, received sound levels were calculated using FWRAM only along a few radials, and transmission loss

was calculated using MONM on a long-range three-dimensional grid. A far-field point source representation of the acoustic PDSM signature from the pile was then determined by back-propagating the received sound levels generated with FWRAM using the transmission loss calculated with MONM. This point source representation accurately characterises the vertical directivity of the pile-driving signature, with the advantage that it can be applied to MONM for computationally efficient long-range modelling.

In the present study, FWRAM was applied along three 20 km long radials with azimuths 0^0, 90^0, and 180^0 centred at both pile locations. This allowed us to examine the effect of predominantly downward, flat, and upward bathymetries on source levels. Back propagation using MONM transmission loss resulted in three equivalent monopole sources per scenario. The final 1/3-octave-band levels for each scenario (Figure 3) were obtained by taking the maximum SEL at each band, which resulted in the most conservative choice. Source levels above 800 Hz were obtained by extrapolation, following the decay trend observed in the modelled 1/3-ocatave-bands from 200 Hz to 800 Hz. Source levels were similar for scenarios that differed only on the site (i.e., Scenarios 1, 2, 3, 4, and 9 compared to 5, 6, 7, 8, and 10, respectively).
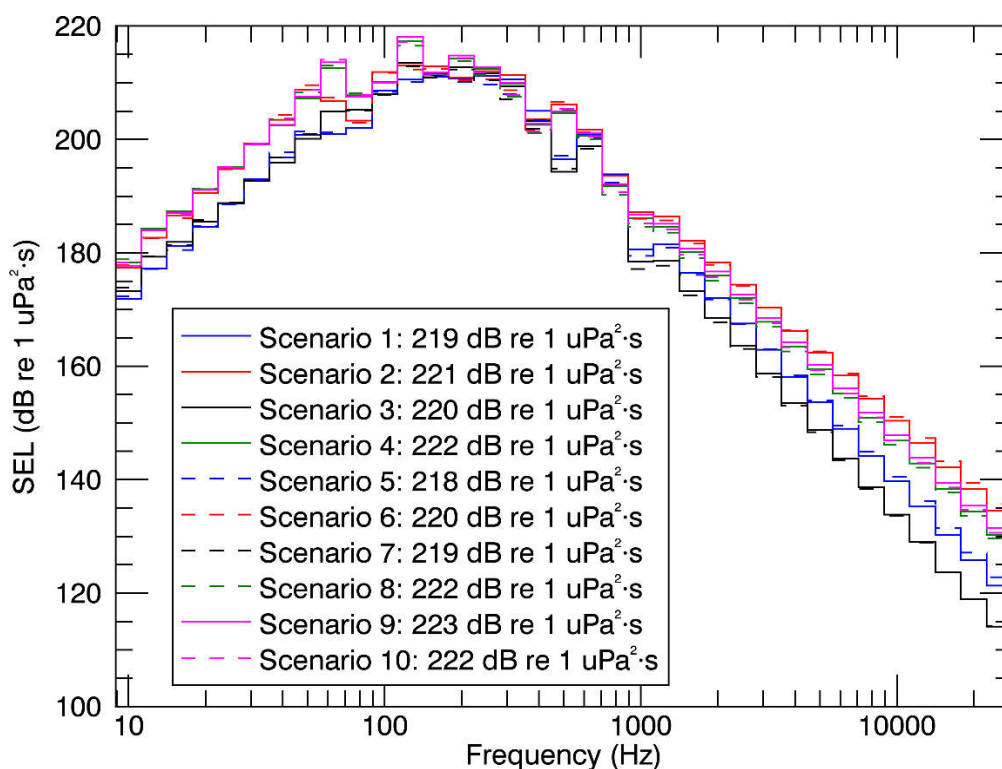
Figure 3. 1/3-octave-band and broadband sound exposure source level for impact pile driving that correspond to the modelling scenarios in Table 4.

3.3. Accumulated SEL

The modelling approach outlined in Section 3.1 provides per-strike SEL. At this early stage of project definition, information on soil resistance as a function of pile depth was not available at the time of this report. The source level of the pile driving was calculated based on the assumption that the pile was at its final penetration into the sediment, with maximum soil resistance and hammer energy. The sound speed profile (Section 3.6.3) will cause transmission loss to vary only slightly with increasing depth, and therefore changes in source depth will not influence the result.

The total number of strikes required to install a pile for each scenario (Table 4) was used in this report to obtain SEL over the period of installation, referred to in this report as SEL_{24h} as only one pile was predicted to be driven per day, by applying Equation 1:

$$SEL = \text{per-strike SEL} + 10\log_{10}N_{24h} \qquad (1)$$

where N_{24h} represents the total number of hammer blows for impact pile driving.

3.4. Estimating SPL from Modelled SEL Results

The per-strike SEL of sound pulses is an energy-like metric related to the dose of sound received over the pulse's entire duration. The pulse SPL on the other hand is related to its intensity over a specified time interval. The time interval often applied to assess seismic pulses is the 90% time window (T_{90}) (Appendix A). Pile driving pulses typically lengthen in duration as they propagate away from their source, due to seafloor and sea surface reflections, as well as other waveguide dispersion effects. The changes in pulse length, and therefore T_{90}, affect the numeric relationship between SPL and SEL. Full-waveform modelling is often used to estimate T_{90}, but this type of modelling is computationally intensive, and can be prohibitively time consuming when run at high spatial resolution over large areas.

For the current study, the Full Waveform Range-dependent Acoustic Model (FWRAM; Appendix B.2.3) was used to model pile driving pulses over the frequency range 10–1024 Hz. This was performed for each scenario at three radials along predominantly downward, flat, and upward bathymetry. FWRAM uses Fourier synthesis to recreate the signal in the time domain so that both the SEL and SPL resulting from the source can be calculated. The difference between the SEL and SPL was extracted for all radials, ranges and depths. A 125 millisecond fixed time window positioned to maximise the SPL over the pulse duration was applied. The resulting SEL-to-SPL offsets were averaged in 2.0 km range bins along each modelled radial and depth, and the 90th percentile was selected at each range in order to generate a range-dependent conversion function for each scenario. Due to the similarity of the conversion factor among all scenarios (Figure 4), a single generalised conversion factor was obtained as the mean value per range among all scenarios, and was applied to predicted per-strike SEL results from MONM to model SPL values.
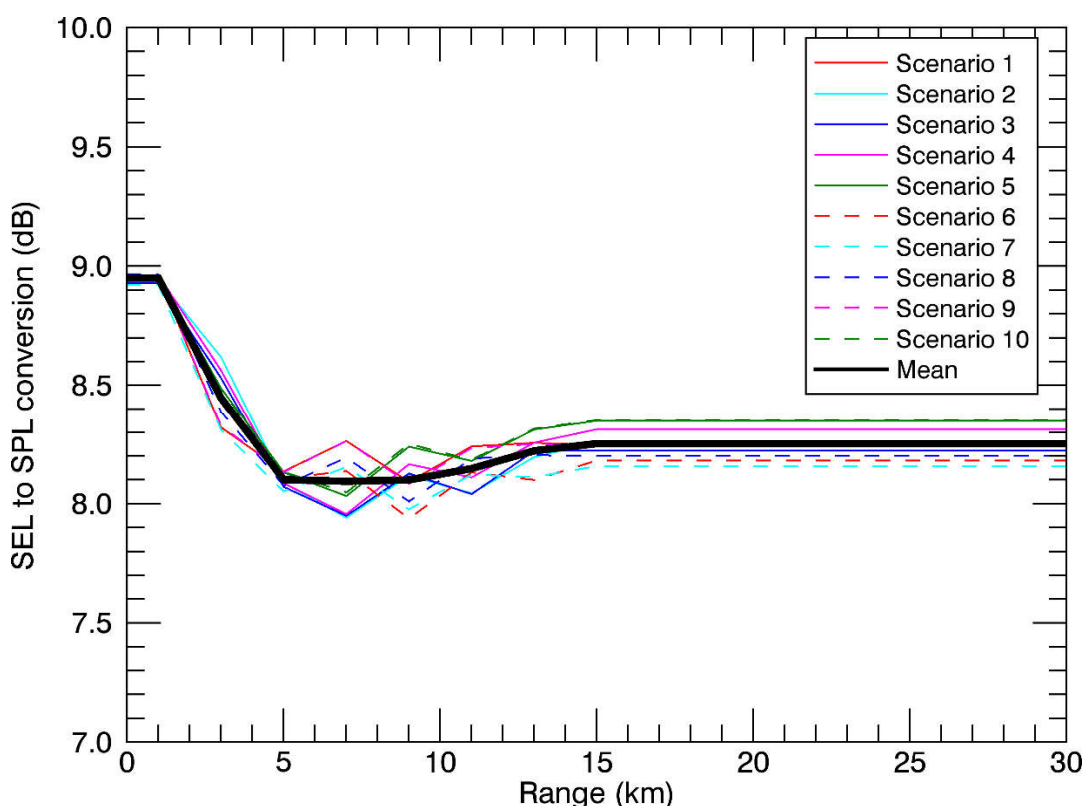
Figure 4. Range-dependent conversion function for converting SEL to SPL for pile driving pulses. Due to the similarity between the conversion factor for each scenario, modelling was conducted using a mean conversion function.

3.5. Estimating Ranges to Threshold Levels

Sound level contours were calculated based on the underwater sound fields predicted by the propagation models, sampled by taking the maximum value over all modelled depths above the sea floor for each location in the modelled region. The predicted distances to specific levels were computed from these contours. Two distances relative to the source are reported for each sound level: 1) R_{max}, the maximum range to the given sound level over all azimuths, and 2) $R_{95\%}$, the range to the given sound level after the 5% farthest points were excluded (see examples in Figure 5).

The $R_{95\%}$ is used because sound field footprints are often irregularly shaped. In some cases, a sound level contour might have small protrusions or anomalous isolated fringes (Figure 5a). In such cases, where relatively few points are excluded in any given direction, R_{max} can misrepresent the area of the region exposed to such effects, and $R_{95\%}$ is considered more representative. On the other hand, in strongly asymmetric cases (Figure 5b), $R_{95\%}$ does not account for significant protrusions in the footprint. In such cases R_{max} might better represent the region of effect in specific directions. These situations are usually associated with bathymetric features that affect propagation. The difference between R_{max} and $R_{95\%}$ depends on the source directivity and how uniform the acoustic environment is.

(a)   (b)
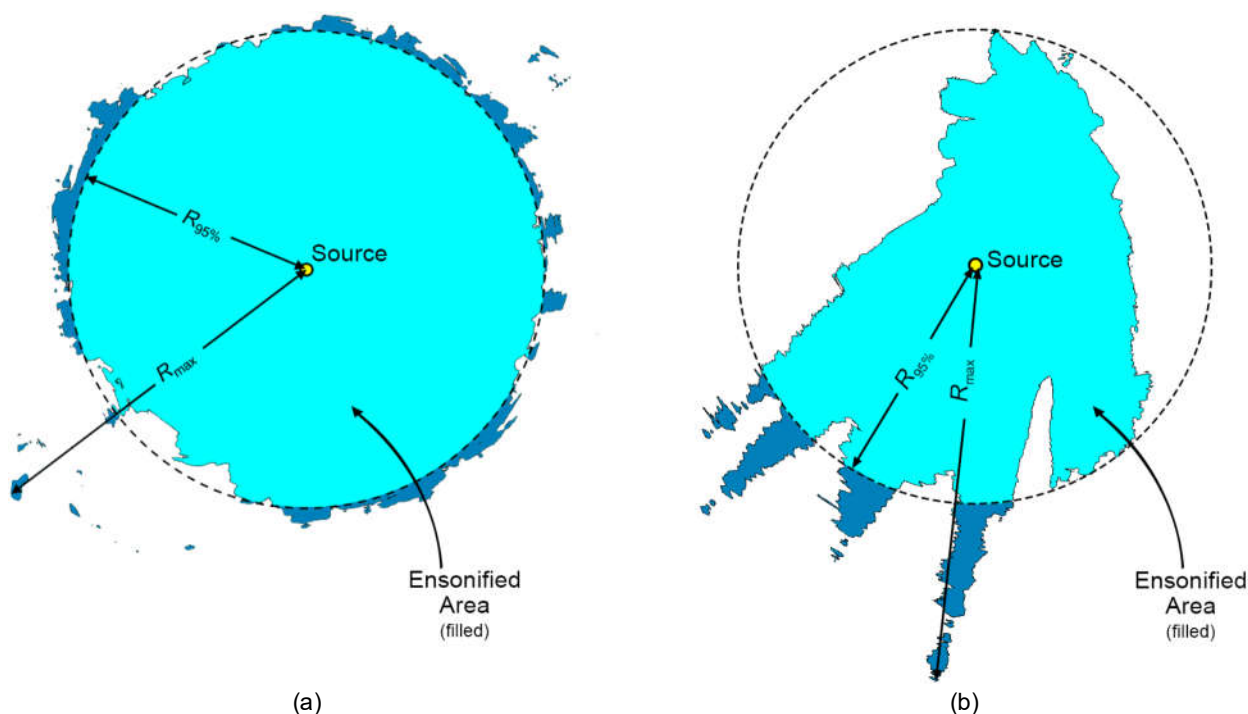
Figure 5. Sample areas ensonified to an arbitrary sound level with R_{max} and $R_{95\%}$ ranges shown for two different scenarios. (a) Largely symmetric sound level contour with small protrusions. (b) Strongly asymmetric sound level contour with long protrusions. Light blue indicates the ensonified areas bounded by $R_{95\%}$; darker blue indicates the areas outside this boundary which determine R_{max}.

3.6. Environmental Parameters

3.6.1. Bathymetry

ConocoPhillips provided accurate bathymetry data for the Barossa field and the surrounding area with a regular grid spacing of 500 × 500 m. This dataset has been supplemented by bathymetry data extracted from a 250 × 250 m resolution grid of Australian waters (Whiteway 2009). For the modelling, bathymetry data for a region of 280 × 280 km, encompassing a 100 km buffer zone around the potential piling locations, were extracted and re-gridded with a regular spacing of 250 × 250 m. The resulting bathymetry contour map and the extent of the modelling regions at Site 1 and Site 2 are shown in Figure 6.
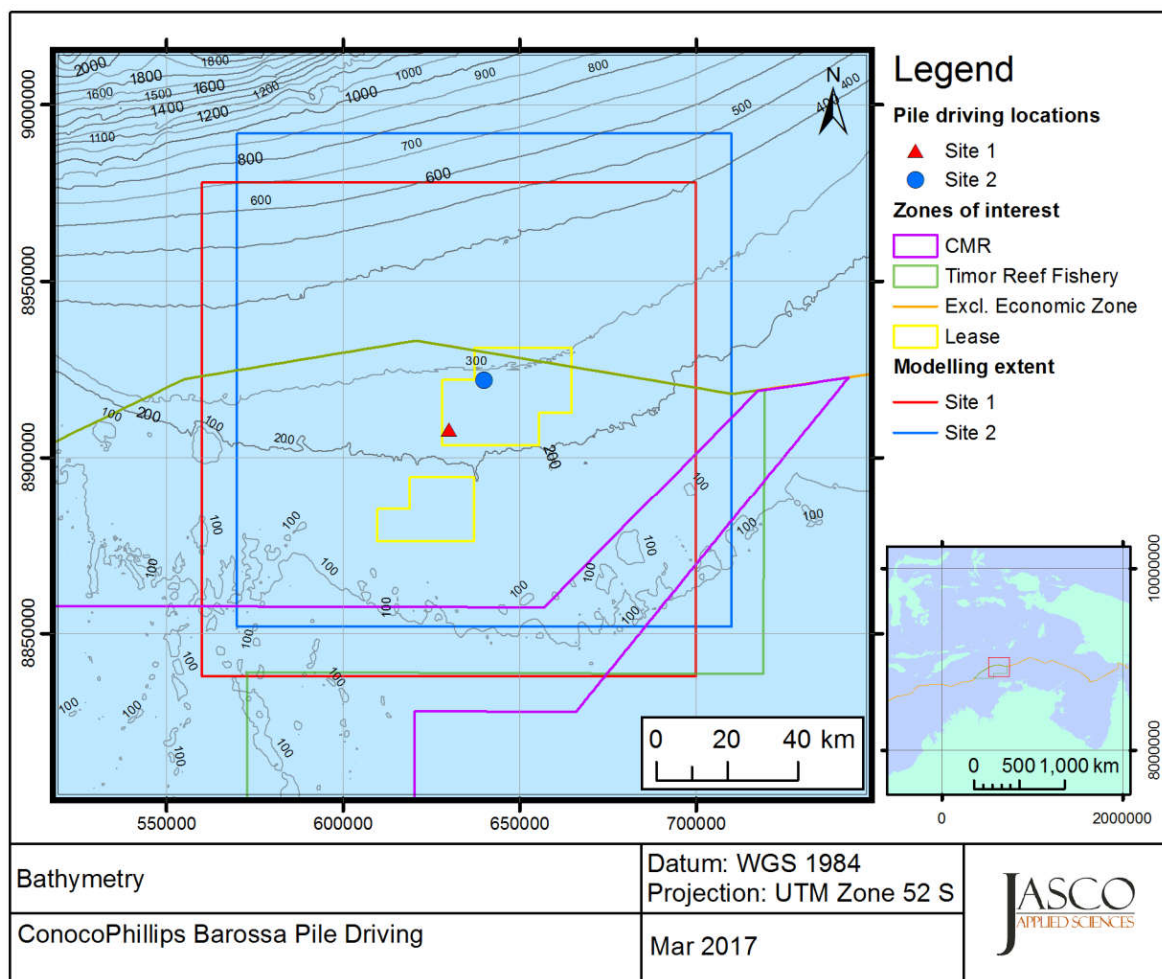
Figure 6. The bathymetry used for the modelling. The edge of the contour area indicates the extent of the modelling grids sampled at a 250 × 250 m resolution.

3.6.2. Geoacoustics

Geotechnical data were obtained from the ARUP report (Lane 2015), supplied by ConocoPhillips to JASCO, and a single geoacoustic profile representing the top sediment layer was created from that analysis. The sediment thickness in the region is over 1,200 m according to the World Ocean Atlas (Whittaker et al. 2013) and therefore this report assumes that the sediment is composed of similar grain types beyond 35 m depths. The parameters derived were based on empirical relationships from Buckingham (2005). The geoacoustic profile used in the modelling is shown in Table 5.

Table 5. Estimated geoacoustic profile used in the modelling. Within each depth range, each parameter varies linearly within the stated range.

Depth below seafloor (m)	Material	Density (g/cm³)	P-wave speed (m/s)	P-wave attenuation (dB/λ)	S-wave speed (m/s)	S-wave attenuation (dB/λ)
0–9	Coarse Sand	2.09	1655.3–2133.8	0.76–1.46		
9–35	Clay	1.46	1539.8–1582.9	0.33–0.51	322.7	0.246
35–500	Medium Sand	2.08	2275.2–3453.2	1.73–2.82		

3.6.3. Sound speed profile

The sound speed profiles (SSPs) for the modelled sites were provided to JASCO by ConocoPhillips. The profiles were principally derived from monthly measurements of temperature and salinity profiles over an entire year. The data were from two sites and included sample depths from 33 m to the seafloor. Data from the US Naval Oceanographic Office's *Generalized Digital Environmental Model V 3.0* (GDEM; Teague et al. 1990, Carnes 2009) supplemented those profiles. GDEM provides an ocean climatology of temperature and salinity for the world's oceans on a latitude-longitude grid with 0.25° resolution, with a temporal resolution of one month, based on global historical observations from the US Navy's Master Oceanographic Observational Data Set (MOODS). The temperature-salinity profiles were converted to sound speed profiles according to Coppens (1981).

For each monthly profile, the supplied data were extrapolated to provide results to the water surface based on the gradients of the profile from the GDEM data. The average of the SSPs taken across all months provides a representative SSP for the area across the year (Figure 7).

The resulting SSP represents a mixed isothermal surface layer with a slight upward-refracting profile. Below 80 m depth the profile is driven by lower temperatures, which produce a steep downward-refracting profile. For depths within the modelling extent, no sound channel is realised in deeper waters.
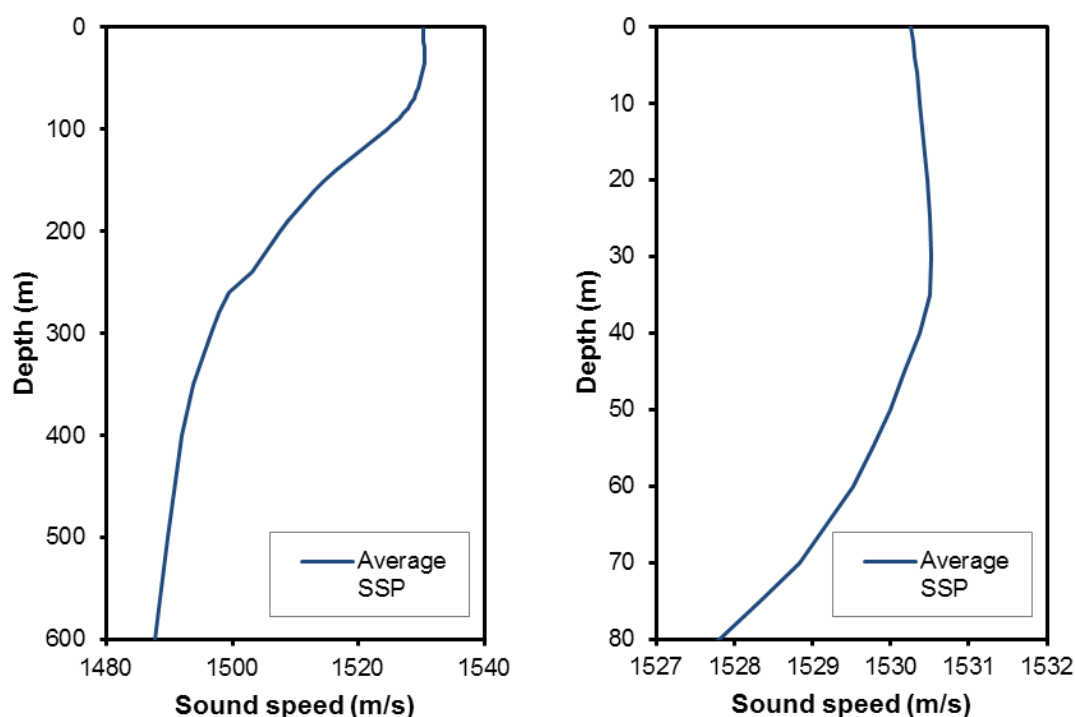
Figure 7. Sound speed profile used for the modelling (a) the average of all monthly profiles, (b) detail of the top 80 m of the SSP.

3.7. Geometry and Modelled Regions

The sound field from pile driving pulses at the two sites shown in Figure 1 were modelled using MONM in the frequency range 10 Hz–25 kHz (Appendix B.2.2) up to distances of 70 km from the source, with a horizontal separation of 20 m between receiver points along the modelled radials. Sound fields were modelled with a horizontal angular resolution of $\Delta\theta = 2.5°$ for a total of N = 144 radial planes. To provide greater fidelity close to the source positions, additional model runs were carried out over an area of 1 × 1 km with a horizontal separation of 5 m between receiver points, with the same horizontal angular resolution. In both cases, receiver depths were chosen to span the entire water column over the modelled areas, from 1 m to a maximum of 2500 m, with step sizes that

increased with depth. At depths closer to the pile, receivers were 2 m apart over the entire length of the pile.

FWRAM (Appendix B.2.3) was run in the frequency range 10–1024 Hz, a bandwidth wide enough to include most of the energy typically generated by impact pile driving (Figure 3). 20 km radials with 5 m step size (only 3 per site for computational efficiency) were simulated to obtain equivalent 1/3-octave-band levels for input to MONM, the SEL-to-SPL offsets (Section 3.2), and to estimate radii to peak criteria thresholds.

4. Modelling Results

The modelling scenarios are grouped per modelling site, with the order of pile size and hammer applied the same for both sites (Table 4). Scenarios 9 and 10, although considering a different soil resistance to all other scenarios are grouped in association with their location in the tabulated results presented in Section 4.1. The results presented for each scenario can be compared to examine the effect on noise footprints of hammer size and pile dimensions at either possible location (site), the influence of bathymetry and depth between the two sites for similar scenarios, and the effect of different soil resistance for the same pile and hammer inputs at both modelling sites.

To assist with the comparison of the results for different hammer sizes, pile dimensions and soil resistance across the same bathymetric environment, maps and graphical representations of the sound fields at Site 1, Scenarios 1–4 and 9, are included in Section 4.2. Site 1 is the premise case for the indicative FPSO facility location and is also the site closest to the Oceanic Shoals CMR, and most central to the Timor Reef Fishery area. Representations for Site 2, Scenarios 5–8 and 10, are included in Appendix C.

4.1. Tables

Table 6 shows the estimated ranges to unweighted per-strike SEL isopleths. Tables 7–11 show the estimated ranges for the various applicable effects criteria (Section 2).

Table 6. Horizontal distances (in km) modelled maximum-over-depth unweighted per-strike SEL isopleths.

Isopleth SEL (dB re 1 µPa²·s)	Distance (km)																			
	Site 1										Site 2									
	Scenario 1		Scenario 2		Scenario 3		Scenario 4		Scenario 9		Scenario 5		Scenario 6		Scenario 7		Scenario 8		Scenario 10	
	R_{max}	$R_{95\%}$	R_{max}	$R_{95\%}$	R_{max}	$R_{95\%}$	R_{max}	$R_{95\%}$	R_{max}	$R_{95\%}$	R_{max}	$R_{95\%}$	R_{max}	$R_{95\%}$	R_{max}	$R_{95\%}$	R_{max}	$R_{95\%}$	R_{max}	$R_{95\%}$
185	0.07	0.07	0.07	0.07	0.07	0.07	0.11	0.11	0.07	0.07	0.07	0.07	0.07	0.07	0.11	0.11	0.07	0.07	0.07	0.07
180	0.14	0.14	0.14	0.14	0.14	0.14	0.22	0.22	0.11	0.11	0.14	0.14	0.14	0.14	0.22	0.22	0.14	0.14	0.14	0.14
170	0.61	0.59	0.81	0.78	0.71	0.70	1.08	1.03	0.54	0.51	0.71	0.66	0.61	0.60	0.89	0.85	0.61	0.59	0.81	0.78
160	5.92	5.48	6.42	6.00	6.07	5.66	8.99	8.16	4.39	3.92	7.24	6.72	4.92	4.40	7.81	7.34	5.92	5.48	6.42	6.00
150	20.27	17.12	23.80	20.83	23.45	18.99	30.86	24.28	21.09	17.72	27.39	21.74	23.56	19.45	31.94	25.76	20.27	17.12	23.80	20.83

Table 7. Maximum (R_{max}) and 95% ($R_{95\%}$) horizontal distances (in km) to modelled maximum-over-depth M-weighted 24 h SEL permanent hearing threshold shift (PTS) thresholds for marine mammals (Wood et al. 2012).

Threshold (SEL$_{24h}$)	Distance (km)																			
	Site 1												Site 2							
	Scenario 1		Scenario 2		Scenario 3		Scenario 4		Scenario 9		Scenario 5		Scenario 6		Scenario 7		Scenario 8		Scenario 10	
	R_{max}	$R_{95\%}$	R_{max}	$R_{95\%}$	R_{max}	$R_{95\%}$	R_{max}	$R_{95\%}$	R_{max}	$R_{95\%}$	R_{max}	$R_{95\%}$	R_{max}	$R_{95\%}$	R_{max}	$R_{95\%}$	R_{max}	$R_{95\%}$	R_{max}	$R_{95\%}$
Low-frequency cetaceans (192 dB re 1 µPa²·s)	5.98	5.60	3.09	2.94	6.07	5.66	3.26	3.10	3.20	3.05	4.88	4.31	2.04	1.85	4.92	4.37	3.34	3.20	2.57	2.03
Mid-frequency cetaceans (198 dB re 1 µPa²·s)	0.79	0.69	0.32	0.31	0.76	0.63	0.32	0.31	0.30	0.28	0.52	0.50	0.27	0.26	0.54	0.51	0.27	0.27	0.26	0.25
High-frequency cetaceans (179 dB re 1 µPa²·s)	16.59	14.05	8.86	7.60	15.39	13.17	8.27	7.48	7.95	6.37	18.75	13.39	7.47	6.95	16.66	12.66	7.42	6.89	7.24	6.81

Table 8. Maximum (R_{max}) and 95% ($R_{95\%}$) horizontal distances (in km) to modelled maximum-over-depth DEWHA (2008) criterion and applied marine mammal and turtle behavioural response thresholds.

Threshold	Distance (km)																			
	Site 1												Site 2							
	Scenario 1		Scenario 2		Scenario 3		Scenario 4		Scenario 9		Scenario 5		Scenario 6		Scenario 7		Scenario 8		Scenario 10	
	R_{max}	$R_{95\%}$	R_{max}	$R_{95\%}$	R_{max}	$R_{95\%}$	R_{max}	$R_{95\%}$	R_{max}	$R_{95\%}$	R_{max}	$R_{95\%}$	R_{max}	$R_{95\%}$	R_{max}	$R_{95\%}$	R_{max}	$R_{95\%}$	R_{max}	$R_{95\%}$
DEWHA (2008), Unweighted SEL (160 dB re 1 µPa²·s)	5.92	5.48	6.42	6.00	6.07	5.66	8.99	8.16	9.68	8.59	4.39	3.92	7.24	6.72	4.92	4.40	7.81	7.34	9.80	7.52
NMFS (2013) Marine mammal behaviour, Unweighted SPL (160 dB re 1 µPa)	17.16	14.26	20.23	16.96	18.14	15.65	23.83	20.34	26.93	21.92	17.88	14.23	22.12	17.83	19.46	15.43	28.30	21.40	28.76	22.39
Turtle behaviour (NSF 2011), unweighted SPL (166 dB re 1 µPa)	7.53	6.18	9.90	8.62	8.84	7.90	12.04	10.19	13.82	11.09	7.29	6.87	9.58	7.49	7.54	6.99	14.25	10.47	14.41	10.99

JASCO APPLIED SCIENCES

Table 9. Maximum (R_{max}) and 95% ($R_{95\%}$) horizontal distances (in km) to modelled maximum-over-depth 24 h SEL mortality and potential mortal injury thresholds for fish, turtles, fish eggs, and fish larvae.

Threshold (SEL$_{24h}$)	Distance (km)																			
	Site 1										Site 2									
	Scenario 1		Scenario 2		Scenario 3		Scenario 4		Scenario 9		Scenario 5		Scenario 6		Scenario 7		Scenario 8		Scenario 10	
	R_{max}	$R_{95\%}$	R_{max}	$R_{95\%}$	R_{max}	$R_{95\%}$	R_{max}	$R_{95\%}$	R_{max}	$R_{95\%}$	R_{max}	$R_{95\%}$	R_{max}	$R_{95\%}$	R_{max}	$R_{95\%}$	R_{max}	$R_{95\%}$	R_{max}	$R_{95\%}$
Fish I: no swim bladder (219 dB re 1 µPa²·s)	0.08	0.08	0.05	0.05	0.08	0.08	0.05	0.05	0.05	0.05	0.07	0.07	0.04	0.04	0.07	0.07	0.05	0.05	0.05	0.04
Fish II: swim bladder involved in hearing (207 dB re 1 µPa²·s)	0.34	0.31	0.18	0.17	0.34	0.33	0.20	0.19	0.19	0.18	0.28	0.27	0.16	0.16	0.29	0.28	0.19	0.18	0.18	0.17
Fish III: swim bladder not involved in hearing (210 dB re 1 µPa²·s)																				
Turtles, fish eggs, and fish larvae (210 dB re 1 µPa²·s)	0.22	0.21	0.13	0.12	0.23	0.22	0.14	0.14	0.14	0.13	0.20	0.19	0.12	0.11	0.20	0.20	0.13	0.13	0.12	0.12

Table 10. Maximum (R_{max}) and 95% ($R_{95\%}$) horizontal distances (in km) to modelled maximum-over-depth 24 h SEL recoverable injury and temporary (hearing) threshold shift (TTS) thresholds for fish.

Threshold (SEL$_{24h}$)	Distance (km)																			
	Site 1										Site 2									
	Scenario 1		Scenario 2		Scenario 3		Scenario 4		Scenario 9		Scenario 5		Scenario 6		Scenario 7		Scenario 8		Scenario 10	
	R_{max}	$R_{95\%}$	R_{max}	$R_{95\%}$	R_{max}	$R_{95\%}$	R_{max}	$R_{95\%}$	R_{max}	$R_{95\%}$	R_{max}	$R_{95\%}$	R_{max}	$R_{95\%}$	R_{max}	$R_{95\%}$	R_{max}	$R_{95\%}$	R_{max}	$R_{95\%}$
Fish I: no swim bladder (216 dB re 1 µPa^2·s)	0.11	0.10	0.07	0.06	0.11	0.11	0.07	0.07	0.07	0.07	0.10	0.09	0.06	0.06	0.10	0.10	0.07	0.07	0.06	0.06
Fish II: swim bladder involved in hearing (203 dB re 1 µPa^2·s)																				
Fish III: swim bladder not involved in hearing (203 dB re 1 µPa^2·s)	0.67	0.59	0.30	0.29	0.67	0.59	0.35	0.34	0.34	0.31	0.50	0.48	0.27	0.26	0.53	0.50	0.29	0.28	0.28	0.27
Fish I, II, III TTS (186 dB re 1 µPa^2·s)	14.04	11.79	7.38	6.18	14.81	11.85	8.89	7.97	8.36	6.49	13.93	11.07	7.32	6.90	14.65	11.64	7.79	7.13	7.53	6.86

Table 11. Maximum (R_{max}) horizontal distances (in km) to modelled maximum-over-depth peak mortality and potential mortal recoverable injury thresholds for fish, turtles, fish eggs, and fish larvae.

Threshold (PK)	Distance (km)									
	Site 1					Site 2				
	Scenario 1	Scenario 2	Scenario 3	Scenario 4	Scenario 5	Scenario 6	Scenario 7	Scenario 8	Scenario 9	Scenario 10
	R_{max}	R_{max}	R_{max}	R_{max}	R_{max}	R_{max}	R_{max}	R_{max}	R_{max}	R_{max}
Fish I: no swim bladder (> 213 dB re 1 µPa)	0.08	0.10	0.09	0.10	0.08	0.09	0.09	0.10	0.10	0.10
Fish II: swim bladder not involved in hearing (> 207 dB re 1 µPa)										
Fish III: swim bladder involved in hearing (> 207 dB re 1 µPa)	0.16	0.20	0.15	0.19	0.16	0.20	0.15	0.19	0.19	0.19
Turtles (> 207 dB re 1 µPa)										
Fish eggs and fish larvae (> 207 dB re 1 µPa)										

4.2. Maps and Graphs

Plots of the estimated sound field and threshold contours in the horizontal plane (maps) are shown for Site 1, Scenarios 1–4 and 9. Representations for Site 2, Scenarios 5–8 and 10, are included in Appendix C.

Maps were created to display the unweighted 24 h SEL footprints with the M-weighted 24 h PTS thresholds for marine mammals (Figures 8–12), the unweighted 24 h SEL footprints with the thresholds for fish, turtles, fish eggs, and fish larvae (Figures 13–17), and SPL footprints with thresholds for marine mammals and turtles (Figures 18–22). Graphs of unweighted SEL in the vertical plane for each of the scenarios are shown in Figures 23–27.
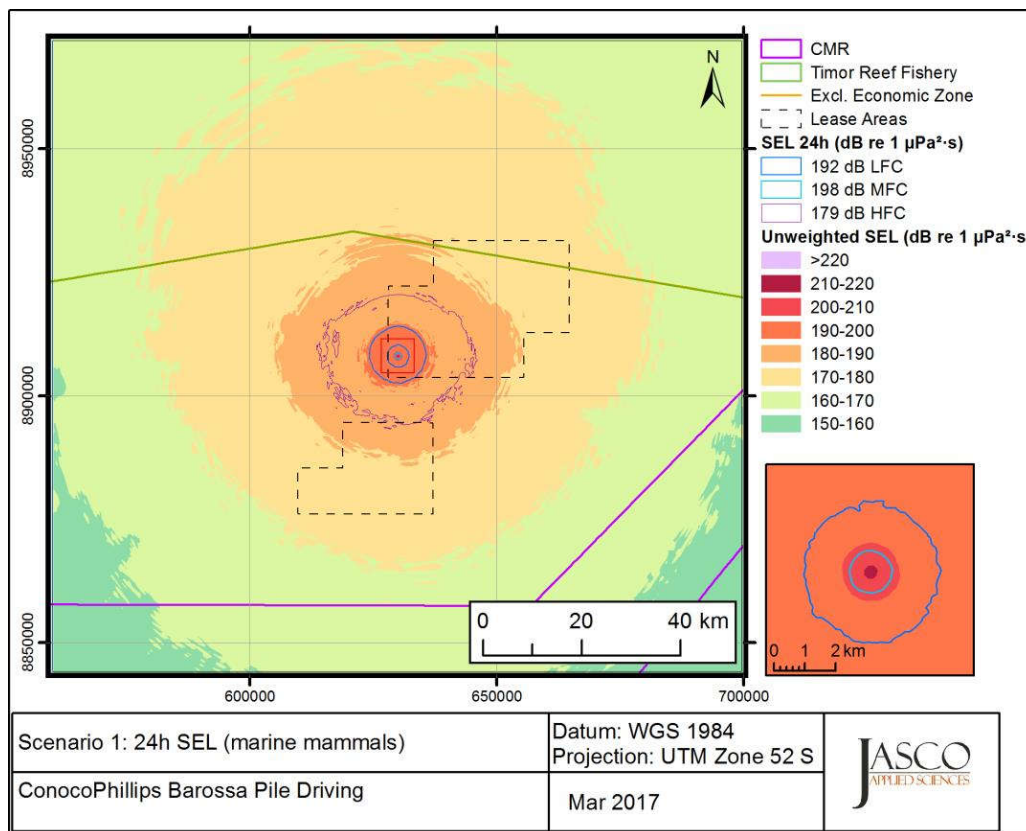
Figure 8. Scenario 1: Sound level contour map showing maximum-over-depth SEL$_{24h}$ results with marine mammal PTS thresholds.
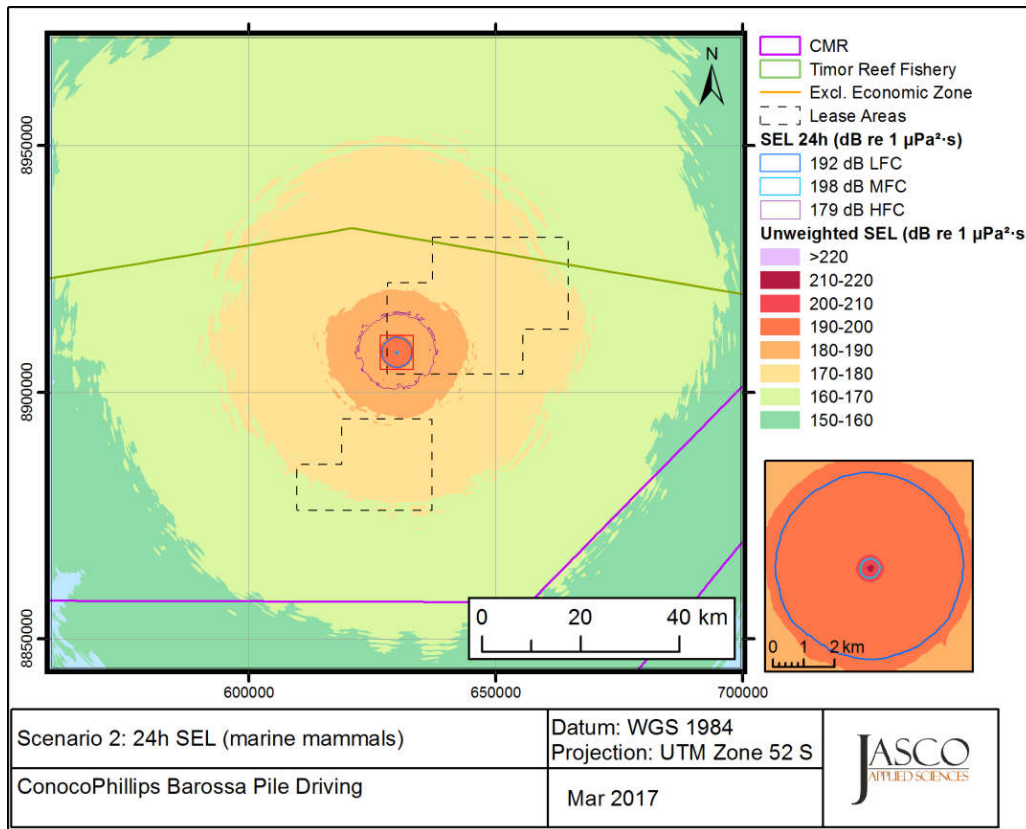
Figure 9. Scenario 2: Sound level contour map showing maximum-over-depth SEL$_{24h}$ results with marine mammal PTS thresholds.
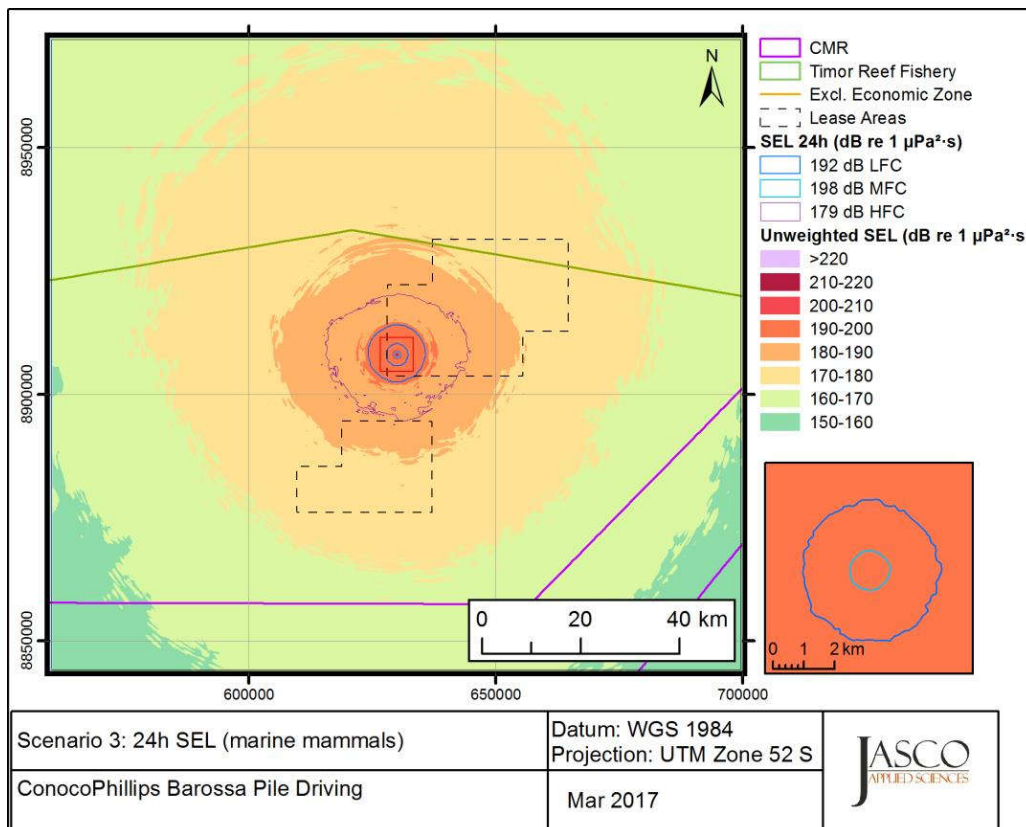
Figure 10. Scenario 3: Sound level contour map showing maximum-over-depth SEL$_{24h}$ results with marine mammal PTS thresholds.
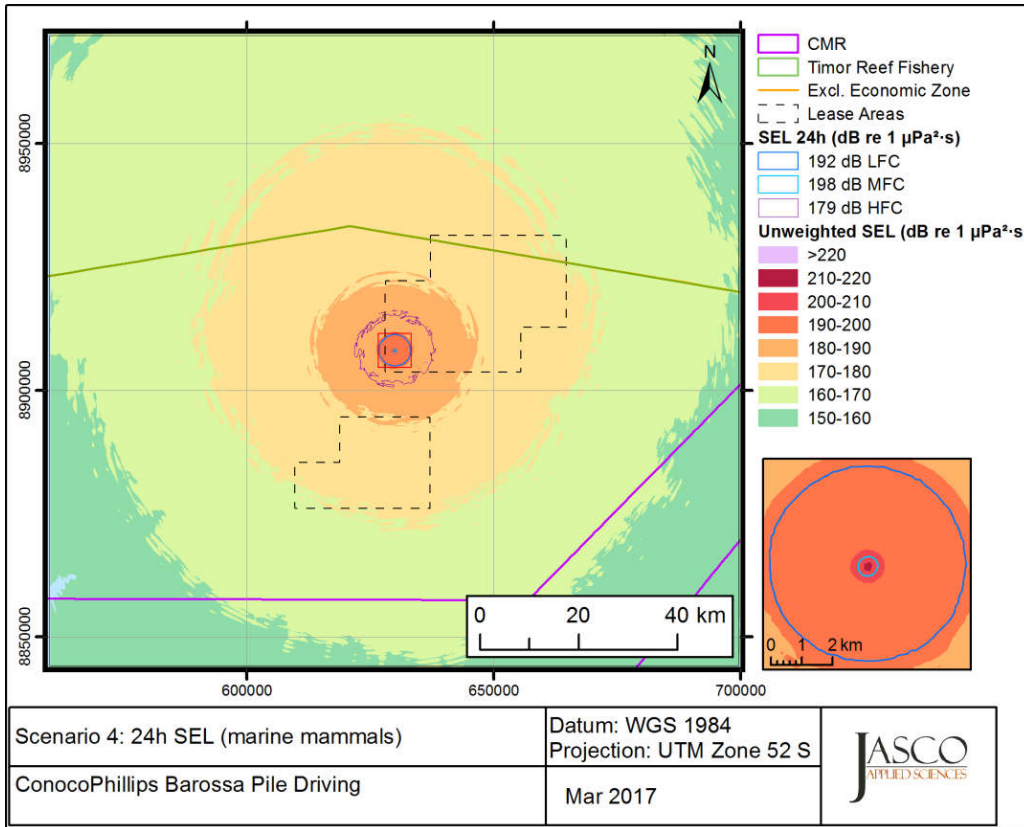
Figure 11. Scenario 4: Sound level contour map showing maximum-over-depth SEL$_{24h}$ results with marine mammal PTS thresholds.
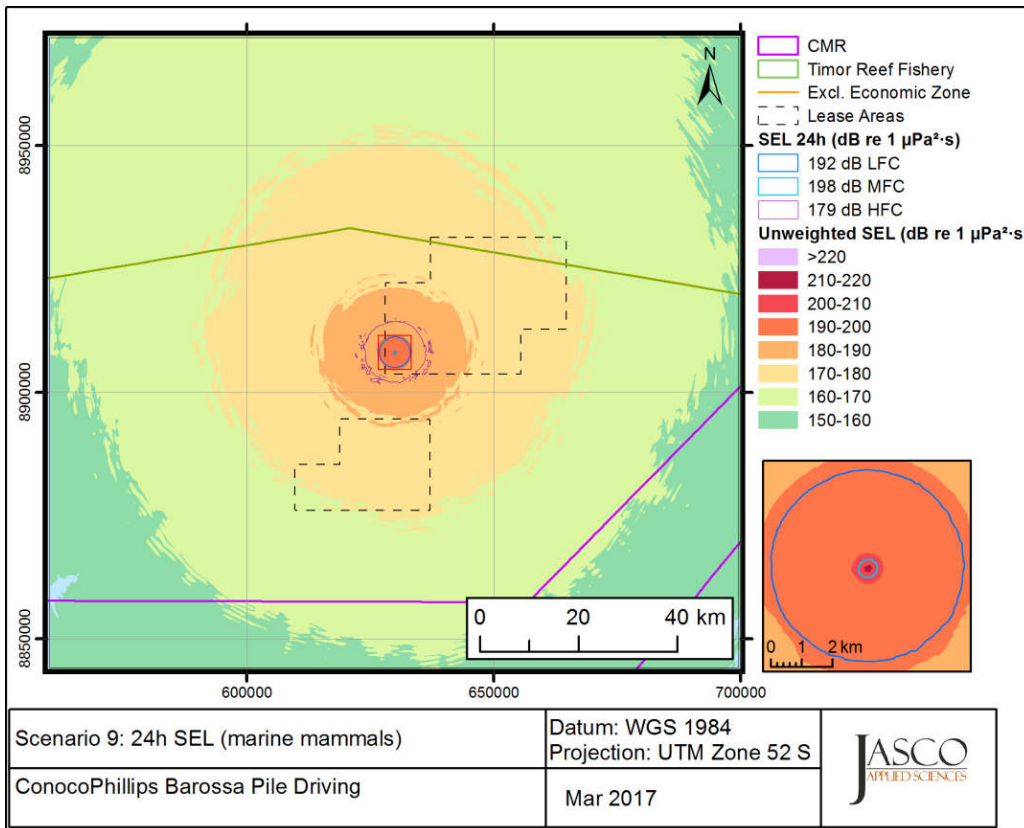
Figure 12. Scenario 9: Sound level contour map showing maximum-over-depth SEL$_{24h}$ results with marine mammal PTS thresholds.
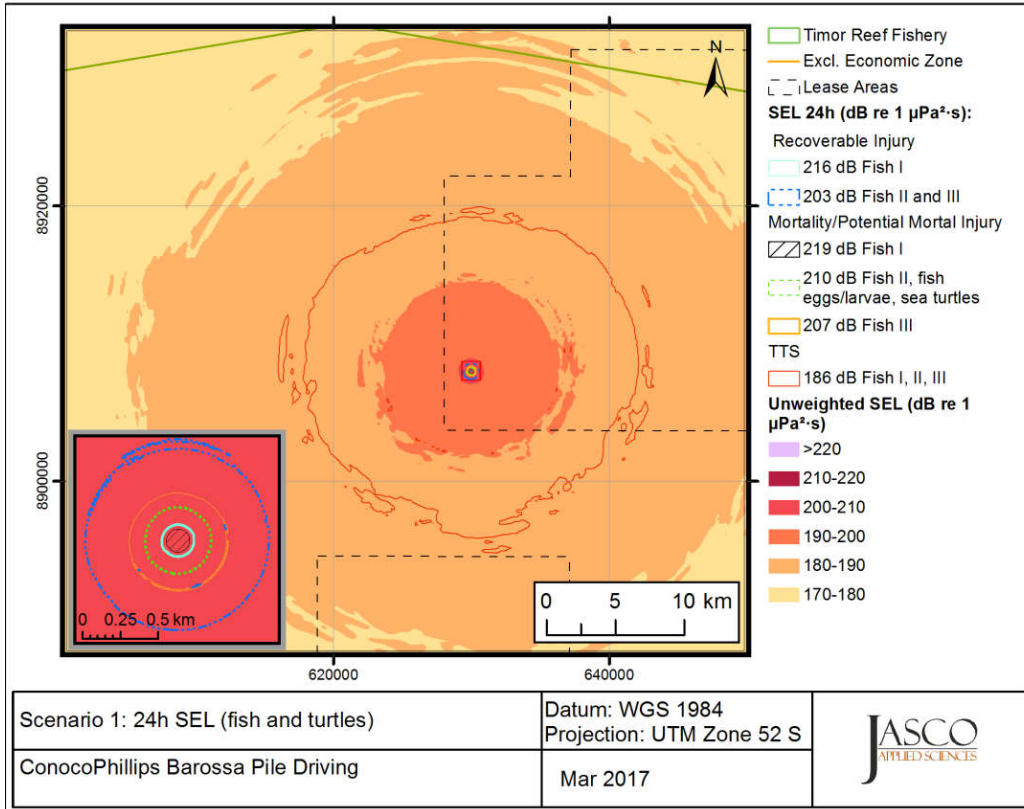
Figure 13. Scenario 1: Sound level contour map showing maximum-over-depth SEL$_{24h}$ results with fish and turtle thresholds.
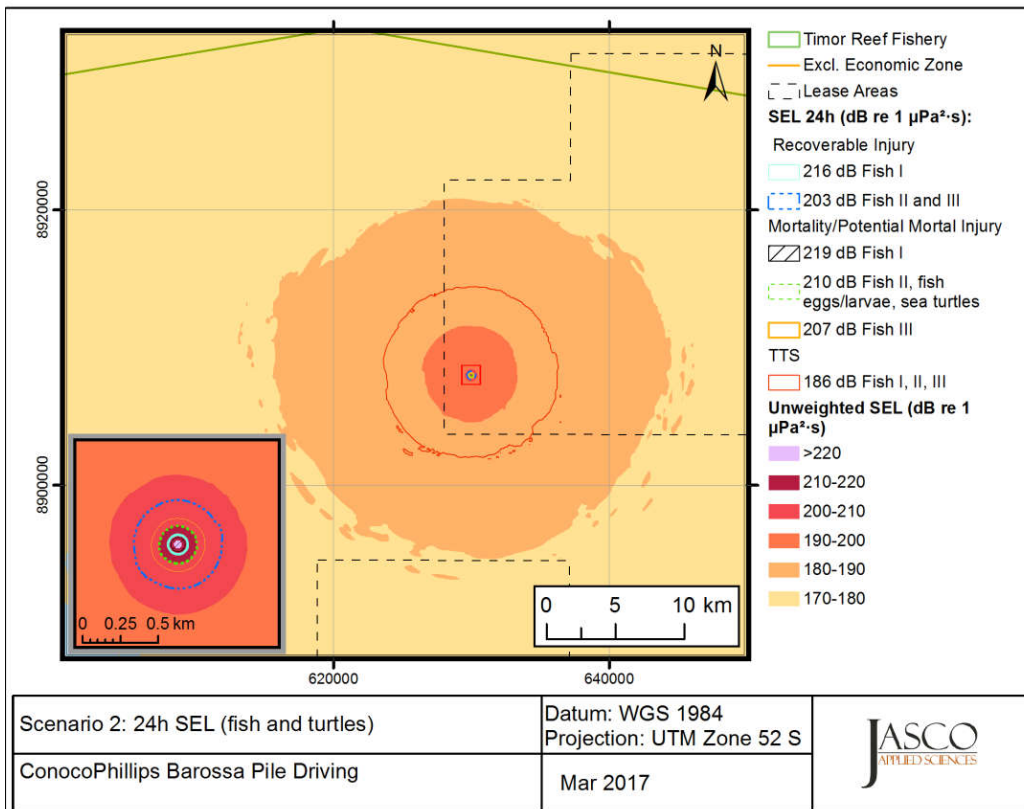
Figure 14. Scenario 2: Sound level contour map showing maximum-over-depth SEL$_{24h}$ results with fish and turtle thresholds.
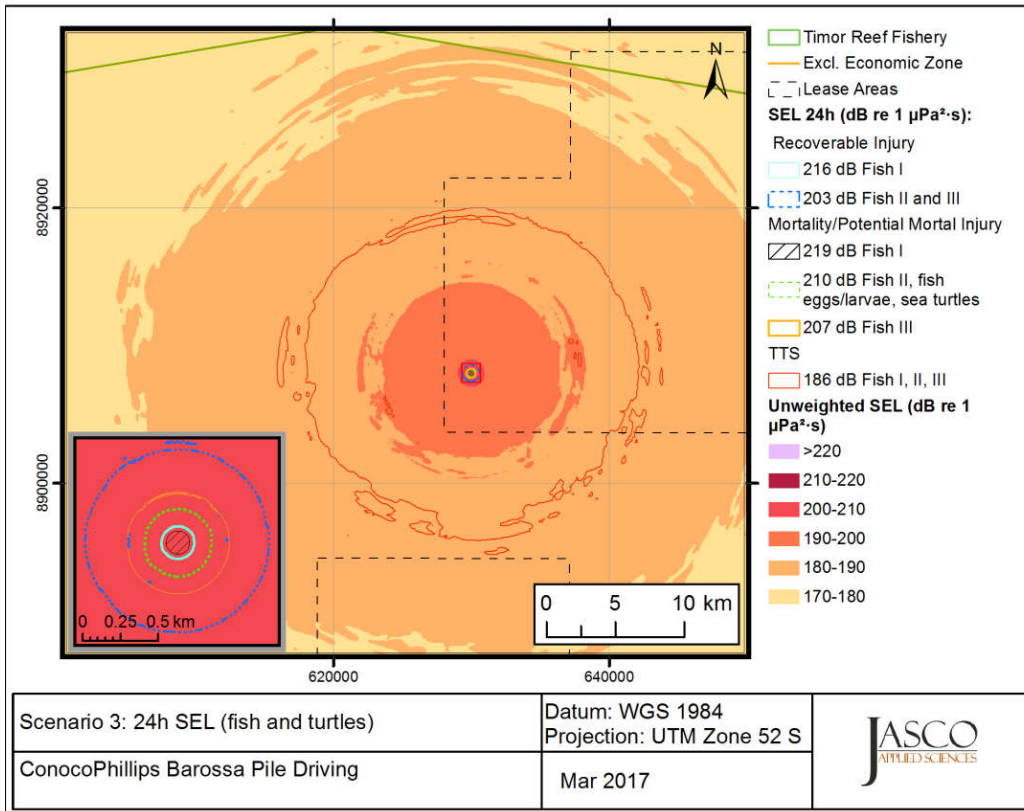
Figure 15. Scenario 3: Sound level contour map showing maximum-over-depth SEL$_{24h}$ results with fish and turtle thresholds.
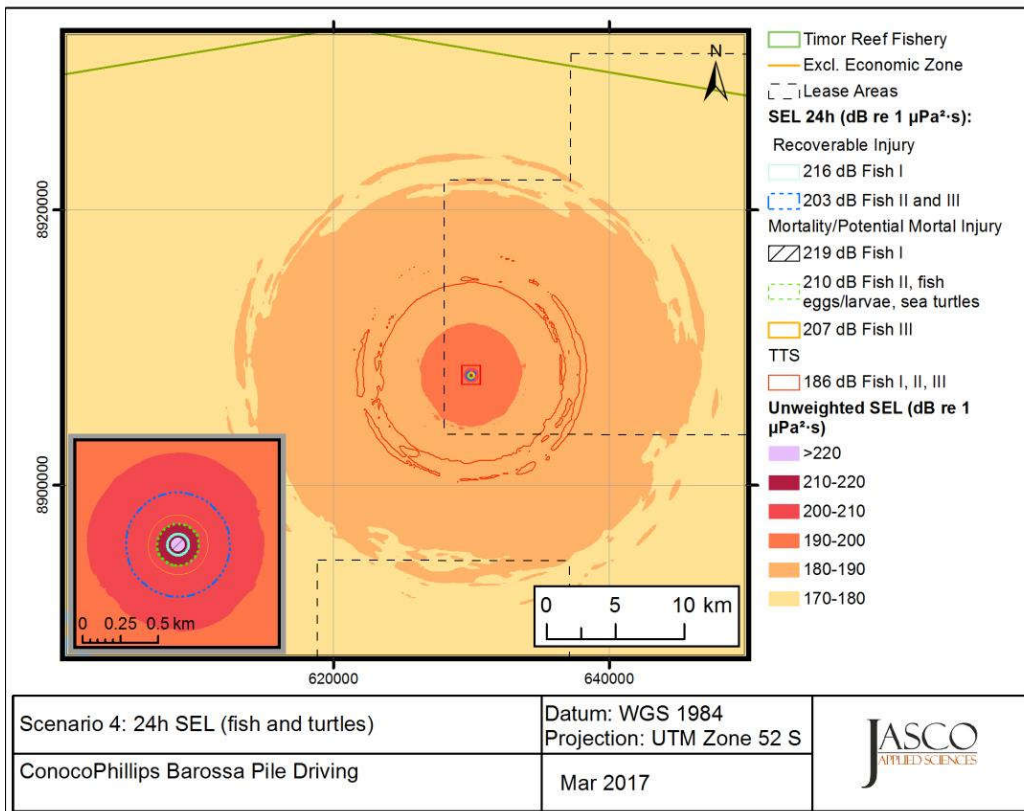
Figure 16. Scenario 4: Sound level contour map showing maximum-over-depth SEL$_{24h}$ results with fish and turtle thresholds.
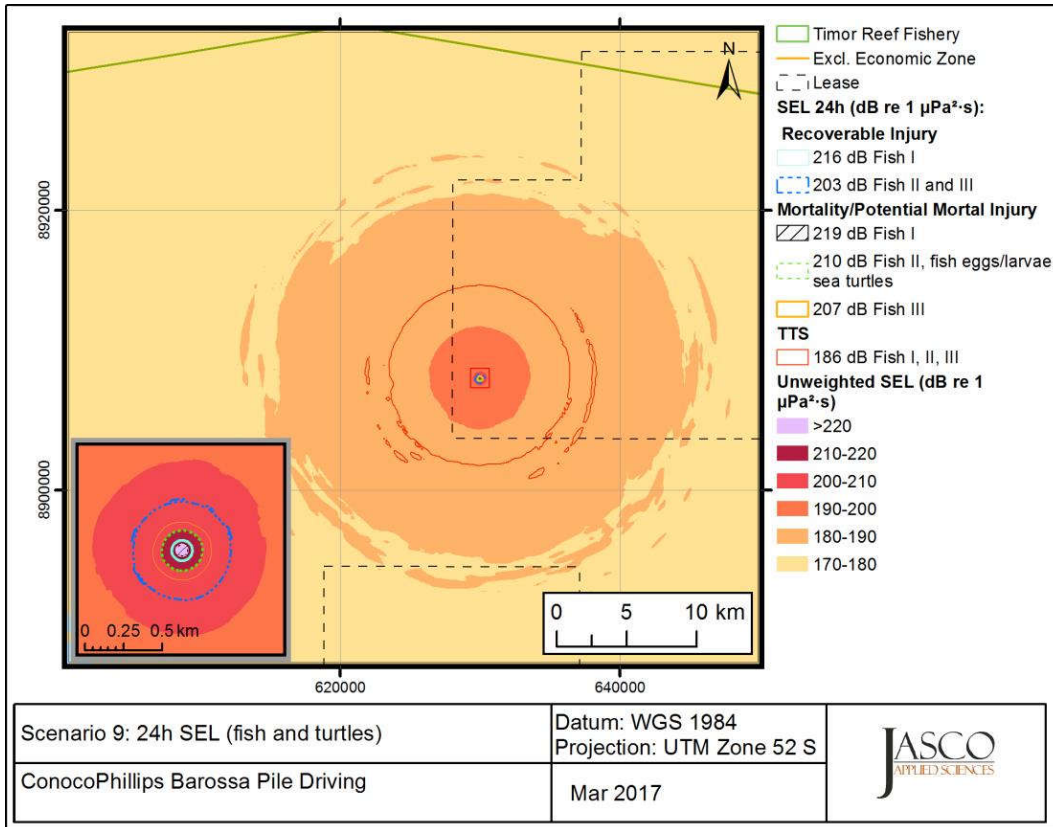
Figure 17. Scenario 9: Sound level contour map showing maximum-over-depth SEL_{24h} results with fish and turtle thresholds.
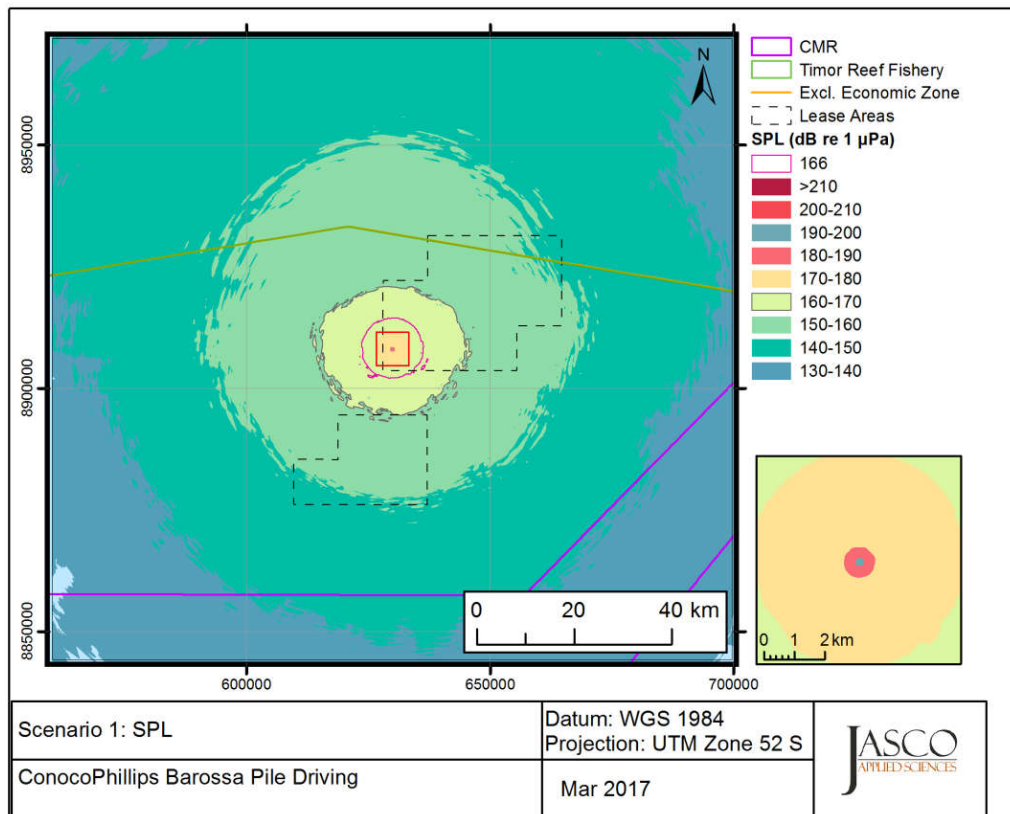
Figure 18. Scenario 1: Sound level contour map showing unweighted maximum-over-depth SPL results, showing isopleths for marine mammal and turtle behaviour thresholds.
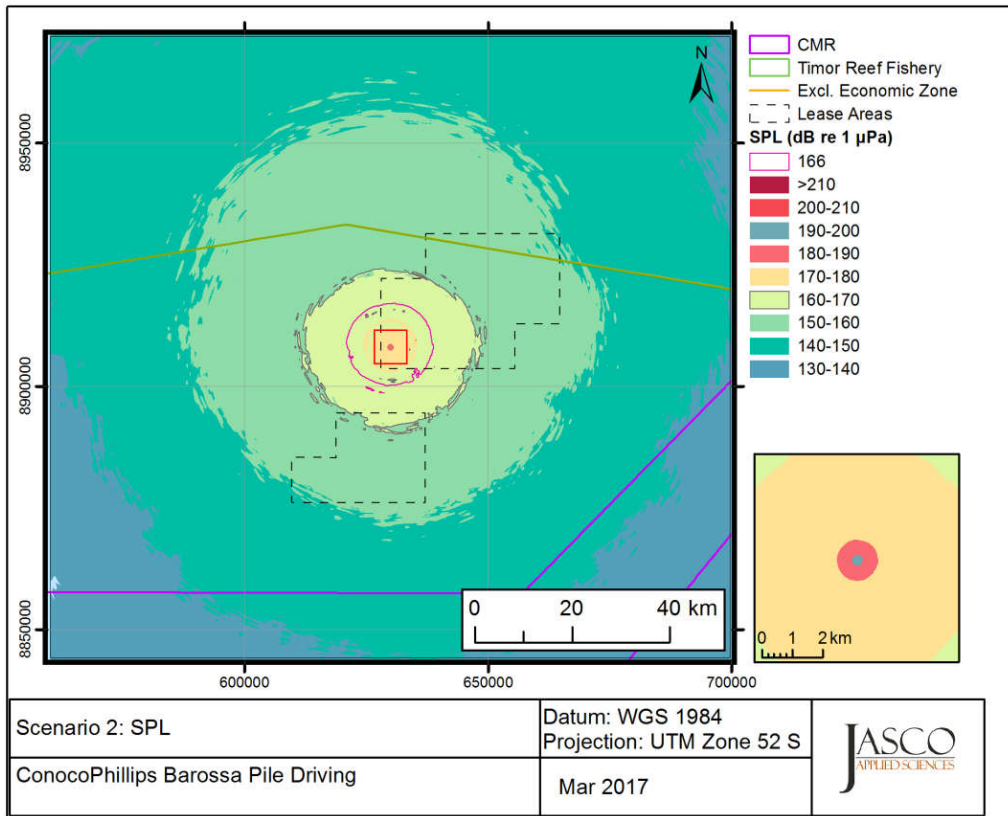
Figure 19. Scenario 2: Sound level contour map showing unweighted maximum-over-depth SPL results, showing isopleths for marine mammal and turtle behaviour thresholds.
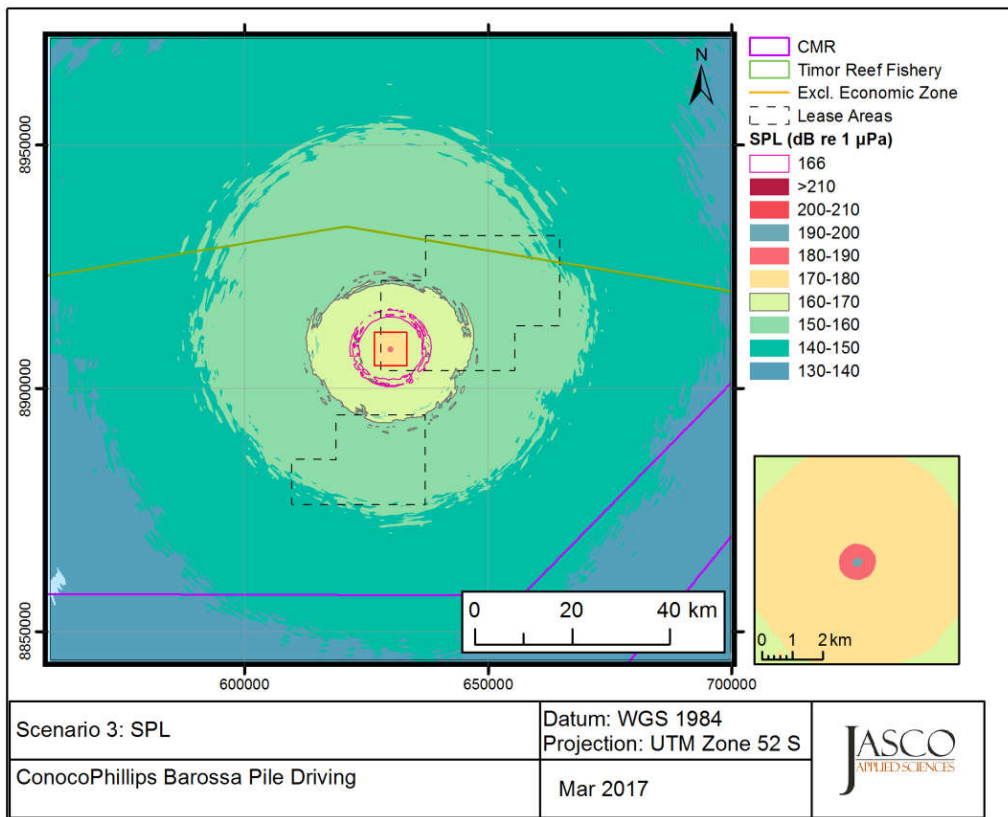
Figure 20. Scenario 3: Sound level contour map showing unweighted maximum-over-depth SPL results, showing isopleths for marine mammal and turtle behaviour thresholds.
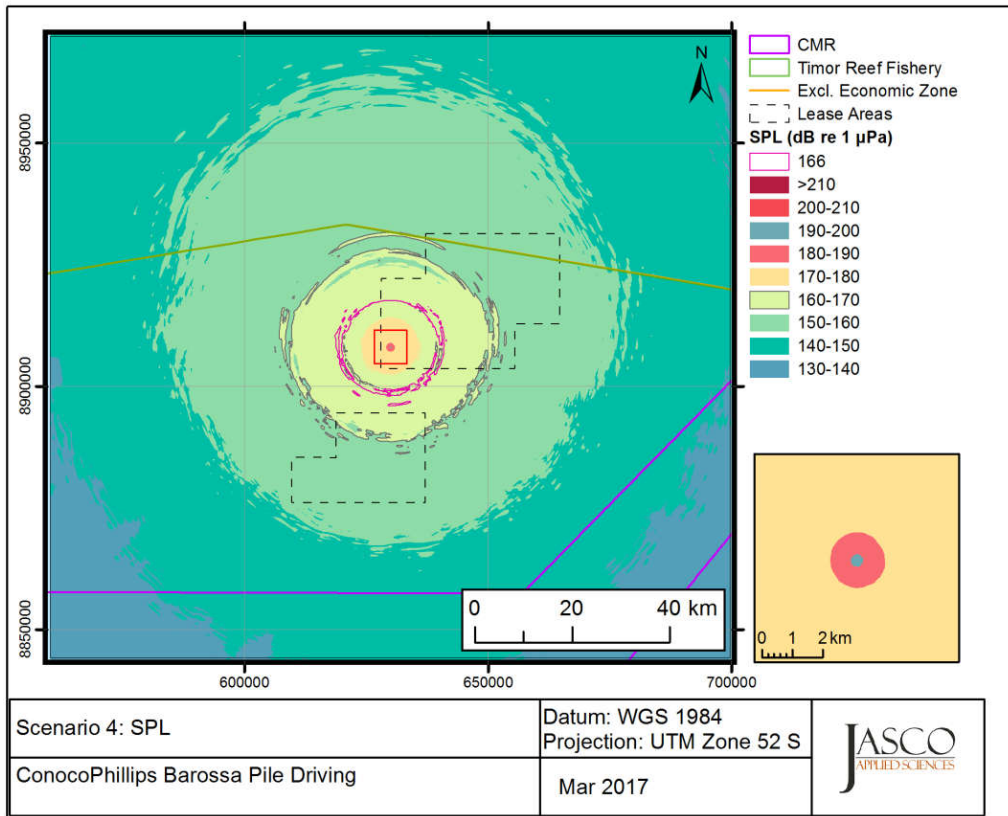
Figure 21. Scenario 4: Sound level contour map showing unweighted maximum-over-depth SPL results, showing isopleths for marine mammal and turtle behaviour thresholds.
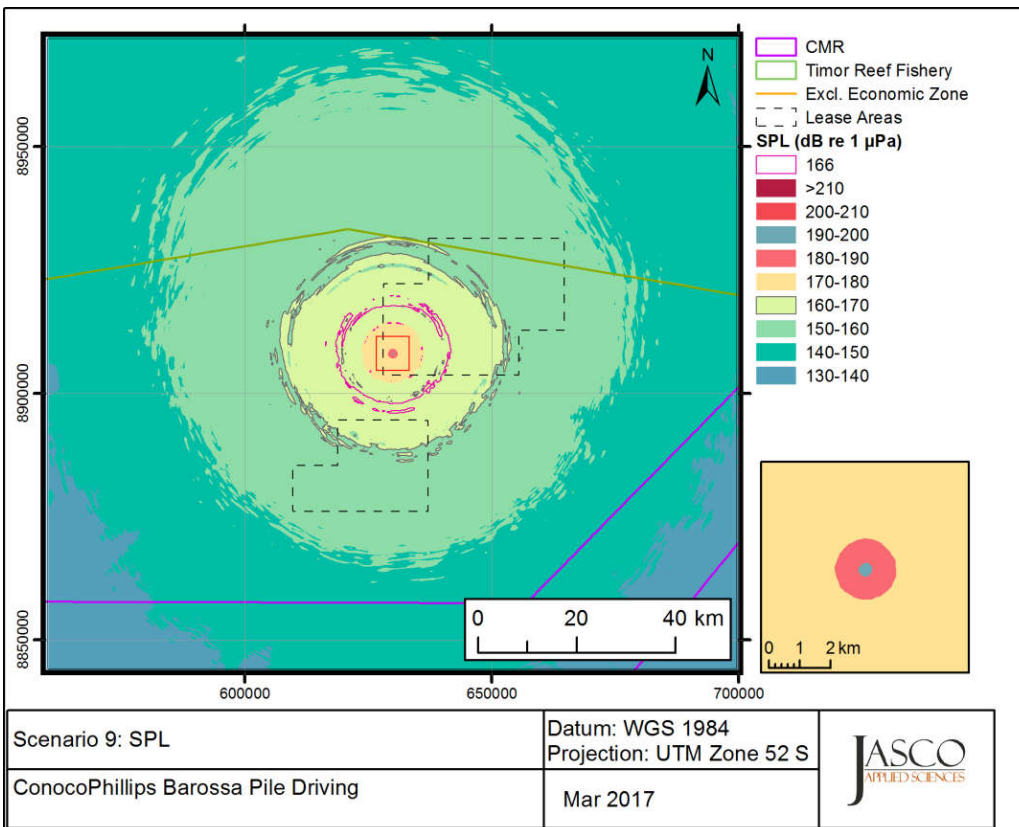
Figure 22. Scenario 9: Sound level contour map showing unweighted maximum-over-depth SPL results, showing isopleths for marine mammal and turtle behaviour thresholds.
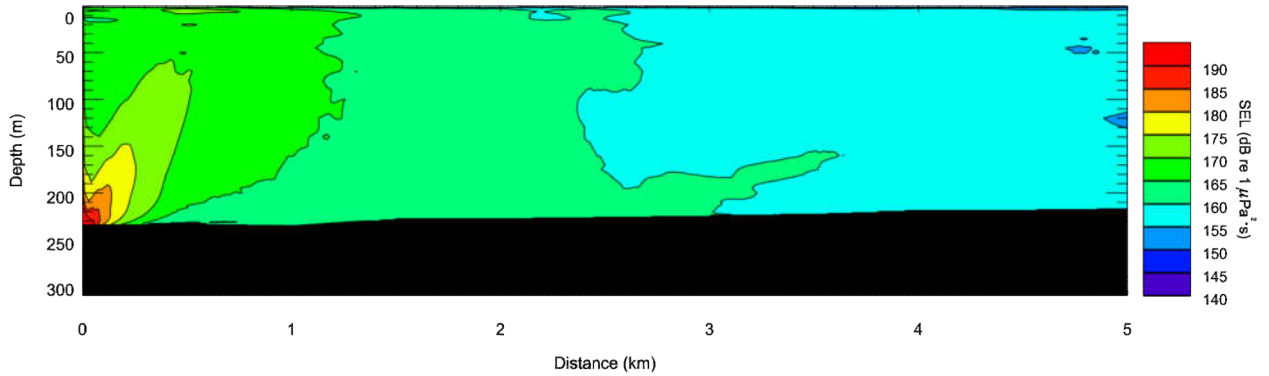
Figure 23. Scenario 1: Predicted unweighted per-strike SEL as a vertical slice. Levels are shown along a single transect of azimuth 180°.
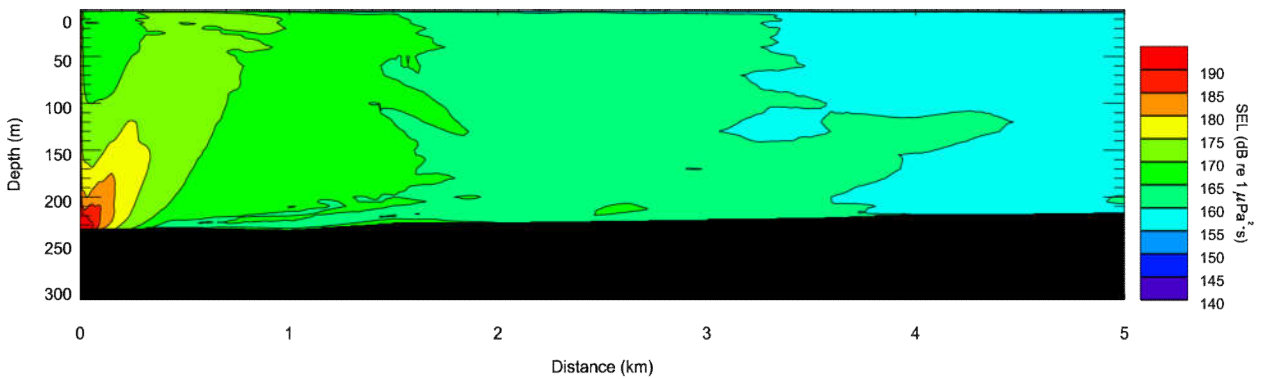
Figure 24. Scenario 2: Predicted unweighted per-strike SEL as a vertical slice. Levels are shown along a single transect of azimuth 180°.
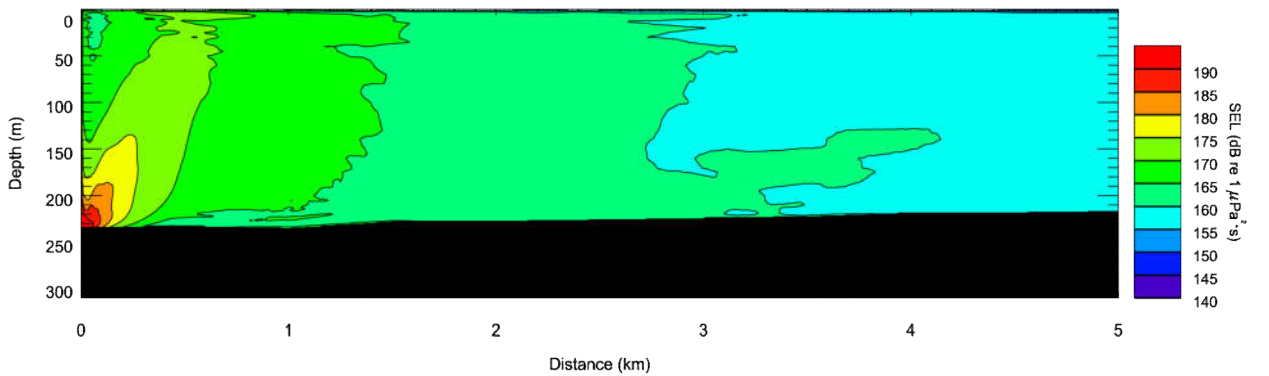
Figure 25. Scenario 3: Predicted unweighted per-strike SEL as a vertical slice. Levels are shown along a single transect of azimuth 180°.
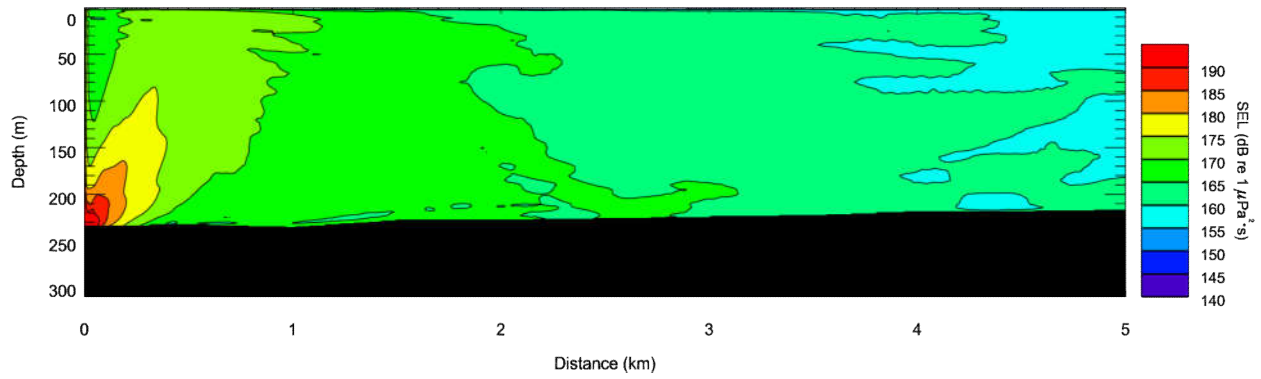
Figure 26. Scenario 4: Predicted unweighted per-strike SEL as a vertical slice. Levels are shown along a single transect of azimuth 180°.
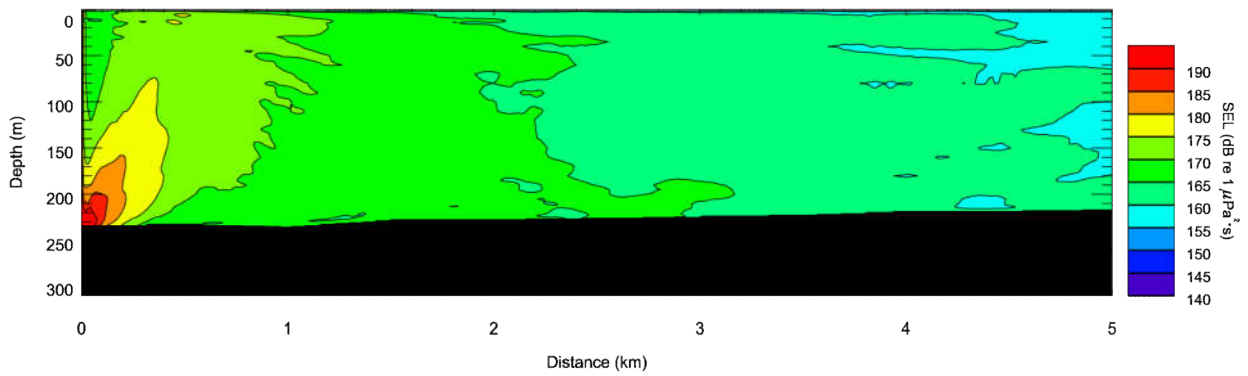
Figure 27. Scenario 9: Predicted unweighted per-strike SEL as a vertical slice. Levels are shown along a single transect of azimuth 180°.

5. Discussion and Conclusion

5.1. Overview

By modelling a combination of possible hammer sizes, pile diameters and lengths at two different water depths, a comprehensive understanding of possible noise footprints, and an understanding of the factors related to sound propagation across the Barossa field development area has been developed. Considering all modelling scenarios, the far-field source level of the pile was predominantly influenced by the hammer size, with the highest far-field per-strike source levels being attributed to the larger hammer (1730 kJ; Figure 3). Water depth marginally influenced the far-field source levels. The peak sound energy from the pile driving is concentrated in the frequency range 40 to 500 Hz (Figure 3). For the modelling scenarios, noise emissions from pile driving are considered to be cylindrically isotropic (i.e. omnidirectional in the horizontal plane). As such, variations in noise that propagates across azimuths are attributed to the bathymetry alone, with this accounted for in the modelling methodology.

Larger effect zones are predicted for per-strike species thresholds of all three metrics (SEL, SPL, and PK) for the 1730 kJ hammer relative to the 660 kJ hammer, regardless of the pile characteristics. The 39 m long, 5 m diameter pile had larger per-strike ranges than the 43 m long, 4 m diameter pile for SEL and SPL metrics, but not always for peak pressure (PK). However, the range differences were small (less than 10 m). The smaller 660 kJ hammer always had larger ranges to 24 h SEL injury isopleths than the larger hammer because it took more blows for this hammer to drive a pile (Table 4).

To compare all scenarios with similar soil resistance (Scenarios 1–8), one metric that can be used is to compare the distances is the per-strike 160 dB re 1 µPa^2·s isopleth, associated with seismic EPBC Act Policy Statement 2.1 (DEWHA 2008). From this, the median difference between R_{max} and $R_{95\%}$ distances across is 470 m, or 8% of R_{max}, with the smallest difference associated with Scenario 3 (407 m), and the largest with Scenario 4 (832 m). These isopleths have $R_{95\%}$ distances of 3.9 to 7.3 km. The SEL$_{24h}$ isopleths associated with PTS follow a similar trend to the per-strike SEL isopleths higher than 160 dB, and differ minimally. At lower isopleths, such as the single-strike 150 dB re 1 µPa^2·s or 160 dB re 1 µPa levels, the difference between R_{max} and $R_{95\%}$ increases, with the median difference being 14.14 km for the 140 dB re 1 µPa^2·s isopleth. This occurs when distances are larger and bathymetry predominantly controls the noise footprint, increasing propagation towards deeper waters (to the north) because it loses less energy when it interacts with the seabed. The R_{max} radius is more representative of the effective extent of the footprint because the source is stationary and is more conservative, given detailed geological profiles of the area are yet to be defined.

The piling scenarios that considered the lower soil resistance and therefore the lower number of average strikes (Scenarios 9 and 10; Table 4) can be compared to Scenarios 4 and 8. The distances to the single strike SEL is smaller for Scenario 9 compared to Scenario 4 (Site 1), but greater for Scenario 10 compared to Scenario 8 (Site 2). However, the ranges to the marine mammal behavioural criteria of 160 dB re 1 µPa for cetaceans (NMFS 2013) are larger for Scenarios 9 and 10, although only slightly larger for Scenario 10 compared to Scenario 8. The distances to PK and SEL$_{24h}$ metrics were slightly smaller for Scenarios 9 and 10.

The subsections that follow focus on the results from the modelling of the eight scenarios with the expected soil resistance based on the assumed average strike count (i.e. Scenarios 1-8). The model assumed no acoustic mitigation around the pile driving operation. Therefore, the modelling scenarios represent the maximum noise footprint from pile driving activities as a conservative estimate given likely soil resistance.

5.2. Marine Mammals

Considering Scenarios 1–8, the maximum distances to the to the DEWHA (2008) per-strike threshold (160 dB re 1 µPa^{2}s) for Sites 1 and 2 are 8.99 and 7.81 km respectively, with Scenarios 4 and 8 based on the wider pile and the larger hammer (Table 8).

Considering Scenarios 1-8, the maximum distances to the NMFS SPL threshold for possible behavioural effects on marine mammals (SPL 160 dB re 1 µPa) (NMFS 2013) at Sites 1 and 2 are 23.83 and 28.30 km respectively (Scenarios 4 and 8; Table 8).

Marine mammals could experience PTS near the piling operations based on the 24 h SEL criteria from Wood et al. (2012). Considering Scenarios 1-8 and Sites 1 and 2 respectively, the maximum distance an animal could be experience PTS is 6.07 or 4.92 km for low-frequency cetaceans, 0.79 or 0.54 km for mid-frequency cetaceans, and 16.59 or 18.75 km for high-frequency cetaceans (Table 7). The 24 h SEL is a cumulative metric that reflects the dosimetric impact of noise levels within 24 hours based on the assumption that an animal is consistently exposed to such noise levels at a fixed position. The corresponding radii are significantly larger than those for peak pressure criteria, but they represent an unlikely worst case scenario since, more realistically, marine mammals would not stay in the same location or at the same range for 24 hours. Therefore, a reported radius of 24 h SEL criteria does not mean that any animal travelling within this radius of the source will be injured, but rather that it could be injured if it remained in that range for 24 hours.

5.3. Turtles

Considering the locations of Site 1 and 2 separately from Scenarios 1–8, the maximum distance to the NMFS SPL threshold for possible behavioural effects on turtles (SPL 160 dB re 1 µPa) (NSF 2011) at modelling Sites 1 and 2 is 12.04 and 14.25 km, respectively, also for Scenarios 4 and 8 (Table 8).

Turtles could suffer a mortal injury based on both 24 h SEL criteria (210 dB re 1 $\mu Pa^2 \cdot s$) and PK criteria. Considering Sites 1 and 2 respectively, for 24 h SEL this could occur at 230 m (Scenario 3) or 200 m (Scenarios 5 and 7; Table 9). For the PK criteria, this could occur at 200 m (Scenario 2 or 6; Table 11). While the larger distance from either criterion should be applied, the distance from the PK is more relevant to operational considerations.

5.4. Fish

Fish could suffer a potential mortal injury based on both 24 h SEL and PK criteria. Of the two metrics mentioned, the larger distance is the measure that should be applied. The results in this section focus on Scenarios 1–8 and modelling Sites 1 and 2 respectively, with results in Tables 9–11. Mortal and potential mortal acoustic injury to fish without a swim bladder (Fish I) could occur within 80 or 70 m (24 h SEL criteria) or 100 m (PK criteria). Fish with a swim bladder (Fish II and III), fish eggs, and fish larvae could sustain the same types of injuries if they are within 340 or 290 m (24 h SEL criteria) or 200 m (PK criteria).

Recoverable injury to fish without a swim bladder (Fish I) could occur within 110 or 100 m (24 h SEL criteria) or 100 m (PK criteria). Similar injury to fish with a swim bladder (Fish II and III) could occur within 670 or 530 m (24 h SEL criteria) or 200 m (PK criteria). The maximum distance at which fish could experience TTS at either modelling site is 14.81 or 14.65 km.

Glossary

1/3-octave-band
Non-overlapping passbands that are one-third of an octave wide (where an octave is a doubling of frequency). Three adjacent 1/3-octave-bands comprise one octave. One-third-octave-bands become wider with increasing frequency. Also see octave.

A-weighting
Frequency-selective weighting for human hearing in air that is derived from the inverse of the idealized 40-phon equal loudness hearing function across frequencies.

absorption
The conversion of acoustic energy into heat, which is captured by insulation.

attenuation
The gradual loss of acoustic energy from absorption and scattering as sound propagates through a medium.

auditory weighting function (frequency-weighting function)
Auditory weighting functions account for marine mammal hearing sensitivity. They are applied to sound measurements to emphasize frequencies that an animal hears well and de-emphasize frequencies they hear less well or not at all (Southall et al. 2007, Finneran and Jenkins 2012, NOAA 2013).

azimuth
A horizontal angle relative to a reference direction, which is often magnetic north or the direction of travel. In navigation it is also called bearing.

bandwidth
The range of frequencies over which a sound occurs. Broadband refers to a source that produces sound over a broad range of frequencies (e.g., seismic airguns, vessels) whereas narrowband sources produce sounds over a narrow frequency range (e.g., sonar) (ANSI/ASA S1.13-2005 R2010).

cetacean
Any animal in the order Cetacea. These are aquatic, mostly marine mammals and include whales, dolphins, and porpoises.

compressional wave
A mechanical vibration wave in which the direction of particle motion is parallel to the direction of propagation. Also called primary wave or P-wave.

continuous sound
A sound whose sound pressure level remains above ambient sound during the observation period (ANSI/ASA S1.13-2005 R2010). A sound that gradually varies in intensity with time, for example, sound from a marine vessel.

decibel (dB)
One-tenth of a bel. Unit of level when the base of the logarithm is the tenth root of ten, and the quantities concerned are proportional to power (ANSI S1.1-1994 R2004).

ensonified
Exposed to sound.

far-field
The zone where, to an observer, sound originating from an array of sources (or a spatially-distributed source) appears to radiate from a single point. The distance to the acoustic far-field increases with frequency.

frequency
The rate of oscillation of a periodic function measured in cycles-per-unit-time. The reciprocal of the period. Unit: hertz (Hz). Symbol: f. 1 Hz is equal to 1 cycle per second.

hearing group
Groups of marine mammal species with similar hearing ranges. Commonly defined functional hearing groups include low-, mid-, and high-frequency cetaceans, pinnipeds in water, and pinnipeds in air.

geoacoustic
Relating to the acoustic properties of the seabed.

hearing threshold
The sound pressure level that is barely audible for a given individual in the absence of significant background noise during a specific percentage of experimental trials.

hertz (Hz)
A unit of frequency defined as one cycle per second.

high-frequency cetacean (HFC)
The functional hearing group that represents odontocetes specialized for using high frequencies.

impulsive sound
Sound that is typically brief and intermittent with rapid (within a few seconds) rise time and decay back to ambient levels (NOAA 2013, ANSI S12.7-1986 R2006). For example, seismic airguns and impact pile driving.

low-frequency cetacean (LFC)
The functional hearing group that represents mysticetes (baleen whales).

median
The 50th percentile of a statistical distribution.

mid-frequency cetacean (MFC)
The functional hearing group that represents some odontocetes (dolphins, toothed whales, beaked whales, and bottlenose whales).

M-weighting
The process of band-pass filtering loud sounds to reduce the importance of inaudible or less-audible frequencies for broad classes of marine mammals. "Generalized frequency weightings for various functional hearing groups of marine mammals, allowing for their functional bandwidths and appropriate in characterizing auditory effects of strong sounds" (Southall et al. 2007).

mysticete
Mysticeti, a suborder of cetaceans, use their baleen plates, rather than teeth, to filter food from water. They are not known to echolocate, but use sound for communication. Members of this group include rorquals (Balaenopteridae), right whales (Balaenidae), and gray whales (*Eschrichtius robustus*).

non-impulsive sound
Sound that is broadband, narrowband or tonal, brief or prolonged, continuous or intermittent, and typically does not have a high peak pressure with rapid rise time (typically only small fluctuations in decibel level) that impulsive signals have (ANSI/ASA S3.20-1995 R2008). For example, marine vessels, aircraft, machinery, construction, and vibratory pile driving (NIOSH 1998, NOAA 2015).

octave
The interval between a sound and another sound with double or half the frequency. For example, one octave above 200 Hz is 400 Hz, and one octave below 200 Hz is 100 Hz.

odontocete
The presence of teeth, rather than baleen, characterizes these whales. Members of the Odontoceti are a suborder of cetaceans, a group comprised of whales, dolphins, and porpoises. The toothed whales' skulls are mostly asymmetric, an adaptation for their echolocation. This group includes sperm whales, killer whales, belugas, narwhals, dolphins, and porpoises.

parabolic equation method
A computationally-efficient solution to the acoustic wave equation that is used to model transmission loss. The parabolic equation approximation omits effects of back-scattered sound, simplifying the computation of transmission loss. The effect of back-scattered sound is negligible for most ocean-acoustic propagation problems.

particle velocity
The physical speed of a particle in a material moving back and forth in the direction of the pressure wave. Unit: meters per second (m/s). Symbol: v.

peak pressure level (PK)
The maximum instantaneous sound pressure level, in a stated frequency band, within a stated period. Also called zero-to-peak pressure level. Unit: decibel (dB).

permanent threshold shift (PTS)
A permanent loss of hearing sensitivity caused by excessive noise exposure. PTS is considered auditory injury.

pinniped
A common term used to describe all three groups that form the superfamily Pinnipedia: phocids (true seals or earless seals), otariids (eared seals or fur seals and sea lions), and walrus.

point source
A source that radiates sound as if from a single point (ANSI S1.1-1994 R2004).

pressure, acoustic
The deviation from the ambient hydrostatic pressure caused by a sound wave. Also called overpressure. Unit: pascal (Pa). Symbol: p.

pressure, hydrostatic
The pressure at any given depth in a static liquid that is the result of the weight of the liquid acting on a unit area at that depth, plus any pressure acting on the surface of the liquid. Unit: pascal (Pa).

received level
The sound level measured at a receiver.

rms
root-mean-square.

shear wave
A mechanical vibration wave in which the direction of particle motion is perpendicular to the direction of propagation. Also called secondary wave or S-wave. Shear waves propagate only in solid media, such as sediments or rock. Shear waves in the seabed can be converted to compressional waves in water at the water-seabed interface.

signature
Pressure signal generated by a source.

sound
A time-varying pressure disturbance generated by mechanical vibration waves travelling through a fluid medium such as air or water.

sound exposure

Time integral of squared, instantaneous frequency-weighted sound pressure over a stated time interval or event. Unit: pascal-squared second ($Pa^2 \cdot s$) (ANSI S1.1-1994 R2004).

sound exposure level (SEL)

A cumulative measure related to the sound energy in one or more pulses. Unit: dB re 1 $\mu Pa^2 \cdot s$. SEL is expressed over the summation period (e.g., per-pulse SEL [for airguns], single-strike SEL [for pile drivers], 24-hour SEL).

sound field

Region containing sound waves (ANSI S1.1-1994 R2004).

sound pressure level (SPL)

The decibel ratio of the time-mean-square sound pressure, in a stated frequency band, to the square of the reference sound pressure (ANSI S1.1-1994 R2004).

For sound in water, the reference sound pressure is one micropascal (p_0 = 1 μPa) and the unit for SPL is dB re 1 μPa:

$$\text{SPL} = 10 \log_{10}\left(p^2 / p_0^2\right) = 20 \log_{10}\left(p / p_0\right)$$

Unless otherwise stated, SPL refers to the root-mean-square sound pressure level. See also 90% sound pressure level and fast-average sound pressure level. Non-rectangular time window functions could be applied to calculate the rms value, in which case the SPL unit should identify the window type.

sound speed profile

The speed of sound in the water column as a function of depth below the water surface.

source level (SL)

The sound level measured in the far-field and scaled back to a standard reference distance of 1 metre from the acoustic centre of the source. Unit: dB re 1 μPa @ 1 m (sound pressure level) or dB re 1 $\mu Pa^2 \cdot s$ (sound exposure level).

temporary threshold shift (TTS)

Temporary loss of hearing sensitivity caused by excessive noise exposure.

transmission loss (TL)

The decibel reduction in sound level between two stated points that results from sound spreading away from an acoustic source subject to the influence of the surrounding environment. Also called propagation loss.

Literature Cited

[DEWHA] Department of the Environment, W., Heritage and the Arts. 2008. *EPBC Act Policy Statement 2.1 - Interaction Between Offshore Seismic Exploration and Whales*. *In*: Department of the Environment, W., Heritage and the Arts. 14 pp.

[ISO] International Organization for Standardization. 2016. *ISO/DIS 18405.2:2016 (Draft). Underwater acoustics—Terminology*. Geneva. https://www.iso.org/obp/ui/#iso:std:iso:18405:dis:ed-1:v2:en.

[NIOSH] National Institute for Occupational Safety and Health. 1998. *Criteria for a recommended standard: Occupational noise exposure*. Document Number 98-126. U.S. Department of Health and Human Services, NIOSH, Cincinnati, Ohio. 122 pp.

[NMFS] National Marine Fisheries Service. 2013. *Marine Mammals: Interim Sound Threshold Guidance* (webpage). National Marine Fisheries Service, National Oceanic and Atmospheric Administration, U.S. Department of Commerce. http://www.westcoast.fisheries.noaa.gov/protected_species/marine_mammals/threshold_guidance.html.

[NMFS] National Marine Fisheries Service. 2016. *Technical Guidance for Assessing the Effects of Anthropogenic Sound on Marine Mammal Hearing: Underwater Acoustic Thresholds for Onset of Permanent and Temporary Threshold Shifts*. U.S. Department of Commerce, NOAA. NOAA Technical Memorandum NMFS-OPR-55. 178 pp. http://www.nmfs.noaa.gov/pr/acoustics/Acoustic%20Guidance%20Files/opr-55_acoustic_guidance_tech_memo.pdf.

[NOAA] National Oceanic and Atmospheric Administration. 2013. *Draft guidance for assessing the effects of anthropogenic sound on marine mammals: Acoustic threshold levels for onset of permanent and temporary threshold shifts*, December 2013, 76 pp. Silver Spring, Maryland: NMFS Office of Protected Resources. http://www.nmfs.noaa.gov/pr/acoustics/draft_acoustic_guidance_2013.pdf.

[NOAA] National Oceanic and Atmospheric Administration. 2015. *Draft guidance for assessing the effects of anthropogenic sound on marine mammal hearing: Underwater acoustic threshold levels for onset of permanent and temporary threshold shifts*, July 2015, 180 pp. Silver Spring, Maryland: NMFS Office of Protected Resources. http://www.nmfs.noaa.gov/pr/acoustics/draft%20acoustic%20guidance%20July%202015.pdf.

[NOAA] National Oceanic and Atmospheric Administration. 2016. *Document Containing Proposed Changes to the NOAA Draft Guidance for Assessing the Effects of Anthropogenic Sound on Marine Mammal Hearing: Underwater Acoustic Threshold Levels for Onset of Permanent and Temporary Threshold Shifts*, p. 24. http://www.nmfs.noaa.gov/pr/acoustics/draft_guidance_march_2016_.pdf.

[NSF] National Science Foundation (U.S.), U.S. Geological Survey, and [NOAA] National Oceanic and Atmospheric Administration (U.S.). 2011. *Final Programmatic Environmental Impact Statement/Overseas. Environmental Impact Statement for Marine Seismic Research Funded by the National Science Foundation or Conducted by the U.S. Geological Survey*. National Science Foundation, Arlington, VA.

AdBm Technologies. 2014. *AdBm Demonstration at Butendiek Offshore Wind Farm with Ballast Nedam*. http://adbmtech.com/technology/demonstration-reports/.

Aerts, L., M. Blees, S. Blackwell, C. Greene, K. Kim, D. Hannay, and M. Austin. 2008. *Marine mammal monitoring and mitigation during BP Liberty OBC seismic survey in Foggy Island Bay, Beaufort Sea, July-August 2008: 90-day report*. Document Number LGL Report P1011-1. Report by LGL Alaska Research Associates Inc., LGL Ltd., Greeneridge Sciences Inc. and

JASCO Applied Sciences for BP Exploration Alaska. 199 pp.
http://www.nmfs.noaa.gov/pr/pdfs/permits/bp_liberty_monitoring.pdf.

ANSI S12.7-1986. R2006. *American National Standard Methods for Measurements of Impulsive Noise*. American National Standards Institute, New York.

ANSI S1.1-1994. R2004. *American National Standard Acoustical Terminology*. American National Standards Institute, New York.

ANSI S1.1-2013. R2013. *American National Standard Acoustical Terminology*. American National Standards Institute, New York.

ANSI/ASA S1.13-2005. R2010. *American National Standard Measurement of Sound Pressure Levels in Air*. American National Standards Institute and Acoustical Society of America, New York.

ANSI/ASA S3.20-1995. R2008. *American National Standard Bioacoustical Terminology*. American National Standards Institute and Acoustical Society of America, New York.

Buckingham, M.J. 2005. Compressional and shear wave properties of marine sediments: Comparisons between theory and data. *Journal of the Acoustical Society of America* 117(1): 137-152. http://link.aip.org/link/?JAS/117/137/1.

Buehler, D., R. Oestman, J. Reyff, K. Pommerenck, and B. Mitchell. 2015. *Technical Guidance for Assessment and Mitigation of the Hydroacoustic Effects of Pile Driving on Fish*. Report Number CTHWANP-RT-15-306.01.01. California Department of Transportation (CALTRANS), Division of Environmental Analysis. 532 pp.
http://www.dot.ca.gov/hq/env/bio/files/bio_tech_guidance_hydroacoustic_effects_110215.pdf.

Carnes, M.R. 2009. *Description and Evaluation of GDEM-V 3.0*. Document Number NRL Memorandum Report 7330-09-9165. US Naval Research Laboratory, Stennis Space Center, MS. 21 pp.

Collins, M.D. 1993. A split-step Padé solution for the parabolic equation method. *Journal of the Acoustical Society of America* 93(4): 1736-1742.

Collins, M.D., R.J. Cederberg, D.B. King, and S. Chin-Bing. 1996. Comparison of algorithms for solving parabolic wave equations. *Journal of the Acoustical Society of America* 100(1): 178-182.

Coppens, A.B. 1981. Simple equations for the speed of sound in Neptunian waters. *Journal of the Acoustical Society of America* 69(3): 862-863. http://link.aip.org/link/?JAS/69/862/1.

Finneran, J.J. and C.E. Schlundt. 2010. Frequency-dependent and longitudinal changes in noise-induced hearing loss in a bottlenose dolphin (*Tursiops truncatus*). *Journal of the Acoustical Society of America* 128(2): 567-570.

Finneran, J.J. and A.K. Jenkins. 2012. *Criteria and thresholds for U.S. Navy acoustic and explosive effects analysis*. SPAWAR Systems Center Pacific, San Diego, California.

François, R.E. and G.R. Garrison. 1982a. Sound absorption based on ocean measurements: Part II: Boric acid contribution and equation for total absorption. *Journal of the Acoustical Society of America* 72(6): 1879-1890.

François, R.E. and G.R. Garrison. 1982b. Sound absorption based on ocean measurements: Part I: Pure water and magnesium sulfate contributions. *Journal of the Acoustical Society of America* 72(3): 896-907.

Funk, D., D. Hannay, D. Ireland, R. Rodrigues, and W. Koski (eds.). 2008. *Marine mammal monitoring and mitigation during open water seismic exploration by Shell Offshore Inc. in the Chukchi and Beaufort Seas, July–November 2007: 90-day report*. LGL Report P969-1. Prepared by

LGL Alaska Research Associates Inc., LGL Ltd., and JASCO Research Ltd. for Shell Offshore Inc., National Marine Fisheries Service (US), and US Fish and Wildlife Service. 218 pp.

Gunderboom. *Product News: Sound Attenuation System (SAS)* (pamphlet). http://www.gunderboom.com/PDFfiles/Sound%20Attenuation%20Update.pdf.

Hannay, D. and R. Racca. 2005. *Acoustic Model Validation*. Document Number 0000-S-90-04-T-7006-00-E, Revision 02. Technical report for Sakhalin Energy Investment Company Ltd. by JASCO Research Ltd. 34 pp.

Hermannsen, L., J. Tougaard, K. Beedholm, J. Nabe-Nielsen, and P.T. Madsen. 2015. Characteristics and propagation of airgun pulses in shallow water with implications for effects on small marine mammals. *PLoS ONE* 10(7): e0133436. http://journals.plos.org/plosone/article?id=10.1371/journal.pone.0133436.

ICF Jones & Stokes and Illingworth and Rodkin, Inc. 2009. *Technical Guidance for Assessment and Mitigation of the Hydroacoustic Effects of Pile Driving on Fish*. Prepared for California Department of Transportation (CALTRANS), Sacramento, CA. 298 pp. www.dot.ca.gov/hq/env/bio/files/Guidance_Manual_2_09.pdf.

IHC Offshore Systems. 2012. *Symposium Sound Solutions* (pamphlet). http://www.noordzee.nl/wp-content/uploads/2011/11/ihc-noise-mitigation-screen.pdf.

Ireland, D.S., R. Rodrigues, D. Funk, W. Koski, and D. Hannay. 2009. *Marine mammal monitoring and mitigation during open water seismic exploration by Shell Offshore Inc. in the Chukchi and Beaufort Seas, July–October 2008: 90-Day Report*. Document Number LGL Report P1049-1. 277 pp.

Lane, A. 2015. *Barossa Field Development – Shallow Geophysical and Geotechnical Interpretation including Preliminary Analysis of 3D Exploration Seismic (3DX) Data*. Document Number CBAR-650-PL-R02-V-00001. Arup. 28 pp.

Lucke, K., U. Siebert, P. Lepper, A., and M.-A. Blanchet. 2009. Temporary shift in masked hearing thresholds in a harbor porpoise (*Phocoena phocoena*) after exposure to seismic airgun stimuli. *Journal of the Acoustical Society of America* 125(6): 4060-4070.

MacGillivray, A. 2014. A model for underwater sound levels generated by marine impact pile driving. *Proceedings of Meetings on Acoustics* 20(1): 045008. http://scitation.aip.org/content/asa/journal/poma/20/1/10.1121/2.0000030.

MacGillivray, A.O. and N.R. Chapman. 2012. Modeling underwater sound propagation from an airgun array using the parabolic equation method. *Canadian Acoustics* 40(1): 19-25. http://jcaa.caa-aca.ca/index.php/jcaa/article/view/2502.

Martin, B., K. Broker, M.-N.R. Matthews, J. MacDonnell, and L. Bailey. 2015. *Comparison of measured and modeled air-gun array sound levels in Baffin Bay, West Greenland. OceanNoise 2015*, 11-15 May, Barcelona, Spain.

McCauley, R.D., J. Fewtrell, A.J. Duncan, C. Jenner, M.-N. Jenner, J.D. Penrose, R.I.T. Prince, A. Adihyta, J. Murdoch, et al. 2000. Marine seismic surveys: A study of environmental implications. *Australian Petroleum Production Exploration Association (APPEA) Journal* 40: 692-708.

McPherson, C.R., M. Wood, and H. Yurk. 2016. *Effects of Seismic Survey Noise on Marine Fauna, ConocoPhillips Barossa MSS*. Document Number 01104, Version 1.0. Technical report by JASCO Applied Sciences for Jacobs.

Moein, S.E., J.A. Musick, J.A. Keinath, D.E. Barnard, M.L. Lenhardt, and R. George. 1994. *Evaluation of Seismic Sources for Repelling Sea Turtles from Hopper Dredges, in Sea Turtle Research*

Program: Summary Report. *In*: Hales, L.Z. (ed.). Report from U.S. Army Engineer Division, South Atlantic, Atlanta GA, and U.S. Naval Submarine Base, Kings Bay GA. Technical Report CERC-95. 90 pp.

Nedwell, J.R. and A.W. Turnpenny. 1998. The use of a generic frequency weighting scale in estimating environmental effect. *Workshop on Seismics and Marine Mammals*. 23–25th June 1998, London, U.K.

Nedwell, J.R., A.W.H. Turnpenny, J. Lovell, S.J. Parvin, R. Workman, and J.A.L. Spinks. 2007. *A validation of the dB$_{ht}$ as a measure of the behavioural and auditory effects of underwater noise*. Report No. 534R1231 prepared by Subacoustech Ltd. for the UK Department of Business, Enterprise and Regulatory Reform under Project No. RDCZ/011/0004. www.subacoustech.com/information/downloads/reports/534R1231.pdf.

O'Neill, C., D. Leary, and A. McCrodan. 2010. Sound Source Verification. (Chapter 3) *In* Blees, M.K., K.G. Hartin, D.S. Ireland, and D. Hannay (eds.). *Marine mammal monitoring and mitigation during open water seismic exploration by Statoil USA E&P Inc. in the Chukchi Sea, August-October 2010: 90-day report*. LGL Report P1119. Prepared by LGL Alaska Research Associates Inc., LGL Ltd., and JASCO Applied Sciences Ltd. for Statoil USA E&P Inc., National Marine Fisheries Service (US), and US Fish and Wildlife Service. 1-34.

Pile Dynamics, Inc. 2010. GRLWEAP.

Popper, A.N., A.D. Hawkins, R.R. Fay, D.A. Mann, S. Bartol, T.J. Carlson, S. Coombs, W.T. Ellison, R.L. Gentry, et al. 2014. *Sound Exposure Guidelines for Fishes and Sea Turtles: A Technical Report prepared by ANSI-Accredited Standards Committee S3/SC1 and registered with ANSI*. SpringerBriefs in Oceanography, Volume ASA S3/SC1.4 TR-2014. ASA Press. 87 pp.

Racca, R., A. Rutenko, K. Bröker, and M. Austin. 2012a. A line in the water - design and enactment of a closed loop, model based sound level boundary estimation strategy for mitigation of behavioural impacts from a seismic survey. *11th European Conference on Underwater Acoustics 2012*. Volume 34(3), Edinburgh, United Kingdom.

Racca, R., A. Rutenko, K. Bröker, and G. Gailey. 2012b. *Model based sound level estimation and in-field adjustment for real-time mitigation of behavioural impacts from a seismic survey and post-event evaluation of sound exposure for individual whales. Acoustics 2012 Fremantle: Acoustics, Development and the Environment*, Fremantle, Australia. http://www.acoustics.asn.au/conference_proceedings/AAS2012/papers/p92.pdf.

Southall, B.L., A.E. Bowles, W.T. Ellison, J.J. Finneran, R.L. Gentry, C.R. Greene, Jr., D. Kastak, D.R. Ketten, J.H. Miller, et al. 2007. Marine mammal noise exposure criteria: Initial scientific recommendations. *Aquatic Mammals* 33(4): 411-521.

Teague, W.J., M.J. Carron, and P.J. Hogan. 1990. A comparison between the Generalized Digital Environmental Model and Levitus climatologies. *Journal of Geophysical Research* 95(C5): 7167-7183.

Warner, G., C. Erbe, and D. Hannay. 2010. Underwater Sound Measurements. (Chapter 3) *In* Reiser, C.M., D.W. Funk, R. Rodrigues, and D. Hannay (eds.). *Marine Mammal Monitoring and Mitigation during Open Water Shallow Hazards and Site Clearance Surveys by Shell Offshore Inc. in the Alaskan Chukchi Sea, July-October 2009: 90-Day Report*. LGL Report P1112-1. Report by LGL Alaska Research Associates Inc. and JASCO Applied Sciences for Shell Offshore Inc., National Marine Fisheries Service (US), and US Fish and Wildlife Service. 1-54.

Whiteway, T. 2009. *Australian Bathymetry and Topography Grid, June 2009*. GeoScience Australia, Canberra. http://www.ga.gov.au/metadata-gateway/metadata/record/gcat_67703.

Whittaker, J.M., A. Goncharov, S.E. Williams, R.D. Müller, and G. Leitchenkov. 2013. Global sediment thickness data set updated for the Australian-Antarctic Southern Ocean. *Geochemistry, Geophysics, Geosystems* 14(8): 3297-3305.

Wood, J., B.L. Southall, and D.J. Tollit. 2012. *PG&E offshore 3 D Seismic Survey Project EIR-Marine Mammal Technical Draft Report*. SMRU Ltd.

Zhang, Y. and C. Tindle. 1995. Improved equivalent fluid approximations for a low shear speed ocean bottom. *Journal of the Acoustical Society of America* 98(6): 3391-3396. http://scitation.aip.org/content/asa/journal/jasa/98/6/10.1121/1.413789.

Appendix A. Acoustic Metrics

A.1. Acoustic Metrics

Underwater sound pressure amplitude is measured in decibels (dB) relative to a fixed reference pressure of p_0 = 1 µPa. Because the perceived loudness of sound, especially impulsive noise such as from seismic airguns, pile driving, and sonar, is not generally proportional to the instantaneous acoustic pressure, several sound level metrics are commonly used to evaluate noise and its effects on marine life. We provide specific definitions of relevant metrics used in the accompanying report. Where possible we follow the ANSI and ISO standard definitions and symbols for sound metrics, but these standards are not always consistent.

The zero-to-peak sound pressure level, or peak sound pressure level (PK; dB re 1 µPa), is the maximum instantaneous sound pressure level in a stated frequency band attained by an acoustic pressure signal, $p(t)$:

$$L_{p,pk} = 20\log_{10}\left[\frac{\max(|p(t)|)}{p_0}\right] \tag{A-1}$$

$L_{p,pk}$ is often included as a criterion for assessing whether a sound is potentially injurious; however, because it does not account for the duration of a noise event, it is generally a poor indicator of perceived loudness.

The peak-to-peak sound pressure level (dB re 1 µPa) is the difference between the maximum and minimum instantaneous sound pressure levels in a stated frequency band attained by an impulsive sound, $p(t)$:

$$L_{p,pk-pk} = 10\log_{10}\left\{\frac{[\max(p(t)) - \min(p(t))]^2}{p_0^2}\right\} \tag{A-2}$$

The root-mean-square (rms) sound pressure level (SPL; dB re 1 µPa) is the rms pressure level in a stated frequency band over a specified time window (T, s) containing the acoustic event of interest. It is important to note that SPL always refers to an rms pressure level and, therefore, not instantaneous pressure:

$$L_p = 10\log_{10}\left(\frac{1}{T}\int_T p^2(t)dt \bigg/ p_0^2\right) . \tag{A-3}$$

The SPL represents a nominal effective continuous sound over the duration of an acoustic event, such as the emission of one acoustic pulse, a marine mammal vocalisation, the passage of a vessel, or over a fixed duration. Because the window length, T, is the divisor, events with similar sound exposure level (SEL) but more spread out in time have a lower SPL.

In studies of impulsive noise, the time window T is often defined as the "90% time window" (T_{90}): the period over which cumulative square pressure function passes between 5% and 95% of its full per-pulse value. The SPL computed over this T_{90} interval is commonly called the 90% SPL (SPL(T_{90}); dB re 1 µPa):

$$L_{p90} = 10\log_{10}\left(\frac{1}{T_{90}}\int_{T_{90}} p^2(t)dt \bigg/ p_0^2\right) . \tag{A-4}$$

The sound exposure level (SEL, dB re 1 µPa^2·s) is a measure related to the acoustic energy contained in one or more acoustic events (N). The SEL for a single event is computed from the time-integral of the squared pressure over the full event duration (T):

$$L_E = 10 \log_{10} \left(\int_T p^2(t) dt \Big/ T_0 p_0^2 \right) \qquad \text{(A-5)}$$

where T_0 is a reference time interval of 1 s. The SEL continues to increase with time when non-zero pressure signals are present. it therefore can be construed as a dose-type measurement so the integration time used must be carefully considered in terms of relevance for impact to the exposed recipients.

SEL can be calculated over periods with multiple acoustic events or over a fixed duration. For a fixed duration, the square pressure is integrated over the duration of interest. For multiple events, the SEL can be computed by summing (in linear units) the SEL of the N individual events:

$$L_{E,N} = 10 \log_{10} \left(\sum_{i=1}^{N} 10^{\frac{L_{E,i}}{10}} \right) . \qquad \text{(A-6)}$$

To compute the SPL(T_{90}) and SEL of acoustic events in the presence of high levels of background noise, Equations A-4 and A-5 are modified to subtract the background noise energy from the event energy:

$$L_{p90} = 10 \log_{10} \left(\frac{1}{T_{90}} \int_{T_{90}} (p^2(t) - \overline{n^2}) dt \Big/ p_0^2 \right) \qquad \text{(A-7)}$$

$$L_E = 10 \log_{10} \left(\int_T (p^2(t) - \overline{n^2}) dt \Big/ T_0 p_0^2 \right) \qquad \text{(A-8)}$$

where $\overline{n^2}$ is the mean square pressure of the background noise, generally computed by averaging the squared pressure of a temporally-proximal segment of the acoustic recording during which acoustic events are absent (e.g., between pulses).

Because the SPL(T_{90}) and SEL are both computed from the integral of square pressure, these metrics are related by the following expression, which depends only on the duration of the energy time window T:

$$L_p = L_E - 10 \log_{10}(T) \qquad \text{(A-9)}$$

$$L_{p90} = L_E - 10 \log_{10}(T_{90}) - 0.458 \qquad \text{(A-10)}$$

where the 0.458 dB factor accounts for the 10% of SEL missing from the SPL(T_{90}) integration time window.

Energy equivalent SPL (dB re 1 µPa) denotes the SPL of a stationary (constant amplitude) sound that generates the same SEL as the signal being examined, $p(t)$, over the same period of time, T:

$$L_{eq} = 10 \log_{10} \left(\frac{1}{T} \int_T p^2(t) dt \Big/ p_0^2 \right) . \qquad \text{(A-11)}$$

The equations for SPL and the energy-equivalent SPL are numerically identical; conceptually, the difference between the two metrics is that the former is typically computed over short periods (typically of one second or less) and tracks the fluctuations of a non-steady acoustic signal, whereas

the latter reflects the average SPL of an acoustic signal over times typically of one minute to several hours.

If applied, the frequency weighting of an acoustic event should be specified, as in the case of M-weighted SEL (e.g., $SEL_{LFC,24h}$; Appendix A.2). The use of fast, slow, or impulse exponential-time-averaging, or other time-related characteristics should else be specified.

A.2. Impact Criteria

A.2.1. Marine Mammals

In recognition of shortcomings of the SPL-only based injury criteria, in 2005 NMFS sponsored the Noise Criteria Group to review literature on marine mammal hearing to propose new noise exposure criteria. Some members of this expert group published a landmark paper (Southall et al. 2007) that suggested assessment methods similar to those applied for humans. The resulting recommendations introduced dual acoustic injury criteria for impulsive sounds that included peak pressure level thresholds and SEL_{24h} thresholds, where the subscripted 24h refers to the accumulation period for calculating SEL. The peak pressure level criterion is not frequency weighted whereas the SEL_{24h} is frequency weighted according to one of four marine mammal species hearing groups: Low-, Mid- and High-Frequency Cetaceans (LFC, MFC, and HFC respectively) and Pinnipeds in Water (PINN). These weighting functions are referred to as M-weighting filters (analogous to the A-weighting filter for human; Appendix A.2). The SEL_{24h} thresholds were obtained by extrapolating measurements of onset levels of Temporary Threshold Shift (TTS) in belugas by the amount of TTS required to produce Permanent Threshold Shift (PTS) in chinchillas. The Southall et al. (2007) recommendations do not specify an exchange rate, which suggests that the thresholds are the same regardless of the duration of exposure (i.e., it infers a 3 dB exchange rate).

Wood et al. (2012) refined Southall et al.'s (2007) thresholds, suggesting lower injury values for LFC and HFC while retaining the filter shapes (Appendix A.2). Their revised thresholds were based on TTS-onset levels in harbour porpoises from Lucke et al. (2009), which led to a revised impulsive sound PTS threshold for HFC of 179 dB re 1 $\mu Pa^2 \cdot s$. Because there were no data available for baleen whales, Wood et al. (2012) based their recommendations for LFC on results obtained from MFC studies. In particular they referenced Finneran and Schlundt (2010) research, which found mid-frequency cetaceans are more sensitive to non-impulsive sound exposure than Southall et al. (2007) assumed. Wood et al. (2012) thus recommended a more conservative TTS-onset level for LFC of 192 dB re 1 $\mu Pa^2 \cdot s$.

In August 2016, after substantial public and expert input into three draft versions and based largely on the above-mentioned literature (NOAA 2013, 2015, 2016), NMFS finalised technical guidance for assessing the effect of anthropogenic sound on marine mammal hearing (NMFS 2016). The guidance describes injury criteria with new thresholds and frequency weighting functions for the five hearing groups described by Finneran and Jenkins (2012).

As of 2016, an optimal approach to determining the potential for injury is not apparent. There is consensus in the research community that an SEL-based method is preferable either separately or in addition to an SPL-based approach to assess the potential for injuries. While the scientific community is trending towards the NMFS (2016) criteria, for consistency with other recent assessments in the Barossa field, this report applies the criteria recommended by Wood et al. (2012).

A.3. Marine Mammal Frequency Weighting

The potential for noise to affect animals depends on how well the animals can hear it. Noises are less likely to disturb or injure an animal if they are at frequencies that the animal cannot hear well. An exception occurs when the sound pressure is so high that it can physically injure an animal by non-auditory means (i.e., barotrauma). For sound levels below such extremes, the importance of sound components at particular frequencies can be scaled by frequency weighting relevant to an animal's sensitivity to those frequencies (Nedwell and Turnpenny 1998, Nedwell et al. 2007).

A.3.1. Marine Mammal Frequency Weighting Functions

Auditory weighting functions for marine mammals—called *M-weighting* functions—were proposed by Southall et al. (2007). Functions were defined for five functional hearing groups of marine mammals:

- Low-frequency cetaceans (LFCs)—mysticetes (baleen whales)

- Mid-frequency cetaceans (MFCs)—some odontocetes (toothed whales)

- High-frequency cetaceans (HFCs)—odontocetes specialized for using high-frequencies

- Pinnipeds in water—seals, sea lions, and walrus

- Pinnipeds in air (not addressed here)

The M-weighting functions have unity gain (0 dB) through the passband and their high and low frequency roll-offs are approximately –12 dB per octave. The amplitude response in the frequency domain of each M-weighting function is defined by:

$$G(f) = -20 \log_{10}\left[\left(1 + \frac{a^2}{f^2}\right)\left(1 + \frac{f^2}{b^2}\right)\right] \quad\quad\quad (\text{A-12})$$

where $G(f)$ is the weighting function amplitude (in dB) at the frequency f (in Hz), and a and b are the estimated lower and upper hearing limits, respectively, which control the roll-off and passband of the weighting function. The parameters a and b are defined uniquely for each functional hearing group (Table A-1). The auditory weighting functions recommended by Southall et al. (2007) are shown in Figure A-1.
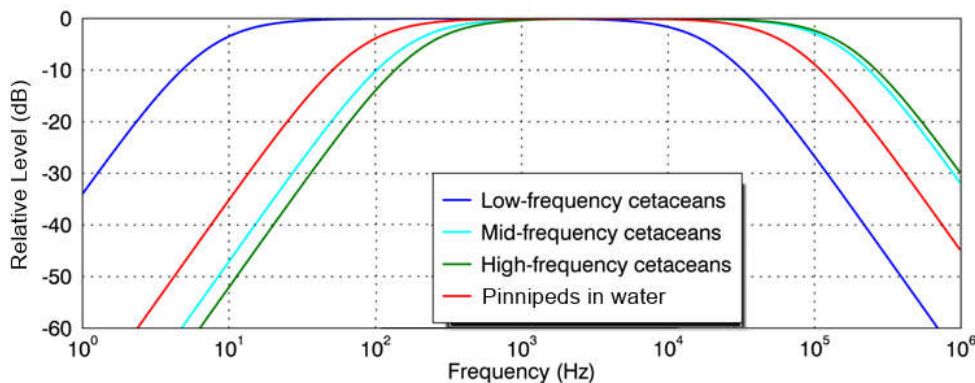
Figure A-1. Auditory weighting functions for functional marine mammal hearing groups as recommended by Southall et al. (2007).

Table A-1. Parameters for the auditory weighting functions recommended by Southall et al. (2007).

Functional hearing group	Southall et al.	
	a (Hz)	*b* (Hz)
Low-frequency cetaceans (LFC)	7	22,000
Mid-frequency cetaceans (MFC)	150	160,000
High-frequency cetaceans (HFC)	200	180,000
Pinnipeds in water (Pw)	75	75,000

Appendix B. Source and Propagation Models

B.1. Pile Driving Source Model

A physical model of pile vibration and near-field sound radiation is used to calculate source levels of piles. The physical model employed in this study computes the underwater vibration and sound radiation of a pile by solving the theoretical equations of motion for axial and radial vibrations of a cylindrical shell. These equations of motion are solved subject to boundary conditions, which describe the forcing function of the hammer at the top of the pile and the soil resistance at the base of the pile (Figure B-1). Damping of the pile vibration due to radiation loading is computed for Mach waves emanating from the pile wall. The equations of motion are discretised using the finite difference (FD) method and are solved on a discrete time and depth mesh.

To model the sound emissions from the piles, the force of the pile driving hammers also had to be modelled. The force at the top of each pile was computed using the GRLWEAP 2010 wave equation model (GRLWEAP, Pile Dynamics 2010), which includes a large database of simulated hammers—both impact and vibratory—based on the manufacturer's specifications. The forcing functions from GRLWEAP were used as inputs to the FD model to compute the resulting pile vibrations.

The sound radiating from the pile itself is simulated using a vertical array of discrete point sources. The point sources are centred on the pile axis. Their amplitudes are derived using an inverse technique, such that their collective particle velocity—calculated using a near-field wave-number integration model—matches the particle velocity in the water at the pile wall. The sound field propagating away from the vertical source array is then calculated using a time-domain acoustic propagation model (Section B.2.3). MacGillivray (2014) describes the theory behind the physical model in more detail.
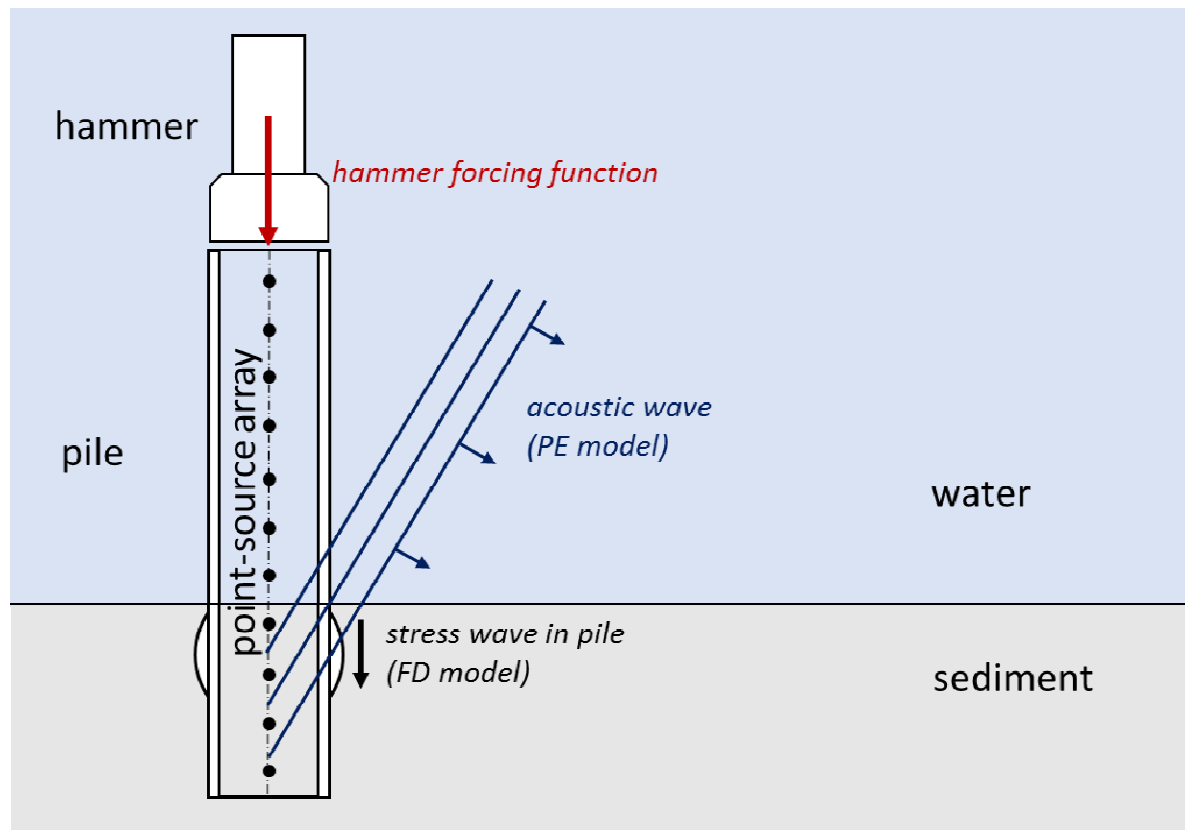
Figure B-1. Physical model geometry for impact driving of a cylindrical pile (vertical cross-section). The hammer forcing function is used with the finite difference (FD) model to compute the stress wave vibration in the pile. A vertical array of point sources is used with the parabolic equation (PE) model to compute the acoustic waves that the pile wall radiates.

B.2. Sound Propagation Models

B.2.1. Transmission Loss

The propagation of sound through the environment was modelled by predicting the acoustic transmission loss—a measure, in decibels, of the decrease in sound level between a source and a receiver some distance away. Geometric spreading of acoustic waves is the predominant way by which transmission loss occurs. Transmission loss also happens when the sound is absorbed and scattered by the seawater, and absorbed scattered, and reflected at the water surface and within the seabed. Transmission loss depends on the acoustic properties of the ocean and seabed; its value changes with frequency.

If the acoustic source level (SL), expressed in dB re 1 µPa @ 1 m, and transmission loss (TL), in units of dB, at a given frequency are known, then the received level (RL) at a receiver location can be calculated in dB re 1 µPa @ 1 m by:

$$RL = SL - TL \qquad\qquad\qquad (B\text{-}1)$$

B.2.2. Noise Propagation with MONM

Underwater sound propagation (i.e., transmission loss) at frequencies of 10 Hz to 5 kHz was predicted with JASCO's Marine Operations Noise Model (MONM). MONM computes received per-pulse SEL (per-strike for pile driving) for directional impulsive sources at a specified source depth.

MONM computes acoustic propagation via a wide-angle parabolic equation solution to the acoustic wave equation (Collins 1993) based on a version of the U.S. Naval Research Laboratory's Range-dependent Acoustic Model (RAM), which has been modified to account for a solid seabed (Zhang and Tindle 1995). The parabolic equation method has been extensively benchmarked and is widely employed in the underwater acoustics community (Collins et al. 1996). MONM accounts for the additional reflection loss at the seabed, which results from partial conversion of incident compressional waves to shear waves at the seabed and sub-bottom interfaces, and it includes wave attenuations in all layers. MONM incorporates the following site-specific environmental properties: a bathymetric grid of the modelled area, underwater sound speed as a function of depth, and a geoacoustic profile based on the overall stratified composition of the seafloor.

MONM computes acoustic fields in three dimensions by modelling transmission loss within two-dimensional (2-D) vertical planes aligned along radials covering a 360° swath from the source, an approach commonly referred to as N×2-D. These vertical radial planes are separated by an angular step size of $\Delta\theta$, yielding N = 360°/$\Delta\theta$ number of planes (Figure B-2).
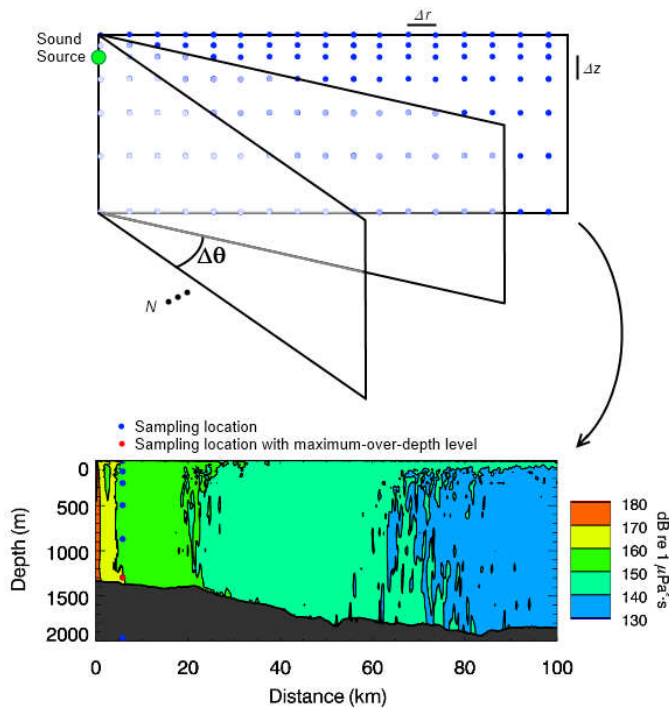
Figure B-2. The N×2-D and maximum-over-depth modelling approach used by MONM.

MONM treats frequency dependence by computing acoustic transmission loss at the centre frequencies of 1/3-octave-bands. Sufficiently many 1/3-octave-bands, starting at 10 Hz, are modelled to include the majority of acoustic energy emitted by the source. At each centre frequency, the transmission loss is modelled within each of the N vertical planes as a function of depth and range from the source. The 1/3-octave-band received per-pulse SELs are computed by subtracting the band transmission loss values from the directional source level in that frequency band. Composite broadband received SELs are then computed by summing the received 1/3-octave-band levels.

The frequency-dependent transmission loss computed by MONM can be corrected to account for the acoustic energy attenuating by molecular absorption in seawater. The volumetric sound absorption is quantified by an attenuation coefficient, expressed in units of decibels per kilometre (dB/km). The absorption coefficient depends on the temperature, salinity, and pressure of the water as well as the sound frequency. In general, the absorption coefficient increases with the square of the frequency. The absorption of acoustic wave energy has a noticeable effect (> 0.05 dB/km) at frequencies above 1 kHz. For example, at 10 kHz the absorption loss over 10 km distance can exceed 10 dB. The coefficient for seawater can be computed according to the formulae of François and Garrison (1982b, b), which consider the contributions of pure seawater, magnesium sulfate, and boric acid. The formula applies to all oceanic conditions and frequencies from 200 Hz to 1 MHz. For this project, absorption coefficients were computed and applied for all modelled frequencies greater than 2 kHz. Because of the computational expense associated with parabolic equation modelling at frequencies at or above several kHz and the relative importance of absorption at such frequencies, the transmission loss in each frequency band between 6.3 and 25 kHz was approximated from the transmission loss computed at 5 kHz by applying the correct frequency-dependent absorption coefficient in each band.

The received per-pulse SEL sound field within each vertical radial plane is sampled at various ranges from the source, generally with a fixed radial step size. At each sampling range along the surface, the sound field is sampled at various depths, with the step size between samples increasing with depth below the surface. The step sizes are chosen to provide increased coverage near the depth of the source and at depths of interest in terms of the sound speed profile. For areas with deep water, sampling is not performed at depths beyond those reachable by marine mammals. The received per-pulse SEL at a surface sampling location is taken as the maximum value that occurs over all samples within the water column, i.e., the maximum-over-depth received per-pulse SEL. These maximum-over-depth per-pulse SELs are presented as colour contours around the source.

MONM's predictions have been validated against experimental data from several underwater acoustic measurement programs conducted by JASCO (Hannay and Racca 2005, Aerts et al. 2008, Funk et al.

2008, Ireland et al. 2009, O'Neill et al. 2010, Warner et al. 2010, Racca et al. 2012a, Racca et al. 2012b, Martin et al. 2015).

B.2.3. Noise Propagation with FWRAM

For impulsive sounds from impact pile driving, time-domain representations of the pressure waves generated in the water are required to calculate SPL and peak pressure level. Furthermore, the pile must be represented as a distributed source to accurately characterise vertical directivity effects in the near-field zone. For this study, synthetic pressure waveforms were computed using FWRAM, which is a time-domain acoustic model based on the same wide-angle parabolic equation (PE) algorithm as MONM. FWRAM computes synthetic pressure waveforms versus range and depth for range-varying marine acoustic environments, and it takes the same environmental inputs as MONM (bathymetry, water sound speed profile, and seabed geoacoustic profile). Unlike MONM, FWRAM computes pressure waveforms via Fourier synthesis of the modelled acoustic transfer function in closely spaced frequency bands. FWRAM employs the array starter method to accurately model sound propagation from a spatially distributed source (MacGillivray and Chapman 2012).

Besides providing direct calculations of the peak pressure level and SPL, the synthetic waveforms from FWRAM can also be used to convert the SEL values from MONM to SPL.

Appendix C. Results

Maps and graphical representations of the sound fields for Site 2, Scenarios 5–8 and 10 are shown in the following section. Representations for Site 1, Scenarios 1–4 and 9, are included in Section 4.2.

Maps were created to display the unweighted 24 h SEL footprints with the M-weighted 24 h PTS thresholds for marine mammals (Figures C-1 to C-5), the unweighted 24 h SEL footprints with the thresholds for fish, turtles, fish eggs, and fish larvae (Figures C-6 to C-10), and SPL footprints with thresholds for marine mammals and turtles (Figures C-11 to C-15). Graphs of unweighted SEL in the vertical plane for each of the scenarios are shown in Figures C-16 to C-20.
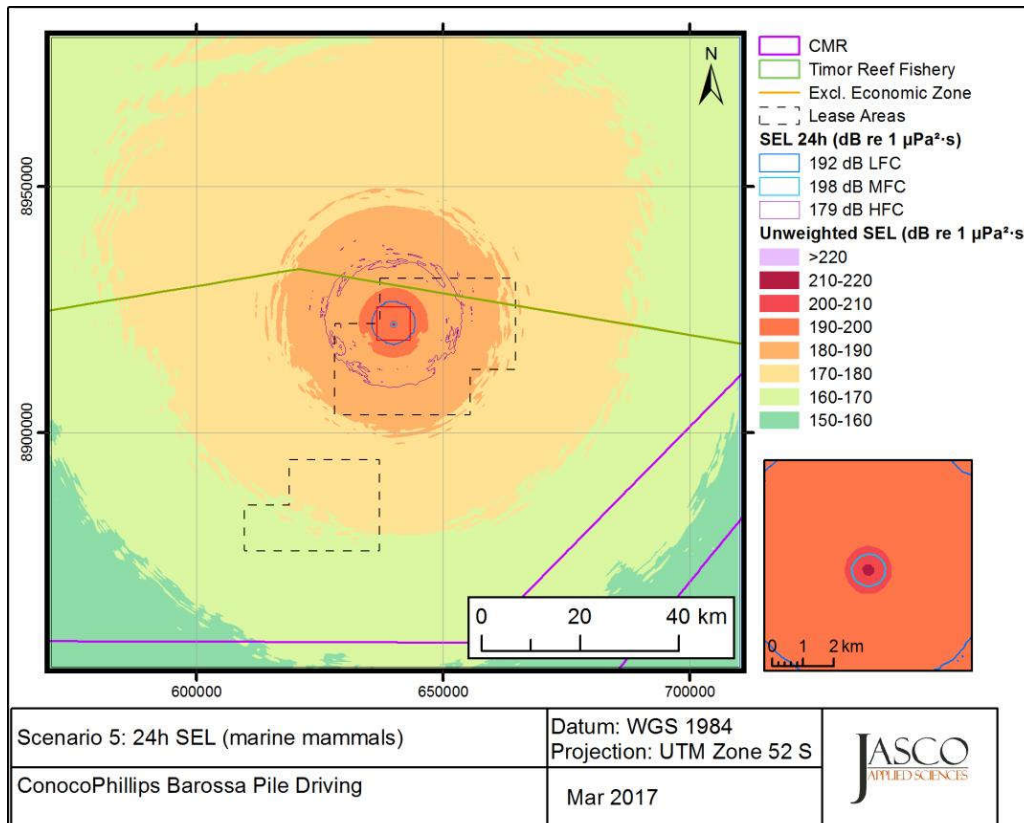
Figure C-1. Scenario 5: Sound level contour map showing maximum-over-depth SEL_{24h} results with marine mammal PTS thresholds.
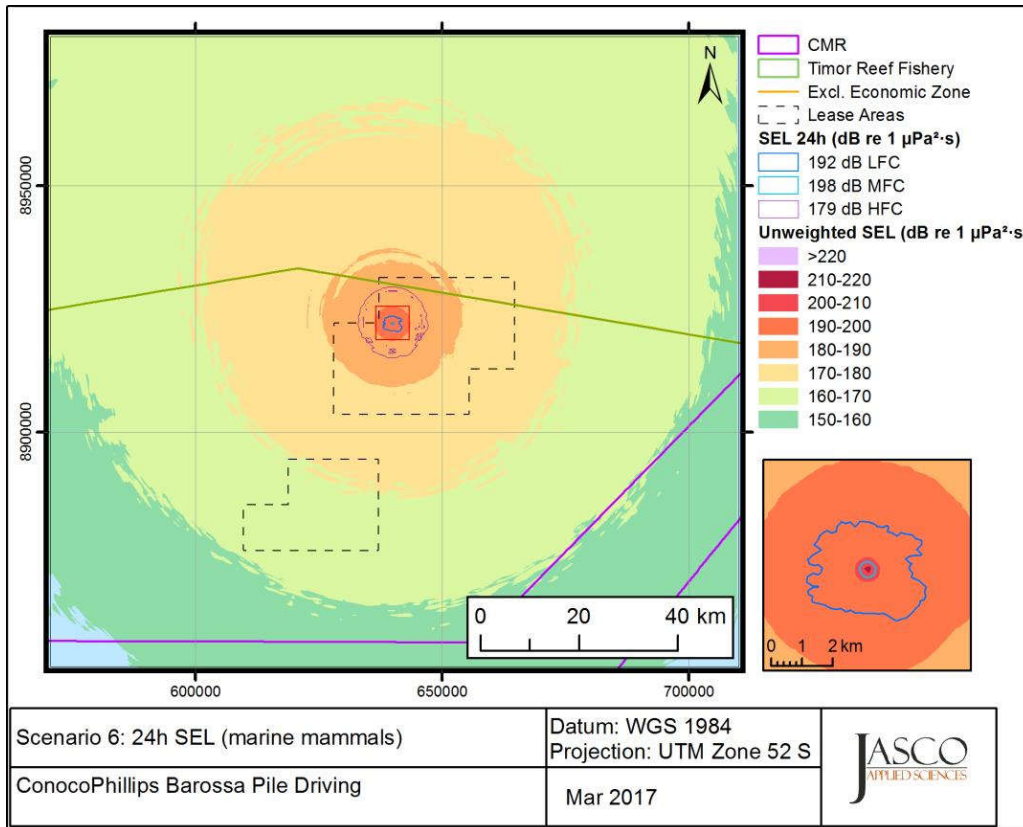
Figure C-2. Scenario 6: Sound level contour map showing maximum-over-depth SEL$_{24h}$ results with marine mammal PTS thresholds.
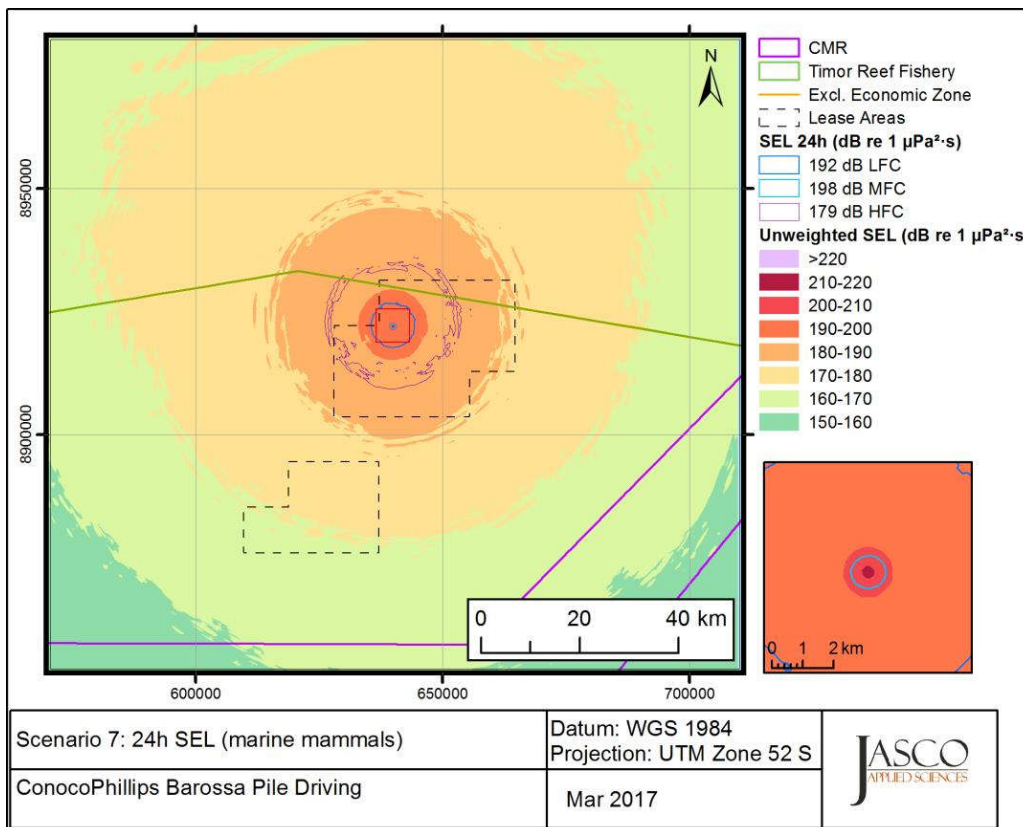
Figure C-3. Scenario 7: Sound level contour map showing maximum-over-depth SEL$_{24h}$ results with marine mammal PTS thresholds.
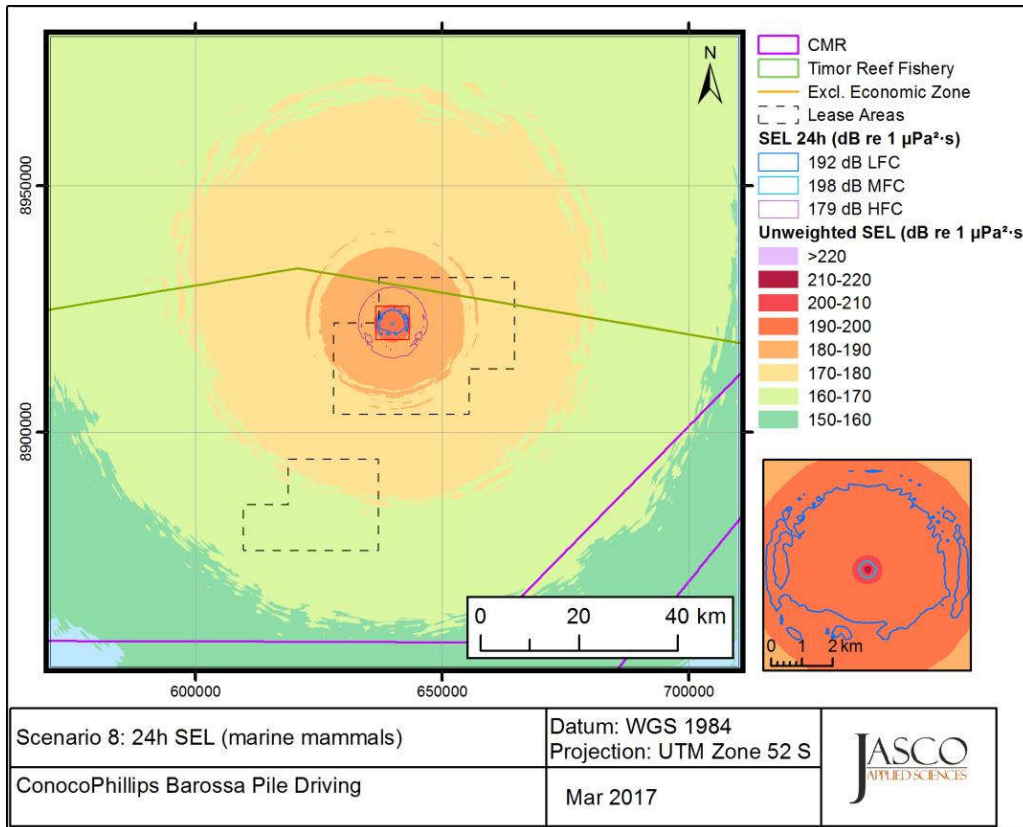
Figure C-4. Scenario 8: Sound level contour map showing maximum-over-depth SEL$_{24h}$ results with marine mammal PTS thresholds.
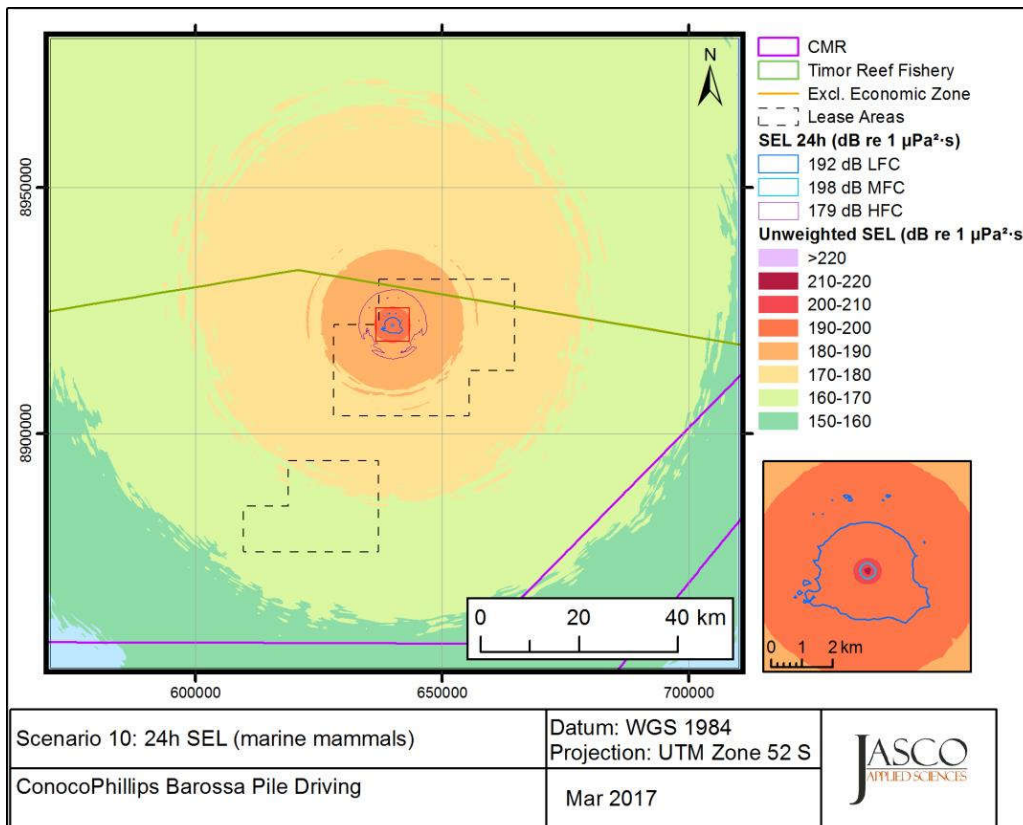
Figure C-5. Scenario 10: Sound level contour map showing maximum-over-depth SEL$_{24h}$ results with marine mammal PTS thresholds.
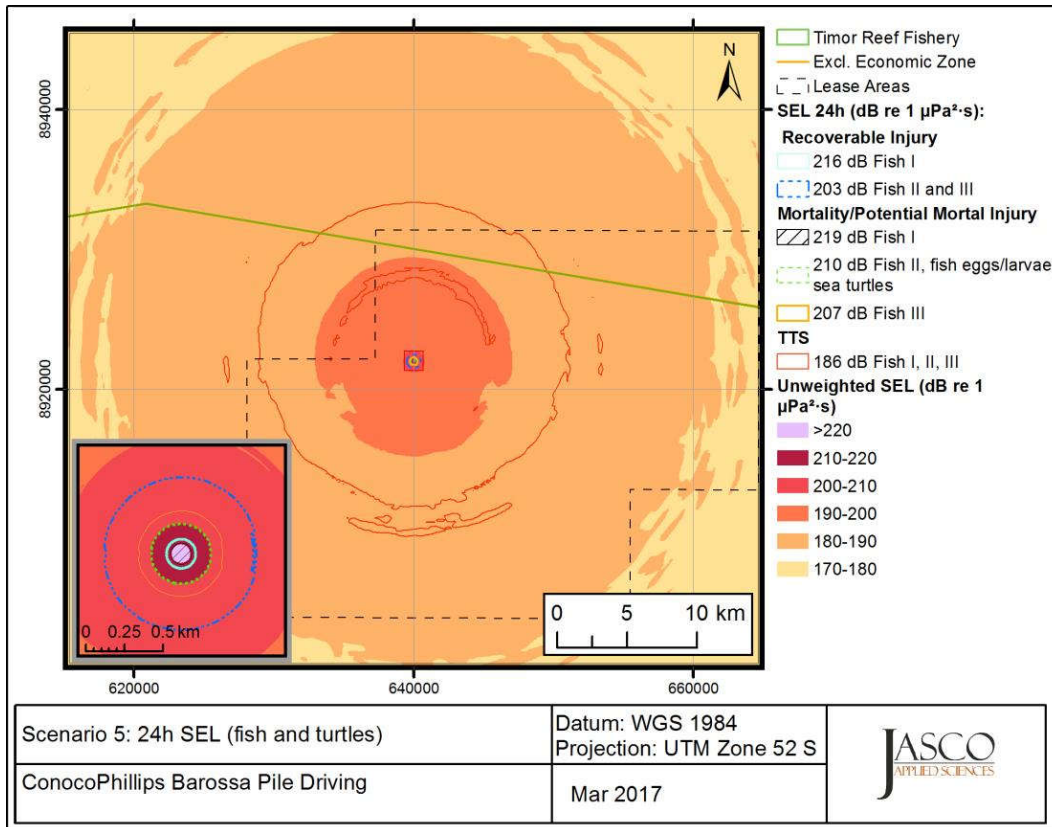
Figure C-6. Scenario 5: Sound level contour map showing maximum-over-depth SEL$_{24h}$ results with fish and turtle thresholds.
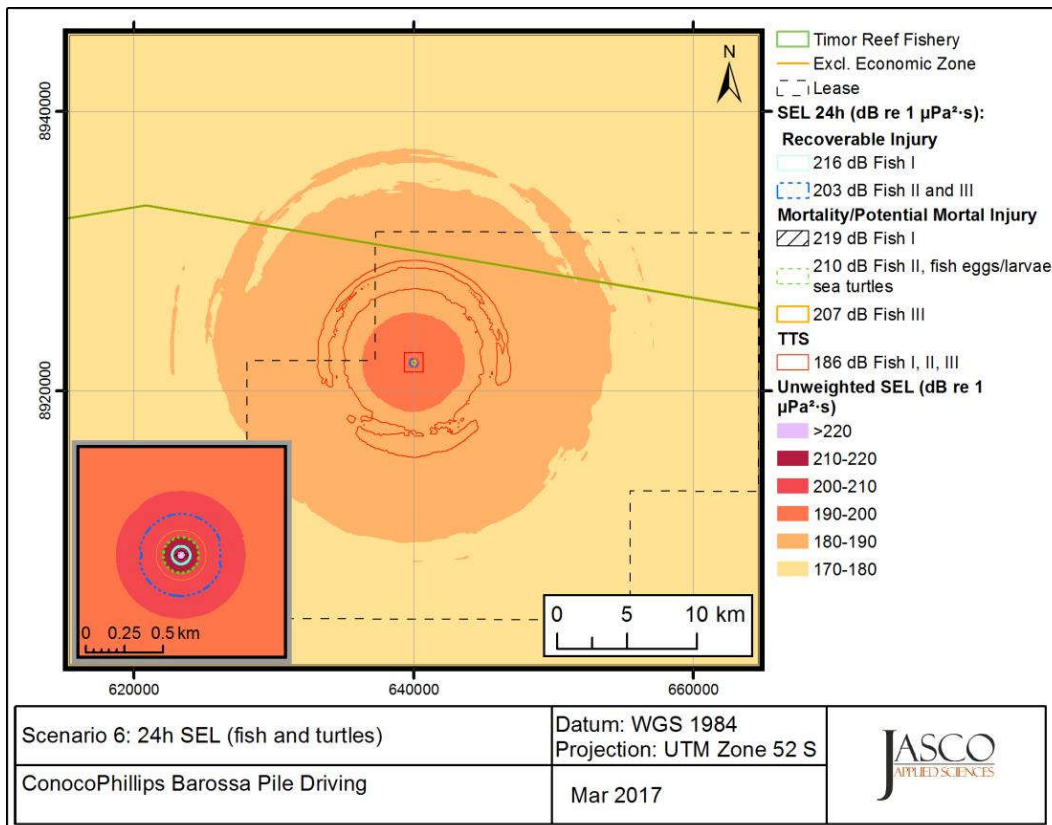
Figure C-7. Scenario 6: Sound level contour map showing maximum-over-depth SEL$_{24h}$ results with fish and turtle thresholds.
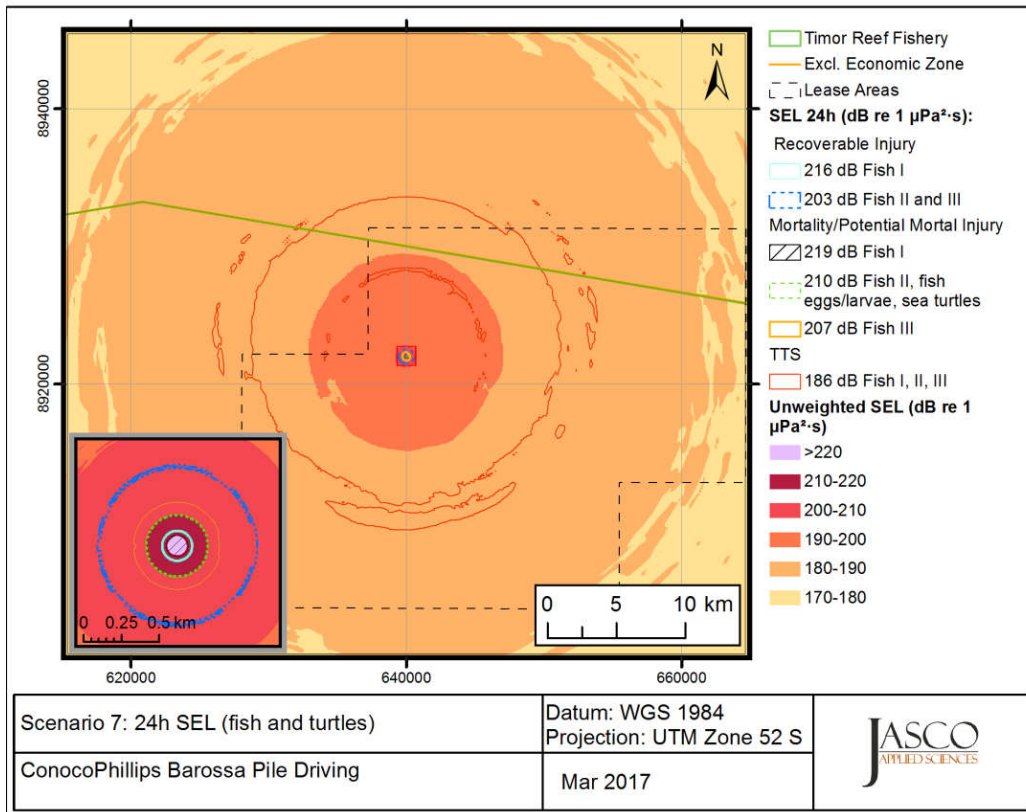
Figure C-8. Scenario 7: Sound level contour map showing maximum-over-depth SEL$_{24h}$ results with fish and turtle thresholds.
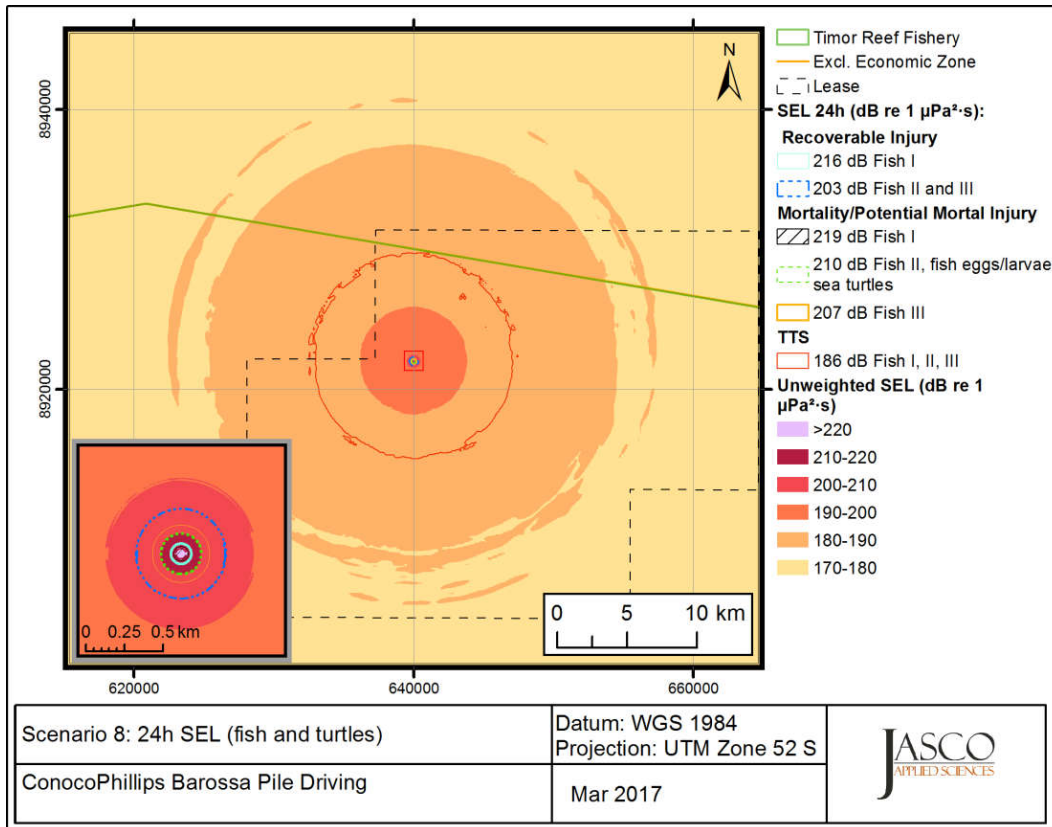
Figure C-9. Scenario 8: Sound level contour map showing maximum-over-depth SEL$_{24h}$ results with fish and turtle thresholds.
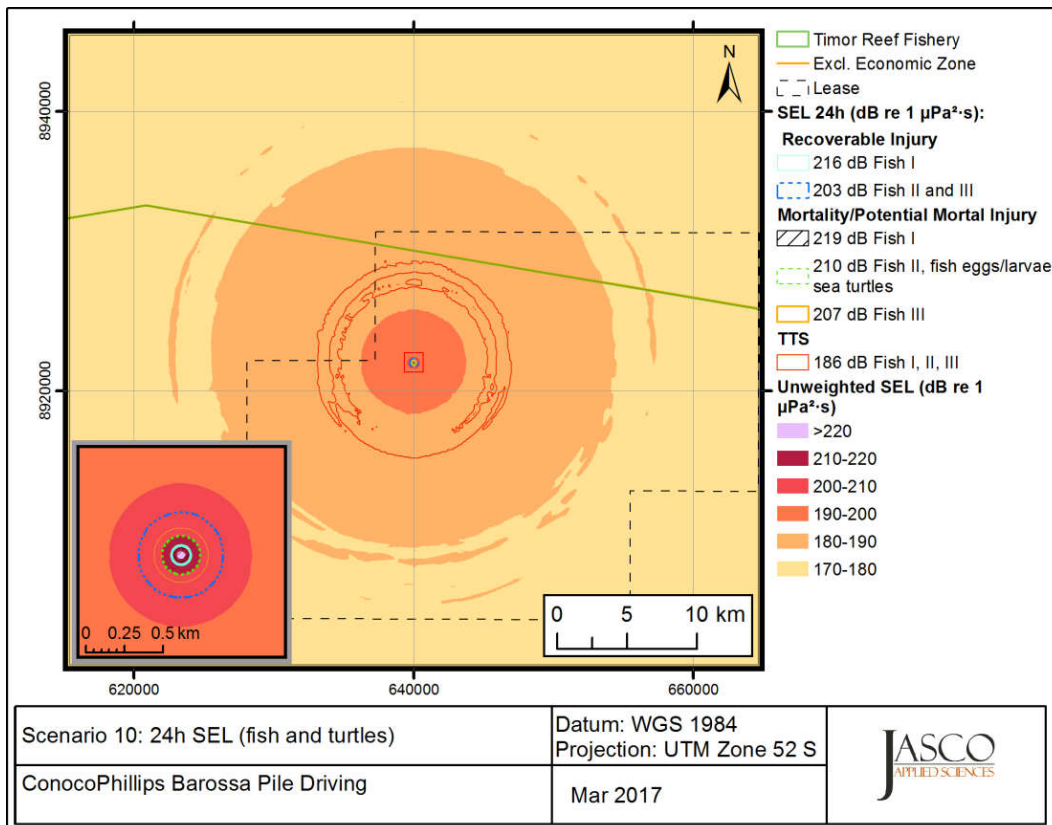
Figure C-10. Scenario 10: Sound level contour map showing maximum-over-depth SEL$_{24h}$ results with fish and turtle thresholds.

Scenario 5: SPL	Datum: WGS 1984 Projection: UTM Zone 52 S	JASCO APPLIED SCIENCES
ConocoPhillips Barossa Pile Driving	Mar 2017	
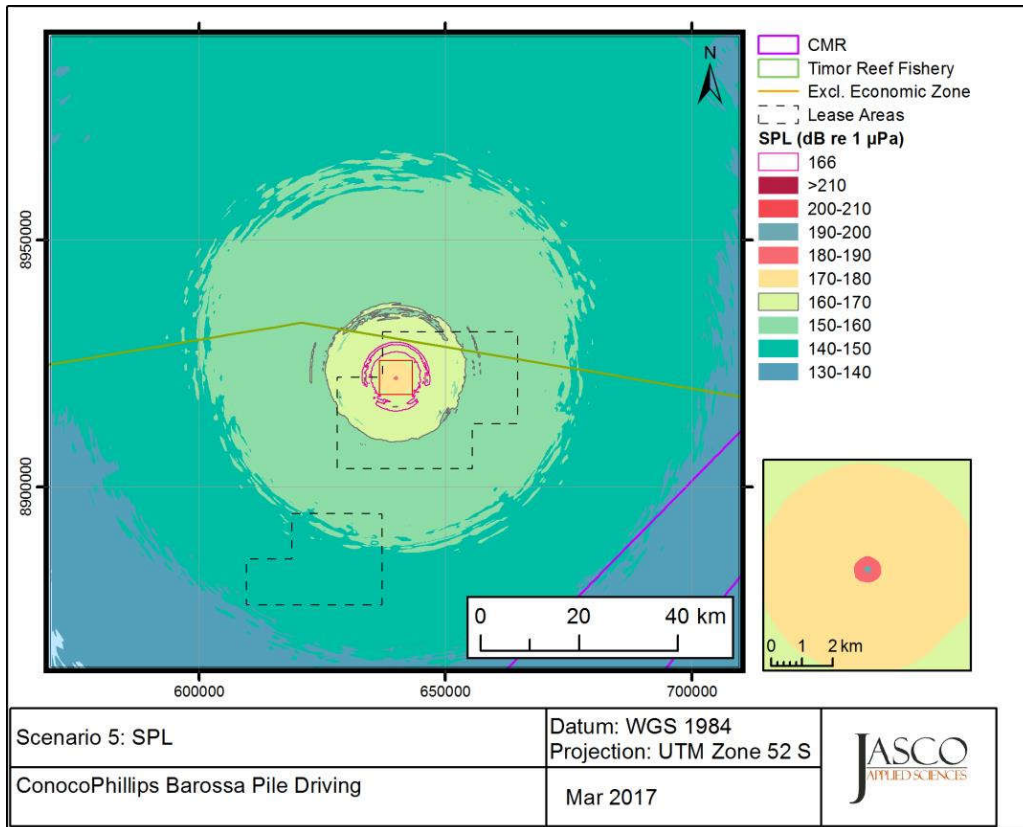
Figure C-11. Scenario 5: Sound level contour map showing unweighted maximum-over-depth SPL results, showing isopleths for marine mammal and turtle behaviour thresholds.

Figure C-12. Scenario 6: Sound level contour map showing unweighted maximum-over-depth SPL results, showing isopleths for marine mammal and turtle behaviour thresholds.
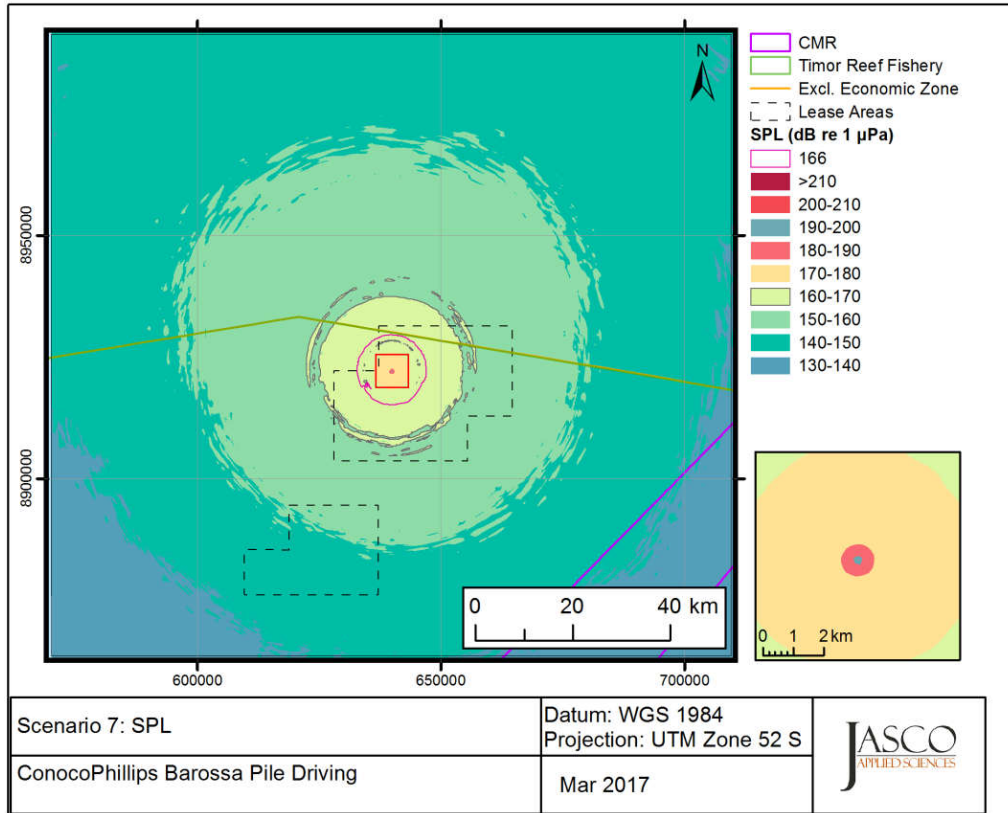
Figure C-13. Scenario 7: Sound level contour map showing unweighted maximum-over-depth SPL results, showing isopleths for marine mammal and turtle behaviour thresholds.
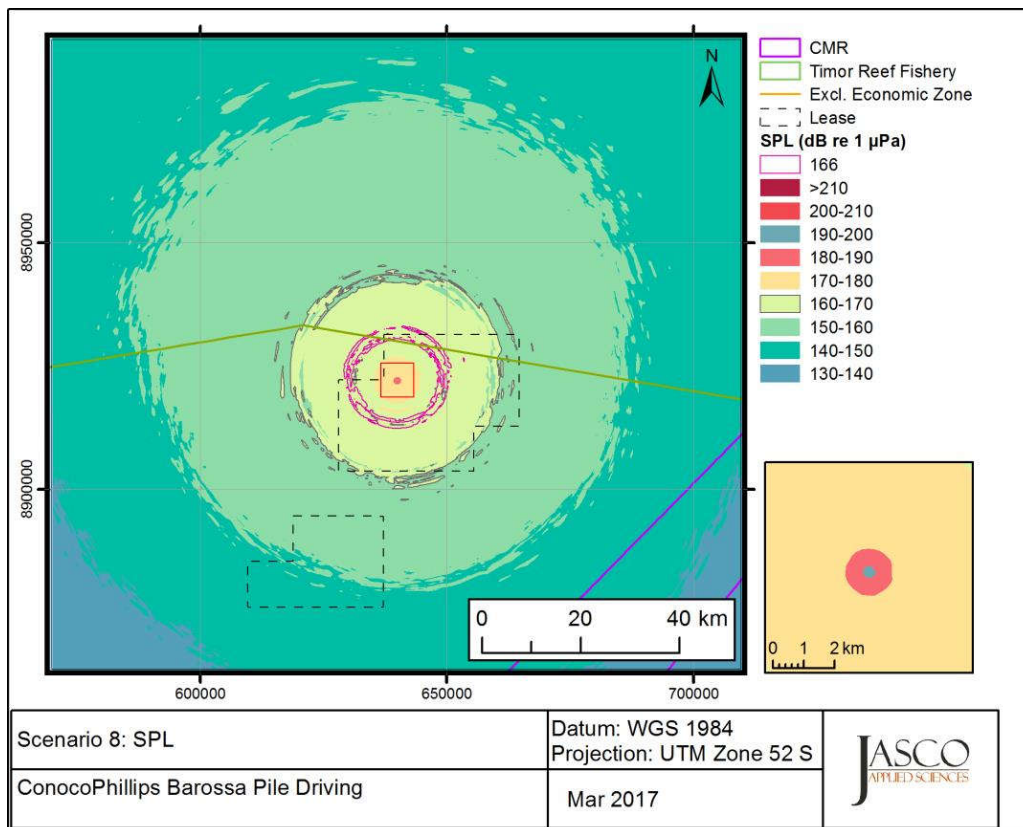
Figure C-14. Scenario 8: Sound level contour map showing unweighted maximum-over-depth SPL results, showing isopleths for marine mammal and turtle behaviour thresholds.
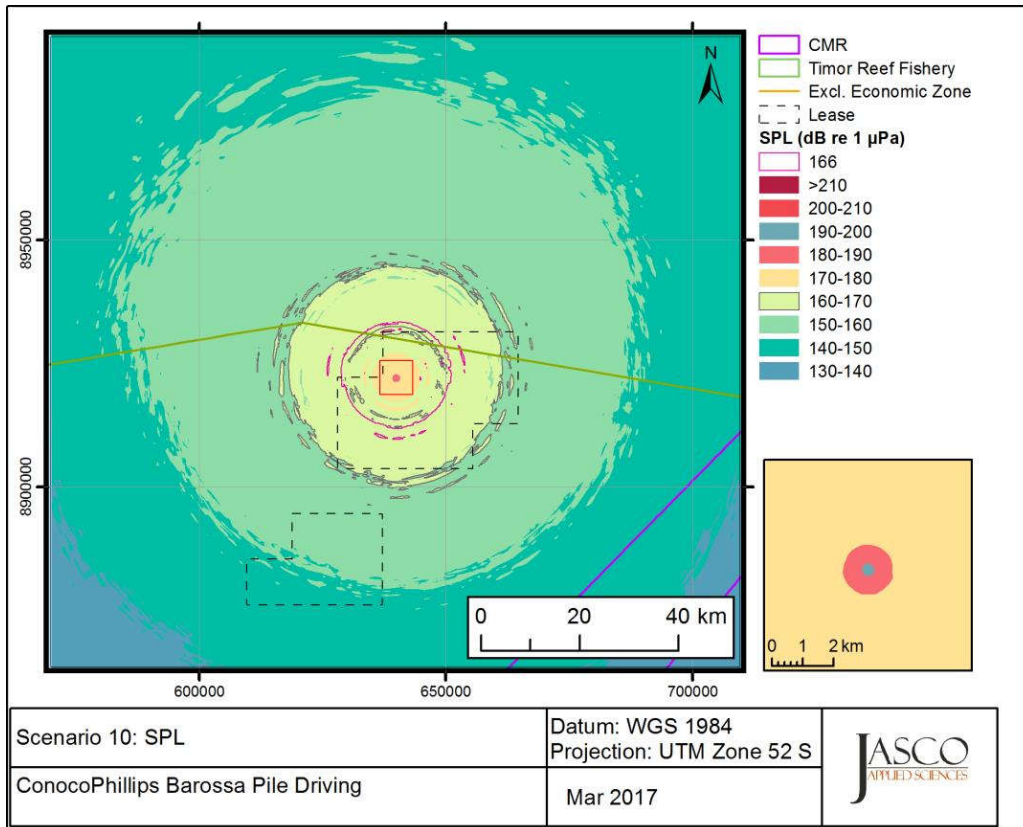
Figure C-15. Scenario 10: Sound level contour map showing unweighted maximum-over-depth SPL results, showing isopleths for marine mammal and turtle behaviour thresholds.
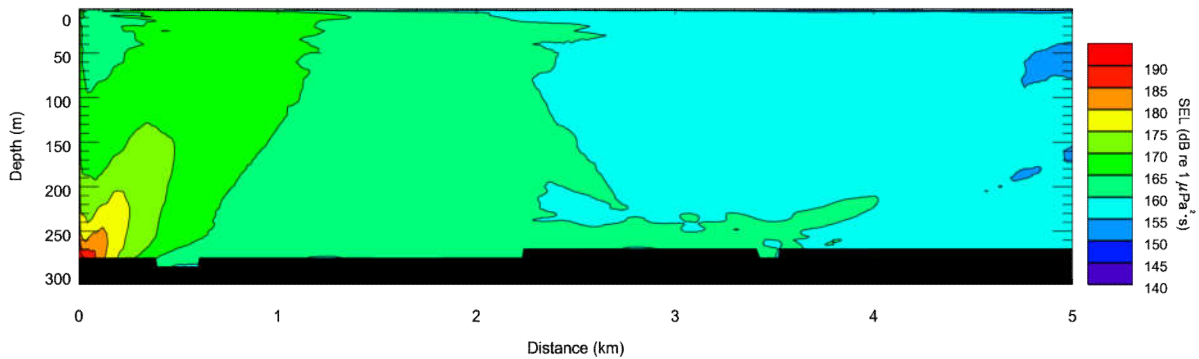
Figure C-16. Scenario 5: Predicted unweighted per-strike SEL as a vertical slice. Levels are shown along a single transect of azimuth 180°.
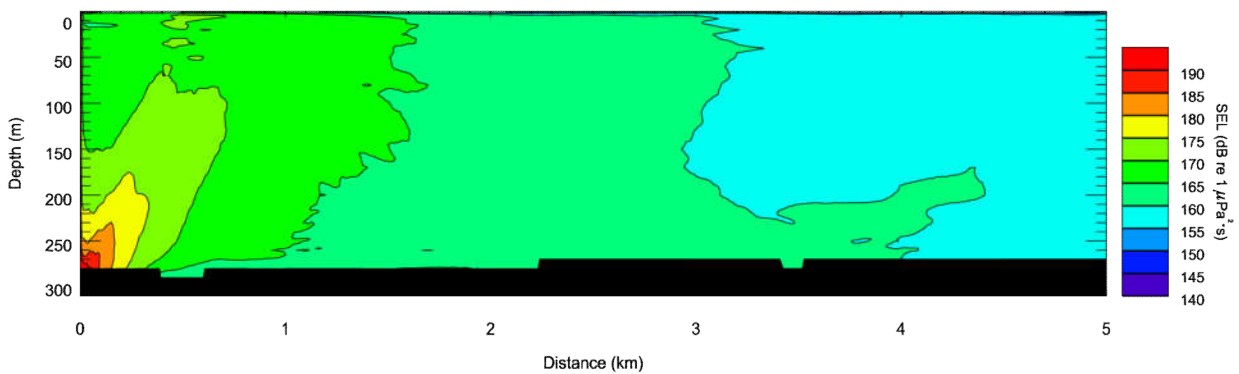
Figure C-17. Scenario 6: Predicted unweighted per-strike SEL as a vertical slice. Levels are shown along a single transect of azimuth 180°.
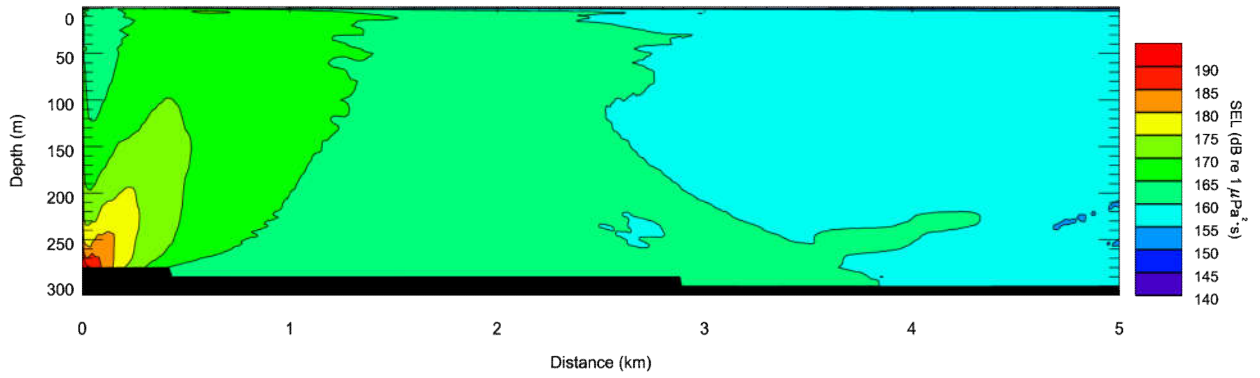
Figure C-18. Scenario 7: Predicted unweighted per-strike SEL as a vertical slice. Levels are shown along a single transect of azimuth 180°.
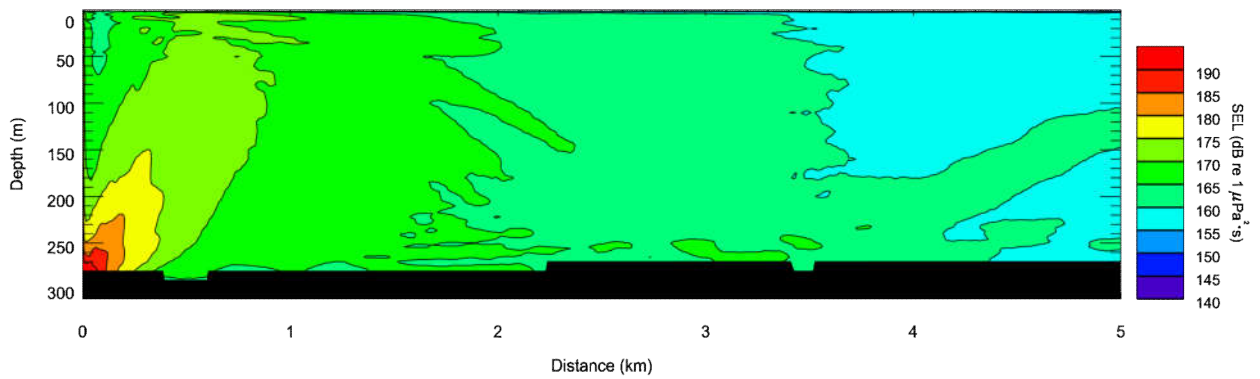
Figure C-19. Scenario 8: Predicted unweighted per-strike SEL as a vertical slice. Levels are shown along a single transect of azimuth 180°.
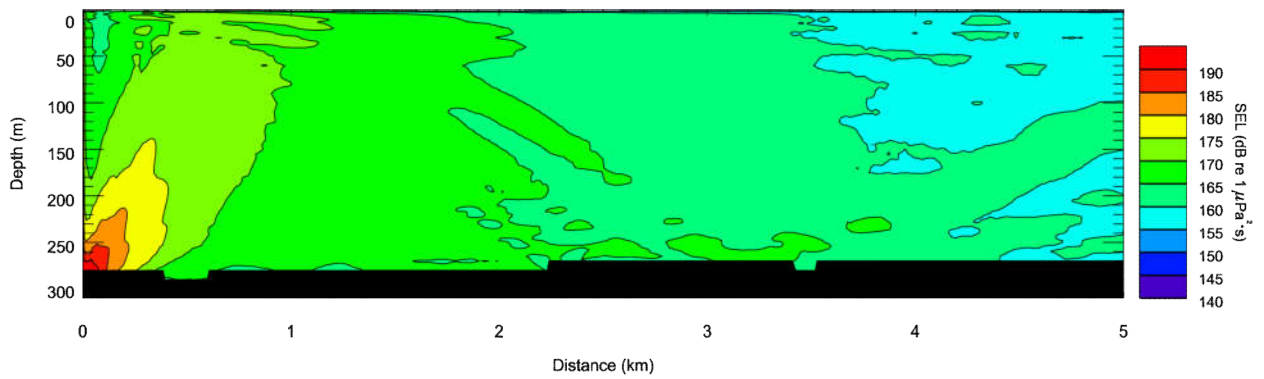
Figure C-20. Scenario 10: Predicted unweighted per-strike SEL as a vertical slice. Levels are shown along a single transect of azimuth 180°.